5 General Principles of Neutron Transport

Anil K. Prinja[1] · *Edward W. Larsen*[2]

[1]Chemical and Nuclear Engineering Department,
University of New Mexico, Albuquerque, NM, USA
prinja@unm.edu
[2]Department of Nuclear Engineering and Radiological
Sciences, University of Michigan, Ann Arbor, MI, USA
edlarsen@umich.edu

Abstract: This chapter describes the basic theory underlying the neutron transport equation and the principal approximations used in this equation's applications to reactor physics. In addition to presenting detailed classical derivations of various forms of the transport equation, we discuss several important topics in a more rigorous manner than is found in typical derivations. For instance, we include (i) a discussion of the lack of smoothness of the angular flux in multidimensional geometries (this has a negative impact on numerical simulations); (ii) derivations of the transport equation in specialized 1-D, 2-D, and 3-D geometries; (iii) a derivation of the time-dependent integral transport equation; (iv) an asymptotic derivation of the point kinetics equation; and (v) an asymptotic derivation of the multigroup P_1 and diffusion equations. The basic approach taken by the authors in this chapter is theoretical, in the hope that this will complement more intuitive presentations of related topics found in other chapters of this handbook.

1 Introduction

A central problem in the design and analysis of nuclear reactors is the accurate and detailed prediction of the space, angle, energy, and time-dependence of neutron and photon distributions in all components of the reactor. Neutrons are responsible for propagating the chain reaction and releasing energy through fission, but neutrons and photons, through fission, capture, scattering, and excitation/ionization interactions, also induce a thermal-mechanical response in the reactor core and, moreover, cause degradation of structural components, fuel rods, and the control system, through radiation damage, depletion, and fission product poison buildup. These consequences, in turn, affect the distribution of the radiation field itself through several feedback mechanisms. A synergistic description of all nuclear and nonnuclear processes is therefore essential for the economic development and safe operation of nuclear power plants, and driving much of this challenge is the need to have an appropriate mathematical and computational framework for adequately characterizing the neutron and photon distributions.

The transport of neutral radiation, including but not restricted to neutrons and photons, through matter is extremely well described by the transport equation, a linear version of Boltzmann's celebrated equation originally developed within the framework of the kinetic theory of gases (for this reason, the transport equation is sometimes also referred to as the linear Boltzmann equation). This equation is an integrodifferential equation having (generally) seven independent variables, whose solution is not smooth, and which can only be solved exactly for the simplest of problems. Essentially, all neutron transport problems of practical interest must be solved either approximately or numerically.

In this chapter, we present the basic theory underlying the neutron transport equation, and we describe some of this equation's principal approximations. In ❯ Sect. 2, we derive the transport equation and discuss some of its general properties. In ❯ Sect. 3, we discuss problems with special spatial symmetries, which enable the transport equation to be formulated using fewer independent variables; these formulations are at the heart of all practical 1-D and 2-D computer simulations of neutron transport. In ❯ Sect. 4, we discuss the integral form of the transport equation, which, under certain conditions, is advantageous for computer simulations. In ❯ Sect. 5, we describe the adjoint transport equation and some of its applications. ❯ Sect. 6 describes the standard multigroup approximation to the energy variable, along with the one-speed transport equation. ❯ Sect. 7 develops the Age and Wigner approximations, which enable certain neutron slowing-down problems to be solved analytically. ❯ Sect. 8 is

devoted to the diffusion approximation, the most important approximate form of the transport equation for nuclear reactor core problems. ❯ Sect. 9 describes the point kinetics approximation, which is used for time-dependent simulations of nuclear reactors. ❯ Sect. 10 provides a brief discussion of numerical methods for simulating neutron and photon transport problems, and we close ❯ Chap. 5 with some concluding remarks in ❯ Sect. 11.

We have consciously adopted a somewhat theoretical approach to this chapter of the handbook, but we have strived for an exposition that presents advanced material in a pedagogical manner that will hopefully appeal both to the novice and to the expert in the field of neutron transport. We include detailed, self-contained presentations of classical material, such as the derivation of the forward and adjoint integrodifferential equations and the forward integral equation, but also, in several of the sections in this chapter, we present material that is either not commonly found in standard texts, or represents a different and more rigorous theoretical approach than standard approaches to the topics under discussion. For instance, ❯ Sect. 2 includes a discussion of the (lack of) smoothness of the angular flux in multidimensional problems; this negatively affects the accuracy of numerical solutions of multidimensional transport problems. Also, ❯ Sect. 3 on the different forms of the Boltzmann equation for 1-D, 2-D, and 3-D geometries is exceptionally important in practice, but this material is not found in standard texts. ❯ Sect. 9 presents a new asymptotic derivation of the point kinetics equation; formerly, this equation has been derived by ad hoc, or at best by variational approaches. Also, ❯ Sect. 7 derives the standard Age and Wigner approximations without introducing the lethargy variable, and ❯ Sect. 8 on the diffusion approximation attempts to put some rigor into the standard P_1 approximation that leads to the multigroup form of this approximation.

Overall, we have attempted to cover significant material in a way that makes use of theoretical approaches that have been developed in recent years, but that has not found its way yet into standard texts. We hope that this will make the chapter more interesting, and that it will provide a more fundamental approach to basic material that may be presented more intuitively in other chapters of this handbook.

2 Derivation of the Neutron Transport (Linear Boltzmann) Equation

Neutron transport is the process in which neutrons propagate through the atoms in a physical system. This includes the *streaming* of neutrons from one collision site (an atomic nucleus) to the next, the *scattering* of neutrons off nuclei, the *capture* of neutrons by nuclei, and the initiation by neutrons of *fission events*, in which a nucleus splits and two or more neutrons are emitted. In this chapter, we develop the mathematical equations that describe the neutron transport process. We begin by defining the necessary independent variables. Then we (i) outline the relevant physics, (ii) define the relevant unknowns (angular flux, precursor densities – for problems with delayed neutrons), and (iii) derive the appropriate mathematical equations for these unknowns. (Our derivation is patterned closely on previous derivations in classic texts [Bell and Glasstone 1970; Case and Zweifel 1967; Henry 1975; Weinberg and Wigner 1958].) Finally, we discuss conditions under which the transport equation is valid and some properties of its solution.
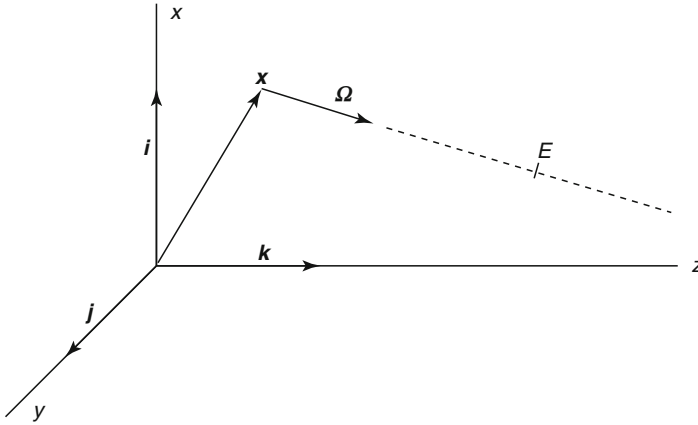
Figure 1
The spatial (*x*), direction-of-flight or angular (Ω), and energy (*E*) variables

2.1   Independent Variables

To characterize a general 3-D neutron transport process, *seven* independent variables are required: three components of the position vector $\boldsymbol{x}$, two angles to specify the unit vector $\boldsymbol{\Omega}$ denoting the direction of flight, the kinetic energy E, and time t. These variables enable one to specify the population of neutrons (i) at an arbitrary point $\boldsymbol{x}$ in the system, (ii) traveling in an arbitrary direction of flight $\boldsymbol{\Omega}$, (iii) with any energy E, and (iv) at any time t (❯ *Fig. 1*).

In steady-state problems, the time variable is extraneous, and in problems with spatial symmetries (discussed in ❯ Sect. 3), fewer spatial and/or angular variables are required.

To derive the 3-D transport equation, it is convenient to use the familiar Cartesian coordinates, defined in the usual manner by:

$$\boldsymbol{x} = x\boldsymbol{i} + y\boldsymbol{j} + z\boldsymbol{k}, \tag{1}$$

where $\boldsymbol{i}$, $\boldsymbol{j}$, and $\boldsymbol{k}$ are mutually orthogonal unit vectors.

The direction-of-flight vector $\boldsymbol{\Omega}$, a unit vector ($|\boldsymbol{\Omega}| = 1$), is specified using a *polar angle θ*, defined relative to the z-axis, and an *azimuthal angle ω*, defined relative to the x-axis (❯ *Fig. 2*). In terms of the *direction cosines* projected onto the three Cartesian axes, we have:

$$\boldsymbol{\Omega} = \Omega_x\boldsymbol{i} + \Omega_y\boldsymbol{j} + \Omega_z\boldsymbol{k}, \tag{2a}$$

where:

$$\Omega_x = l_3 = \sqrt{1 - \mu^2}\ \cos\omega, \tag{2b}$$

$$\Omega_y = l_4 = \sqrt{1 - \mu^2}\ \sin\omega, \tag{2c}$$

$$\Omega_z = l_1 = \mu. \tag{2d}$$
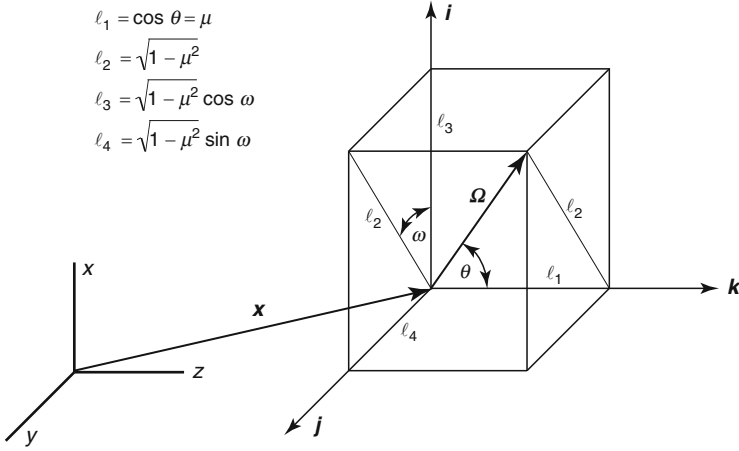
◨ Figure 2
The polar angle θ and azimuthal angle ω
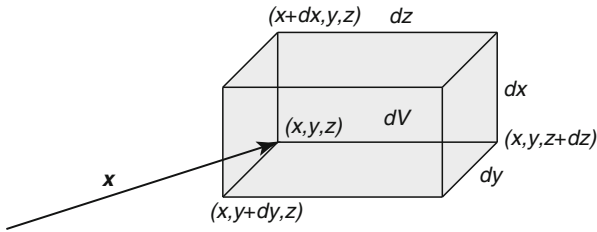
◨ Figure 3
Incremental volume dV

If we independently displace the spatial variables x, y, and z by incremental (very small) amounts dx, dy, and dz, the spatial variable $\boldsymbol{x}$ will sweep out an incremental hexahedral volume $dV = dxdydz$ about $\boldsymbol{x}$ (see ❷ *Fig. 3*).

Similarly, if we independently displace the angular variables μ and ω by incremental amounts $d\mu$ and $d\omega$, then the unit vector $\boldsymbol{\Omega}$ will sweep out an incremental, rectangular, dimensionless *element of area* or *solid angle* $d\Omega = dsd\ell$ on the unit sphere (see ❷ *Fig. 4*).

❷ *Figure 4* shows that $ds = d\omega\sqrt{1 - \mu^2}$, and ❷ *Fig. 5*, drawn in the plane generated by $\boldsymbol{\Omega}$ and $\boldsymbol{k}$, shows that $d\ell = d\mu/\sqrt{1 - \mu^2}$. Thus, $d\Omega$ is given by:

$$d\Omega = dsd\ell = \left(d\omega\sqrt{1 - \mu^2}\right)\left(\frac{d\mu}{\sqrt{1 - \mu^2}}\right) = d\mu d\omega. \tag{3}$$

For example, the surface area of the entire unit sphere is then:

$$\text{Area} = \int_{4\pi} d\Omega = \int_0^{2\pi}\int_{-1}^{1} d\mu d\omega = 4\pi,$$
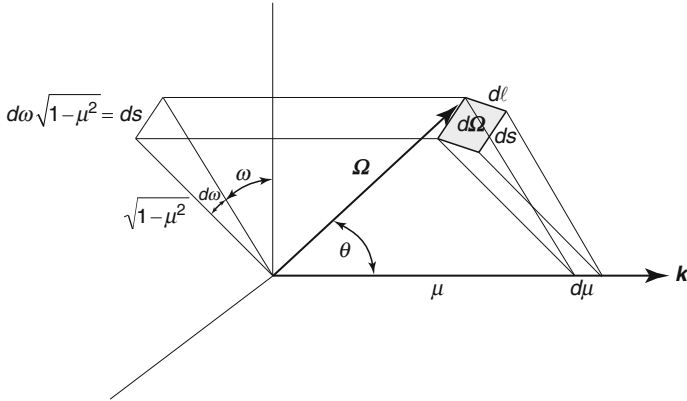
◼ Figure 4
Solid angle $d\Omega$
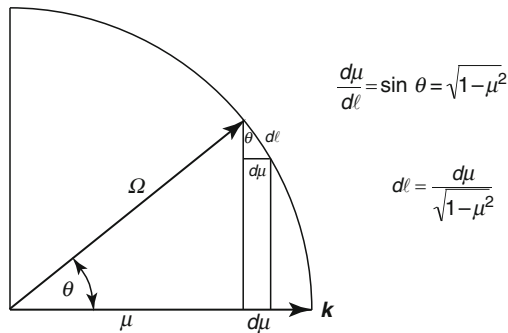
◼ Figure 5
Relationship between $d\mu$ and $d\ell$

where integration over the unit sphere is denoted by:

$$\int_{4\pi} f(\mathbf{\Omega})d\Omega = \int_0^{2\pi}\int_{-1}^{1} f(\mathbf{\Omega})d\mu d\omega = \int_0^{2\pi}\int_{-1}^{1} f(\mu,\omega)d\mu d\omega.$$

2.2 The Basic Physics of Neutron Transport

Let us consider a neutron, streaming with direction $\mathbf{\Omega}$ and energy E inside a material with known physical properties. As the neutron travels an incremental distance ds, there is an incremental probability dp that the neutron will interact with a nucleus. To determine the

relationship between dp and ds, let us consider the neutron to be normally incident, at an arbitrary point, on a target of area A and incremental thickness ds (see ❯ *Fig. 6*).

We assume that the *microscopic cross-sectional area of a target nucleus* $\sigma(E)$ (cm^2) and the *number density of target nuclei* N (cm^{-3}) are known. The *neutron's-eye-view* of the target is depicted in ❯ *Fig. 7*.

If the target is sufficiently thin that one target nucleus does not shield another, then the probability of a collision is:

$$dp = \frac{\text{total area of nuclei}}{\text{area of target}}$$

$$= \frac{n\sigma}{A}, \tag{4}$$

where $n = NdV = N(Ads)$ = the number of nuclei in the target. Equation (4) gives:

$$dp = \frac{N(Ads)\sigma}{A} = (N\sigma)ds.$$

Therefore, dp is proportional to ds:
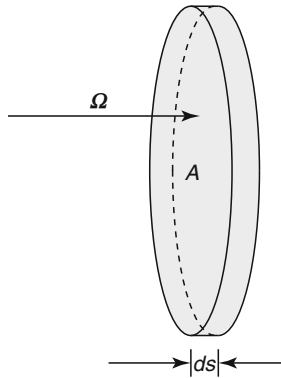
◧ Figure 6
Incrementally thin neutron target
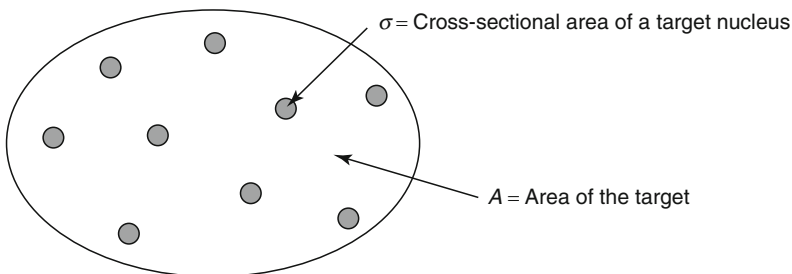
◧ Figure 7
Neutron's-eye-view of the target

$$dp = \Sigma_t(E)ds, \tag{5a}$$

where the "constant" of proportionality is:

$$\Sigma_t(E) = N\sigma(E) = \text{ total macroscopic cross section} \quad (\text{cm}^{-1}). \tag{5b}$$

When a neutron collides with a nucleus, it is captured with probability $p_\gamma(E)$, scatters with probability $p_s(E)$, or initiates a fission event with probability $p_f(E)$. (We ignore other possible, but generally rare, events such as (n, α), (n, p), and $(n, 2n)$.) Then:

$$p_\gamma(E) + p_s(E) + p_f(E) = 1. \tag{6}$$

With $r = (\gamma, s, f)$, the probabilities also define the *macroscopic cross sections* $\Sigma_r(E)$, such that:

$$\Sigma_r(E)ds = \Sigma_t(E)ds \, p_r(E) \tag{7}$$

is the probability that a neutron with energy E, while traveling a distance ds, will experience a collision of type r. The total macroscopic cross section then satisfies:

$$\Sigma_t(E) = \Sigma_\gamma(E) + \Sigma_s(E) + \Sigma_f(E). \tag{8}$$

If the neutron is captured, it is considered to be removed from the system. If the neutron (with direction Ω and energy E) scatters, it emerges from the scattering event with a new direction Ω' and energy E'. We assume that the distribution of post-collision directions Ω' and energies E' is known and can be expressed as:

$$p(\Omega \cdot \Omega', E \to E')d\Omega'dE' = \text{probability that the scattered neutron}$$
$$\text{has direction in } d\Omega' \text{ about } \Omega' \text{ and}$$
$$\text{energy in } dE' \text{ about } E'. \tag{9}$$

In writing p as $p(\Omega \cdot \Omega', E \to E')$, we indicate that scattering in media with randomly distributed scattering centers (nuclei) is *rotationally invariant*. That is, the probability that a neutron will scatter from direction Ω to direction Ω' depends only on the *scattering angle* θ_0 between Ω and Ω' (or, on the cosine of this angle, $\mu_0 = \cos\theta_0 = \Omega \cdot \Omega'$). Thus, all scattered directions of flight Ω' on the cone of equal scattering angle are equally probable (❯ *Fig. 8*).

The distribution function for elastic s-wave neutron scattering, which is isotropic in the center-of-mass frame, can be shown from kinematics (Duderstadt and Hamilton 1976) to be given by:

$$p(\Omega \cdot \Omega', E \to E') = p_0(E \to E') \frac{\delta[\Omega \cdot \Omega' - \mu_0(E \to E')]}{2\pi}. \tag{10a}$$

Here, $p_0(E \to E')$ is a histogram distribution function for outgoing energies E':

$$p_0(E \to E') = \begin{cases} \dfrac{1}{(1-\alpha)E} & \text{if } \alpha E < E' < E, \\ 0 & \text{otherwise,} \end{cases} \tag{10b}$$

where:

$$\alpha = \left(\frac{A-1}{A+1}\right)^2,$$ (10c)

and A is the nucleus-to-neutron mass ratio ($A \geq 1$). Also, δ is the familiar delta-function, and $\mu_0(E \to E')$ is the scattering cosine for a neutron, initially with energy E, that elastically scatters into energy E':

$$\mu_0(E \to E') = \left(\frac{A+1}{2}\right)\sqrt{\frac{E'}{E}} - \left(\frac{A-1}{2}\right)\sqrt{\frac{E}{E'}}.$$ (10d)

Thus, the outgoing neutron energy E' is random and *uniformly distributed* between αE and E. Once E' is known, the scattering cosine $\mu_s(E \to E')$ is uniquely specified by (10d), but the scattering azimuthal angle ω' is random and uniformly distributed on $0 \leq \omega' < 2\pi$. As depicted in ❯ *Fig. 9*, the minimum neutron energy loss is associated with the minimal change in direction of the neutron ("forward" scattering, $\mu_s = +1$), while the maximum neutron energy loss is associated with the maximum change in direction of the neutron ("backward" scattering, $\mu_s = -1$).

We now define the *macroscopic differential scattering cross section* as:

$$\Sigma_s(\boldsymbol{\Omega} \cdot \boldsymbol{\Omega}', E \to E') = \Sigma_s(E)p(\boldsymbol{\Omega} \cdot \boldsymbol{\Omega}', E \to E'),$$ (11)
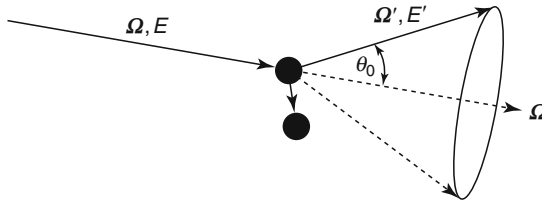
◼ **Figure 8**
Scattering angle θ_0
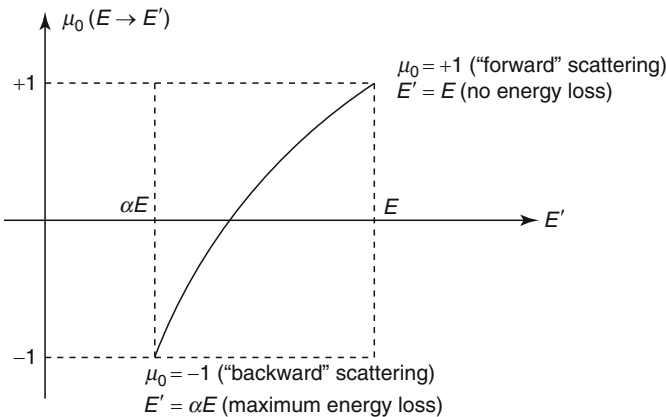
◼ **Figure 9**
Scattering cosine as a function of the outgoing energy E'

which has dimension $\text{cm}^{-1}\,\text{MeV}^{-1}$. Then:

$\Sigma_s(\mathbf{\Omega}\cdot\mathbf{\Omega}',\, E\to E')\,ds\,d\Omega'\,dE'$ = probability that a neutron, with direction $\mathbf{\Omega}$ and energy E

and traveling a distance ds, will scatter into

$d\Omega'$ about $\mathbf{\Omega}'$ and dE' about E'.   (12)

Equations (9)–11 imply:

$$\int_0^\infty \int_{4\pi} p(\mathbf{\Omega}\cdot\mathbf{\Omega}',\, E\to E')\,d\Omega'\,dE' = 1, \tag{13a}$$

$$\int_0^\infty \int_{4\pi} \Sigma_s(\mathbf{\Omega}\cdot\mathbf{\Omega}',\, E\to E')\,d\Omega'\,dE' = \Sigma_s(E). \tag{13b}$$

If a neutron with energy E initiates a fission event, the target nucleus splits into two smaller *daughter nuclei*, and on the average, $\nu(E)$ neutrons are released. Of this number, $\nu(E)[1-\beta(E)]$ are *prompt* (emitted within 10^{-15} s of the fission event) and $\nu(E)\beta(E)$ are *delayed* (emitted roughly 0.1–60 s after the fission event). Thus, the *delayed neutron fraction* $\beta(E)$ is the probability that a fission neutron, created by a neutron with energy E, is delayed ($\beta \approx 0.01$). Delayed fission neutrons are created from the radioactive decay of unstable daughter nuclei, which can be produced during fission events.

Prompt fission neutrons are born at the location of the fission event, their initial direction of flight is *isotropic* (uniformly distributed on the unit sphere), and their initial energy is consistent with the *prompt fission spectrum* $\chi_P(E')$, defined by:

$\chi_P(E')\,dE'$ = the probability that a prompt fission neutron

has energy in dE' about E'.   (14a)

This definition implies:

$$\int_0^\infty \chi_P(E)\,dE = 1. \tag{14b}$$

The unstable daughter nuclei are often grouped into six *precursor groups*, each with its own *radioactive decay constant* λ_j, *delayed fraction* $\beta_j(E)$, and *delayed neutron fission spectrum* $\chi_j(E)$, where $1 \le j \le 6$. The functions $\beta_j(E)$ satisfy:

$$\sum_{j=1}^6 \beta_j(E) = \beta(E). \tag{15}$$

To conclude this discussion, we introduce the notion of the neutron *mean free path*. Let us consider a large number (N_0) of neutrons, all emitted in the same direction of flight, with the same energy E, and from the same spatial point within a large homogeneous region. Each neutron travels along the same flight path within the system and eventually undergoes a collision with a nucleus. Let $N(s, E)$ be the number of neutrons that penetrate to depth s without experiencing a collision. Clearly, $N(s, E)$ is a decreasing function of s, starting with the initial value

$N(0, E) = N_0$. For $s > 0$ and an incremental distance $ds > 0$, the number of neutron–nucleus collisions between s and $s + ds$ is given by:

$$N(s, E) - N(s + ds, E) \approx N(s, E) - \left(N(s, E) + ds \frac{\partial N}{\partial s}(s, E) \right)$$

$$= -ds \frac{\partial N}{\partial s}(s, E). \tag{16}$$

Dividing by $N(s, E)$ and noting that the left side becomes the probability that a neutron will have a collision while traveling a distance ds, we have from (5a):

$$\frac{1}{N(s, E)} \left(-\frac{\partial N}{\partial s}(s, E) \, ds \right) = \Sigma_t(E) \, ds.$$

This relationship can be rearranged to yield the differential equation:

$$\frac{\partial N}{\partial s}(s, E) + \Sigma_t(E) N(s, E) = 0, \quad N(0, E) = N_0,$$

which has the solution:

$$N(s, E) = N_0 e^{-\Sigma_t(E)s}. \tag{17}$$

Next, defining $P(s, E)ds$ as the probability that an uncollided neutron will collide with a nucleus between s and $s + ds$, we have:

$$P(s, E)ds = \frac{\text{the number of collisions between } s \text{ and } s + ds}{\text{the initial number of neutrons (at } s = 0)}$$

$$= \frac{1}{N_0} \left(-\frac{\partial N}{\partial s}(s, E)ds \right) \qquad \text{(by [16])}$$

$$= \Sigma_t(E) e^{-\Sigma_t(E)s} ds \qquad \text{(by [17])}.$$

Thus,

$$P(s, E) = \Sigma_t(E) e^{-\Sigma_t(E)s}. \tag{18a}$$

We note that P satisfies the normalization $\int_0^\infty P(s, E)ds = \int_0^\infty \Sigma_t(E) e^{-\Sigma_t(E)s} ds = 1$, which simply states that in an infinite medium, a neutron must collide somewhere.

The probability density $P(s, E)$ can be used to obtain the mean distance-to-collision, or the *mean free path*:

$$\lambda(E) = \int_0^\infty s P(s, E)ds = \frac{1}{\Sigma_t(E)}. \tag{18b}$$

Thus, the mean free path of a neutron with energy E is equal to the inverse of the macroscopic total cross section at that energy.
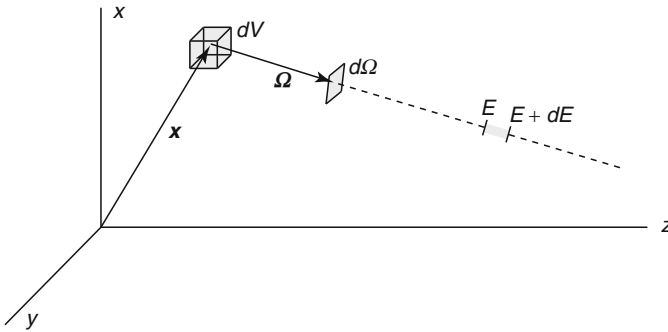
◘ Figure 10
dV about x, dΩ about Ω, and dE about E

2.3 The Angular Neutron Density and Angular Flux

We now define the physical quantities needed to describe the neutron population. We consider all neutrons that, at time t, (i) are geometrically located in a volume increment dV about a point $\boldsymbol{x}$, (ii) travel within a solid angle $d\Omega$ about the direction $\boldsymbol{\Omega}$, and (iii) have energies between E and $E + dE$ (see ❯ *Fig. 10*). The *angular neutron density* $N(\boldsymbol{x}, \boldsymbol{\Omega}, E, t)$, a function of (generally) seven independent variables, is defined by:

$$N(\boldsymbol{x}, \boldsymbol{\Omega}, E, t)\, dV d\Omega dE = \text{the number of neutrons in } dV d\Omega dE$$
$$\text{about } (\boldsymbol{x}, \boldsymbol{\Omega}, E) \text{ at time } t. \tag{19}$$

This definition implies that the value of N is independent of the increments dV, $d\Omega$, and dE. Also, N is a *phase space density*; it has the dimensions $\text{cm}^{-3}\ \text{MeV}^{-1}$.

Knowledge of $N(\boldsymbol{x}, \boldsymbol{\Omega}, E, t)$ enables one to calculate the number of neutrons that exist in any "volume" of 6-D phase space $(\boldsymbol{x}, \boldsymbol{\Omega}, E)$ at any time t. For example, for any $E_1 < E_2$ and any subregion R of the physical system V, we have:

$$\int_{E_1}^{E_2} \int_{4\pi} \int_R N(\boldsymbol{x}, \boldsymbol{\Omega}, E, t)\, dV d\Omega dE = n(t) = \text{the number of neutrons in } R,$$

$$\text{with energies between } E_1 \text{ and } E_2, \text{ at time } t.$$

Next, let us consider a planar surface area element dS, located at any point $\boldsymbol{x}$ in V, with a unit normal vector $\boldsymbol{n}$ (❯ *Fig. 11*). We consider neutrons located near $\boldsymbol{x}$, traveling in directions in $d\Omega$ about $\boldsymbol{\Omega}$, with energies in dE about E, at time t. What is the *rate* (number per second) at which these neutrons flow through dS at time t?

In the plane generated by $\boldsymbol{\Omega}$ and $\boldsymbol{n}$, and with v = neutron speed = $\sqrt{2E/m}$, we consider a volume dV obtained by sweeping dS a distance $ds = v dt$ along the direction of flight $\boldsymbol{\Omega}$ (❯ *Fig. 12*):
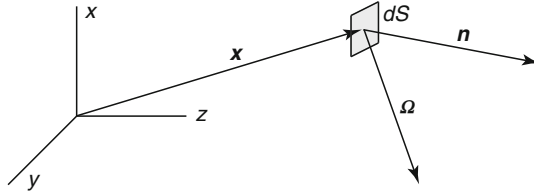
◘ Figure 11
Neutron flow through *dS*

$$\frac{d\ell}{ds} = \cos\theta = \boldsymbol{\Omega}\cdot\boldsymbol{n}$$

$$d\ell = ds\,(\boldsymbol{\Omega}\cdot\boldsymbol{n}) = vdt(\boldsymbol{\Omega}\cdot\boldsymbol{n})$$
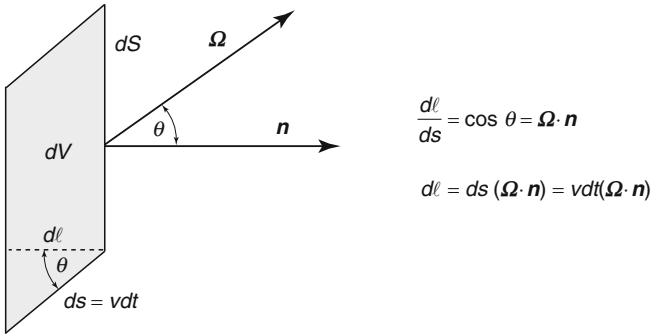
◘ Figure 12
Volume increment *dV*

In time increment dt, neutrons travel the distance $ds = vdt$. Thus, in time dt, among all neutrons traveling in $d\Omega$ about $\boldsymbol{\Omega}$ and dE about E, only those physically located in the incremental volume dV will flow through dS.

The volume of dV is:

$$dV = (dS)(d\ell) = dS(vdt)(\boldsymbol{\Omega}\cdot\boldsymbol{n}).$$

Thus, the number of neutrons located within $dVd\Omega dE$ about $(\boldsymbol{x},\boldsymbol{\Omega},E)$ is:

$$NdVd\Omega dE = NdS(vdt)(\boldsymbol{\Omega}\cdot\boldsymbol{n})d\Omega dE = [(\boldsymbol{\Omega}\cdot\boldsymbol{n})vN]dSd\Omega dEdt,$$

and this is the number of neutrons traveling in $d\Omega dE$ about $(\boldsymbol{\Omega}, E)$ that pass through dS during time dt about t. Dividing by dt, we obtain:

$$(\boldsymbol{\Omega}\cdot\boldsymbol{n})vN(\boldsymbol{x},\boldsymbol{\Omega},E,t)dSd\Omega dE = \text{ the } \textit{rate} \text{ (number per second) at which neutrons,}$$
$$\text{traveling in } d\Omega dE \text{ about } (\boldsymbol{\Omega},E),$$
$$\text{flow through } dS \text{ at time } t. \tag{20}$$

Each incremental surface dS has two normal vectors, $\boldsymbol{n}$ and $-\boldsymbol{n}$. The choice of $\boldsymbol{n}$ determines "positive" and "negative" directions of flow through dS. A positive (negative) rate indicates flow through dS in the hemisphere of directions $\boldsymbol{\Omega}\cdot\boldsymbol{n} > 0$ ($\boldsymbol{\Omega}\cdot\boldsymbol{n} < 0$). (see ◗ *Fig. 13*).
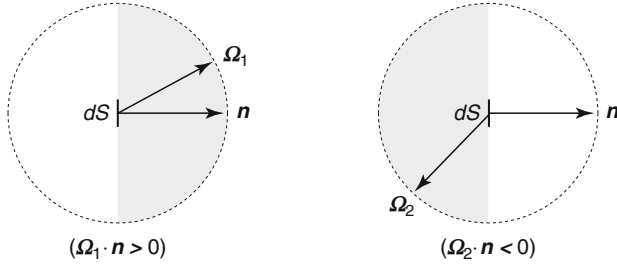
■ **Figure 13**
"Positive" and "negative" directions of neutron flow through *dS*

The *angular flux* (or *fluence rate*) $\psi(\boldsymbol{x}, \boldsymbol{\Omega}, E, t)$ is defined by:

$$\psi(\boldsymbol{x}, \boldsymbol{\Omega}, E, t) = vN(\boldsymbol{x}, \boldsymbol{\Omega}, E, t), \tag{21}$$

where $v = \sqrt{2E/m}$ is the neutron speed. The dimensions of ψ are $\text{cm}^{-2} \text{ MeV}^{-1} \text{ s}^{-1}$. A physical interpretation for ψ is obtained by considering neutrons in $dV d\Omega dE$ about $(\boldsymbol{x}, \boldsymbol{\Omega}, E)$ at time t. During a time increment dt about t,

$$\begin{aligned} \psi dV d\Omega dE dt &= v(N dV d\Omega dE)dt \\ &= (vdt)(N dV d\Omega dE) \\ &= [\text{ distance (path length) traveled by one neutron in time } dt\,] \\ &\quad \times [\text{ number of neutrons in } dV d\Omega dE \text{ about } (\boldsymbol{x}, \boldsymbol{\Omega}, E)\,] \\ &= \text{ total path length traveled by neutrons, in } dV d\Omega dE \\ &\quad \text{ about } (\boldsymbol{x}, \boldsymbol{\Omega}, E), \text{ during time increment } dt \text{ about } t. \end{aligned}$$

Dividing by dt, we obtain the following *volume-based interpretation* for ψ:

$$\begin{aligned} \psi(\boldsymbol{x}, \boldsymbol{\Omega}, E, t)dV d\Omega dE = \ &\text{rate at which path length is generated by neutrons in} \\ &dV d\Omega dE \text{ about } (\boldsymbol{x}, \boldsymbol{\Omega}, E) \text{ at time } t. \end{aligned} \tag{22}$$

(Hence, ψ is sometimes called the *path length density*.) Also, (20) implies the following *surface-based interpretation* for ψ:

$$\begin{aligned} |\boldsymbol{\Omega} \cdot \boldsymbol{n}|\psi(\boldsymbol{x}, \boldsymbol{\Omega}, E, t)dS d\Omega dE = \ &\text{the absolute rate at which neutrons, traveling in } d\Omega dE \\ &\text{about } (\boldsymbol{\Omega}, E), \text{ flow through } dS \text{ at time } t. \end{aligned} \tag{23}$$

If the surface increment dS is perpendicular to the direction of neutron travel (i.e., if $\boldsymbol{n} = \boldsymbol{\Omega}$) (❯ *Fig. 14*), then (23) reduces to:

$$\begin{aligned} \psi(\boldsymbol{x}, \boldsymbol{\Omega}, E, t)dS d\Omega dE = \ &\text{the absolute rate at which neutrons, traveling in} \\ &d\Omega dE \text{ about } (\boldsymbol{\Omega}, E), \text{ flow through a surface} \\ &\text{increment } dS \text{ perpendicular to } \boldsymbol{\Omega} \text{ at time } t. \end{aligned} \tag{24}$$
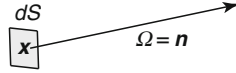
■ **Figure 14**
Neutron flow through *dS* in the direction $\Omega = n$

Equation (22) defines ψ in terms of a volume element dV, while (23) and (24) define ψ in terms of a surface element dS. Both interpretations are useful.

For example, if R is a subregion of V and $\boldsymbol{n}$ is the unit outer normal vector on ∂R, then (23) implies:

$$J_R^+(t) \equiv \int_0^\infty \int_{\partial R} \int_{\Omega \cdot n > 0} \boldsymbol{\Omega} \cdot \boldsymbol{n} \psi(\boldsymbol{x}, \boldsymbol{\Omega}, E, t) d\Omega dS dE$$

$$= \text{ the rate at which neutrons flow (leak) out of } R \text{ at time } t, \tag{25a}$$

$$J_R^-(t) \equiv \int_0^\infty \int_{\partial R} \int_{\Omega \cdot n < 0} |\boldsymbol{\Omega} \cdot \boldsymbol{n}| \psi(\boldsymbol{x}, \boldsymbol{\Omega}, E, t) d\Omega dS dE$$

$$= \text{ the rate at which neutrons flow into } R \text{ at time } t. \tag{25b}$$

Therefore,

$$J_R(t) \equiv J_R^+(t) - J_R^-(t)$$

$$= \int_0^\infty \int_{\partial R} \int_{4\pi} (\boldsymbol{\Omega} \cdot \boldsymbol{n}) \psi(\boldsymbol{x}, \boldsymbol{\Omega}, E, t) d\Omega dS dE$$

$$= \text{ the } net \text{ rate at which neutrons flow (leak) out of } R \text{ at time } t. \tag{26}$$

Using the *divergence theorem*,

$$\int_{\partial R} \boldsymbol{n} f(\boldsymbol{x}) dS = \int_R \nabla f(\boldsymbol{x}) dV, \tag{27}$$

we obtain from (26) the equivalent result:

$$J_R(t) = J_R^+(t) - J_R^-(t)$$

$$= \int_0^\infty \int_R \int_{4\pi} (\boldsymbol{\Omega} \cdot \nabla) \psi(\boldsymbol{x}, \boldsymbol{\Omega}, E, t) d\Omega dV dE$$

$$= \text{ the } net \text{ rate at which neutrons flow (leak) out of } R \text{ at time } t. \tag{28}$$

Thus, the "surface" definition (23) of ψ can be used to determine the rates at which neutrons flow across surfaces. (Equations (25) also hold for surfaces that are not closed, i.e., that do not enclose a volume.)

The "volume" definition (22) of ψ is useful because the number of collisions with nuclei that neutrons experience in an incremental time interval is proportional to the incremental distance that the neutrons travel during that time interval. Thus, *the rate at which neutrons interact with nuclei in a volume is proportional to the rate at which the neutrons generate path length in the volume.* The constants of proportionality are the macroscopic cross sections.

In addition to the neutron angular flux $\psi(x, \Omega, E, t)$, the *precursor densities* $C_j(x, t)$ for the six delayed neutron precursor groups are also required. For $1 \leq j \leq 6$ and for an incremental volume dV about x, these are defined by:

$$C_j(x, t)dV = \text{the number of group-}j \text{ precursor nuclei}$$
$$\text{in } dV \text{ about } x \text{ at time } t. \tag{29}$$

Each precursor nucleus will eventually decay and emit one delayed neutron. Thus, the rate at which group-j precursor nuclei experience radioactive decay equals the rate at which delayed neutrons are emitted by these nuclei.

2.4   Internal and Boundary Sources

In addition to the physical data described above, neutron sources must be prescribed. These exist in two categories: *internal sources* and *boundary sources*.

An internal neutron source $Q(x, E, t)$, generally produced by radioactive decay, is located inside the physical system V and is usually *isotropic* (in radioactive decay, neutrons are emitted in all directions Ω with equal probability). Q is defined by:

$$\frac{Q(x, E, t)}{4\pi} dVd\Omega dE = \text{the incremental rate at which neutrons}$$
$$\text{are produced in } dVd\Omega dE \text{ about } (x, \Omega, E)$$
$$\text{from an internal source, at time } t. \tag{30a}$$

This definition implies that the numerical value of Q is independent of dV, $d\Omega$, and dE. The factor 4π is included so that integration of (30a) over the unit sphere gives the following equivalent (for an isotropic source) definition:

$$Q(x, E, t)dVdE = \text{the incremental rate at which neutrons are}$$
$$\text{isotropically introduced into } dVdE \text{ about } (x, E)$$
$$\text{from an internal source, at time } t. \tag{30b}$$

$Q(x, E, t)$ must be specified for all points x in V, all energies E, and all times after the initial time.

Boundary sources are specified neutron fluxes that enter the physical system V through its outer boundary ∂V. V is usually assumed to be convex; then neutrons leaking out of V cannot reenter through ∂V. The boundary angular flux $\psi^b(x, \Omega, E, t)$ is an external source, independent of the flux within the system, which must be specified for: (i) all points on the outer boundary of the system ($x \in \partial V$), (ii) all directions of flight pointing into the system ($\Omega \cdot n < 0$, where n is the unit outer normal vector at $x \in \partial V$), (iii) all energies, and (iv) all times after the initial time. The angular flux is required to satisfy:

$$\psi(x, \Omega, E, t) = \psi^b(x, \Omega, E, t), \quad x \in \partial V, \;\; \Omega \cdot n < 0, \;\; 0 < E < \infty, \;\; 0 < t. \tag{31}$$

If $\psi^b = 0$, ∂V is called a *vacuum boundary* (⬥ *Fig. 15*).
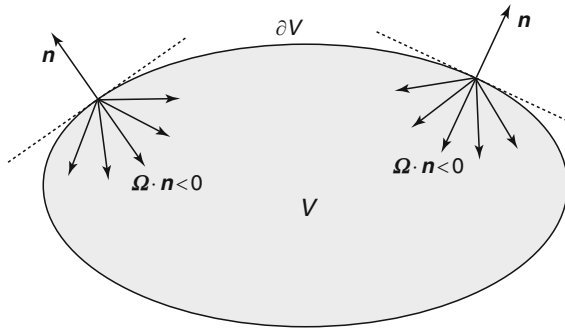
Figure 15
Incident directions of flight on ∂V

The internal and boundary neutron sources are specified and independent of the neutron distribution within V. Generally, neutron transport problems are *driven* by these known sources, which generate the "original" neutrons in the problem. After neutrons are introduced into V by the internal or boundary sources, they "transport" within V according to the physical processes of streaming, absorption, scattering, and fission, discussed above.

In nuclear reactor problems, the term *fission source* describes the neutrons that are produced by fission events in V. This "source" directly depends on ψ and must be calculated. Likewise, the *scattering source* of neutrons emitted from scattering events also directly depends on ψ and must be calculated. (Thus, the term "source" sometimes describes a quantity that depends on ψ.) However, to repeat, the *internal* and *boundary* sources are independent of ψ and must be specified.

2.5 The Time-Dependent Equations of Neutron Transport

Next, we derive seven mathematical equations that determine the neutron angular flux $\psi(\mathbf{x}, \mathbf{\Omega}, E, t)$ and the six neutron precursor densities $C_j(\mathbf{x}, t)$. Each of these seven equations is a *conservation equation* – each is based on the simple physical concept that the rate of change (of neutrons and precursor densities within increments of phase space) equals the rate of gain minus the rate of loss.

We first consider the incremental population of neutrons within $dVd\Omega dE$ about $(\mathbf{x}, \mathbf{\Omega}, E)$ at time t. By (19), the number of these neutrons is:

$$dN = N(\mathbf{x}, \mathbf{\Omega}, E, t)dVd\Omega dE = \frac{1}{v}\psi(\mathbf{x}, \mathbf{\Omega}, E, t)dVd\Omega dE.$$

Thus, the time rate of change of dN is:

$$\frac{\partial N}{\partial t} = \frac{1}{v}\frac{\partial \psi}{\partial t}(\mathbf{x}, \mathbf{\Omega}, E, t)dVd\Omega dE$$
$$= \text{(rate of gain)} - \text{(rate of loss)}. \tag{32a}$$

From our discussion of neutron physics, we have:

$$\text{Rate of loss} = (\text{collision rate} + \text{net leakage rate})$$
$$\text{in } dV d\Omega dE \text{ about } (x, \Omega, E) \text{ at time } t, \tag{32b}$$

and:

$$\text{Rate of gain} = (\text{in-scattering rate} + \text{prompt fission rate} + \text{delayed fission rate}$$
$$+ \text{ source rate}) \text{ in } dV d\Omega dE \text{ about } (x, \Omega, E) \text{ at time } t. \tag{32c}$$

First, we consider the "loss" terms in (32a) and (32b). From (5a) and (19) we have, using $v = ds/dt$, for neutrons in $dV d\Omega dE$ about (x, Ω, E):

$$
\begin{aligned}
\Sigma_t(E)\psi(x, \Omega, E, t)dV d\Omega dE &= \Sigma_t(E)\frac{ds}{dt}N(x, \Omega, E, t)dV d\Omega dE \\
&= \frac{1}{dt}\big[\Sigma_t(E)ds\big]\big[N(x, \Omega, E, t)dV d\Omega dE\big] \\
&= \frac{1}{dt}\big[\text{the probability that a (single) neutron with energy } E \\
&\qquad \text{will undergo a collision in time interval } dt\big] \\
&\qquad \times \big[\text{the number of neutrons in } dV d\Omega dE \text{ about} \\
&\qquad\quad (x, \Omega, E, t) \text{ at time } t\big] \\
&= \frac{1}{dt}\big[\text{the number of collisions in } dV d\Omega dE \text{ about } (x, \Omega, E) \\
&\qquad \text{in time interval } dt \text{ about } t\big] \\
&= \text{Collision rate} \quad (\text{in [32b]}). \tag{33a}
\end{aligned}
$$

Also, in (28), we let R shrink to an incremental volume dV and directly get:

$$\Omega \cdot \nabla\psi(x, \Omega, E, t)dV d\Omega dE = \text{ Net leakage rate} \quad (\text{in [32b]}). \tag{33b}$$

Introducing (33) into (32b), we obtain:

$$\text{Rate of loss} = \big[\Sigma_t(E)\psi(x, \Omega, E, t) + \Omega \cdot \nabla\psi(x, \Omega, E, t)\big]dV d\Omega dE. \tag{34}$$

The derivation of (33b) relies on the use of the divergence theorem (27) to convert a surface integral into a volume integral. A more physically intuitive understanding of (33b) can be obtained by considering dV to be a special cylindrical volume. Specifically, let us consider neutrons in $dV d\Omega dE$ about (x, Ω, E), where dV is an incremental cylindrical volume of length ds and cross-sectional area dA, centered at x and oriented in the direction Ω, as depicted in ▶ *Fig. 16*.
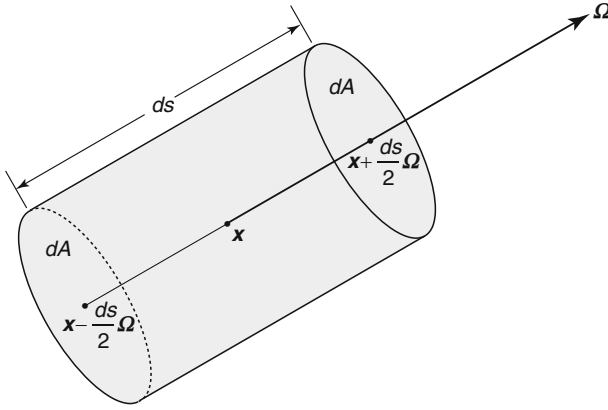
◘ Figure 16
Cylindrical incremental volume *dV*

Then $dV = dsdA$, and neutrons in $d\Omega dE$ about (Ω, E) flow into dV through the surface dA at $x - (ds/2)\Omega$, and flow out of dV through the surface dA at $x + (ds/2)\Omega$. Hence, by (24), we have:

Net rate at which neutrons in $d\Omega dE$ about (Ω, E) leak out of dV

$$
= \left[\psi\left(x + \frac{ds}{2}\Omega, E\right) - \psi\left(x - \frac{ds}{2}\Omega, E\right)\right] dA d\Omega dE
$$

$$
= \left[\frac{\psi\left(x + \frac{ds}{2}\Omega, E\right) - \psi\left(x - \frac{ds}{2}\Omega, E\right)}{ds}\right] dV d\Omega dE
$$

$$
= \left[\Omega \cdot \nabla \psi(x, \Omega, E)\right] dV d\Omega dE. \tag{35}
$$

Next, we consider the "gain" terms in (32a) and (32c). From (12) and (19), we have for neutrons in $dV d\Omega' dE'$ about (x, Ω', E'):

$$
\Sigma_s(\Omega' \cdot \Omega, E' \to E)\psi(x, \Omega', E', t)dV d\Omega' dE' d\Omega dE
$$

$$
= \Sigma_s(\Omega' \cdot \Omega, E' \to E)\frac{ds}{dt}N(x, \Omega', E', t)dV d\Omega' dE' d\Omega dE
$$

$$
= \frac{1}{dt}\left[N(x, \Omega', E', t)dV d\Omega' dE'\right]\left[\Sigma_s(\Omega' \cdot \Omega, E' \to E)ds d\Omega dE\right]
$$

$$
= \frac{1}{dt}\left[\text{ the number of neutrons in } dV d\Omega' dE' \text{ about } (x, \Omega', E') \text{ at time } t \right]
$$

$$
\times \left[\text{ the probability that one of these neutrons will scatter into }\right.
$$

$$
\left. d\Omega dE \text{ about } (\Omega, E) \text{ during time interval } dt \right]
$$

$$
= \frac{1}{dt}\left[\text{ the number of neutrons in } dV \text{ about } x \text{ that scatter from }\right.
$$

$$
d\Omega' dE' \text{ about } (\Omega', E') \text{ into } d\Omega dE \text{ about } (\Omega, E)
$$

$$
\left. \text{during time interval } dt \text{ about } t \right]
$$

=the rate at which neutrons in dV about x scatter from $d\Omega'dE'$

= the rate at which neutrons in dV about x scatter from $d\Omega'dE'$

about (Ω', E') into $d\Omega dE$ about (Ω, E) at time t.

Integrating this expression over all initial directions Ω' and energies E', we obtain:

$$\left[\int_0^\infty \int_{4\pi} \Sigma_s(\Omega' \cdot \Omega, E' \to E)\psi(x, \Omega', E', t)d\Omega'dE'\right]dVd\Omega dE$$

$\qquad\qquad$ = the rate at which neutrons in dV about x scatter

$\qquad\qquad\quad$ into $d\Omega dE$ about (Ω, E) at time t

$\qquad\qquad$ = In-scattering rate   (in [32c]) .   (36a)

Similarly, the rate at which prompt fission neutrons are produced in $dVd\Omega'dE'$ about (x, Ω', E') is given by:

$$\left[1 - \beta(E')\right]\nu(E')\Sigma_f(E')\psi(x, \Omega', E', t)dVd\Omega'dE'.$$

Integrating this expression over all initial directions Ω' and energies E', and multiplying by $[\chi_P(E)/4\pi]d\Omega dE$, we obtain:

$$\left[\frac{\chi_P(E)}{4\pi}\int_0^\infty \int_{4\pi}\left[1 - \beta(E')\right]\nu(E')\Sigma_f(E')\psi(x, \Omega', E', t)d\Omega'dE'\right]dVd\Omega dE$$

$\qquad\qquad$ = the rate at which prompt fission neutrons are

$\qquad\qquad\quad$ produced in $dVd\Omega dE$ about (x, Ω, E) at time t.   (36b)

Also,

$$\sum_{j=1}^6 \frac{\chi_j(E)}{4\pi}\lambda_j C_j(x, t)dVd\Omega dE = \text{ the rate at which delayed neutrons}$$

$\qquad\qquad\qquad\qquad\qquad\qquad\quad$ are emitted into $dVd\Omega dE$

$\qquad\qquad\qquad\qquad\qquad\qquad\quad$ about (x, Ω, E) at time t.   (36c)

Finally, by (30a), we have:

$$\frac{Q(x, E, t)}{4\pi}dVd\Omega dE = \text{ source rate} \quad \text{(in [32c]).} \qquad\qquad\qquad (37)$$

Introducing (36) and (37) into (32c), we obtain:

$$\text{Rate of gain } = \left[\int_0^\infty \int_{4\pi} \Sigma_s(\Omega' \cdot \Omega, E' \to E)\psi(x, \Omega', E', t)d\Omega'dE'\right.$$

$$+ \frac{\chi_P(E)}{4\pi}\int_0^\infty \int_{4\pi}\left[1 - \beta(E')\right]\nu\Sigma_f(E')\psi(x, \Omega', E', t)d\Omega'dE'$$

$$\left. + \frac{1}{4\pi}\sum_{j=1}^6 \chi_j(E)\lambda_j C_j(x, t) + \frac{1}{4\pi}Q(x, E, t)\right]dVd\Omega dE. \qquad (38)$$

Introducing the rate of loss terms (34) and the rate of gain terms (38) into the general conservation equation (32a), we get:

$$\frac{1}{v}\frac{\partial\psi}{\partial t}dVd\Omega dE = \left[\int_0^\infty \int_{4\pi}\Sigma_s\psi d\Omega' dE' + \frac{\chi_p}{4\pi}\int_0^\infty \int_{4\pi}[1-\beta]v\Sigma_f\psi d\Omega' dE' \right.$$
$$\left. + \frac{1}{4\pi}\sum_{j=1}^6 \chi_j\lambda_j C_j + \frac{1}{4\pi}Q \right]dVd\Omega dE - \left[\Sigma_t\psi + \Omega\cdot\nabla\psi\right]dVd\Omega dE.$$

Dividing by $dVd\Omega dE$ and rearranging, we obtain the following first-order *integro-differential* equation:

$$\frac{1}{v}\frac{\partial\psi}{\partial t}(x,\Omega,E,t) + \Omega\cdot\nabla\psi(x,\Omega,E,t) + \Sigma_t(E)\psi(x,\Omega,E,t)$$
$$= \int_0^\infty \int_{4\pi}\Sigma_s(\Omega'\cdot\Omega, E'\rightarrow E)\psi(x,\Omega',E',t)d\Omega' dE'$$
$$+ \frac{\chi_p(E)}{4\pi}\int_0^\infty \int_{4\pi}[1-\beta(E')]v\Sigma_f(E')\psi(x,\Omega',E',t)d\Omega' dE'$$
$$+ \frac{1}{4\pi}\sum_{j=1}^6 \chi_j(E)\lambda_j C_j(x,t) + \frac{1}{4\pi}Q(x,E,t). \tag{39}$$

This is the *time-dependent neutron transport equation (with delayed neutron precursors)*, also called the *linear Boltzmann equation*. The derivation of this equation shows that each of its terms describes a specific physical process that causes a gain or loss of neutrons in each increment of phase space.

We must also derive an equation for each precursor density. The time rate of change of the species-j precursor density may be expressed as:

$$\frac{\partial C_j}{\partial t}(x,t)dV = \text{the rate of change of the number of group-}j$$
$$\text{precursor nuclei in } dV \text{ about } x \text{ at time } t$$
$$= (\text{Rate of gain}) - (\text{rate of loss}). \tag{40}$$

The rate of loss (due to decay) of these precursors is given by:

$$\lambda_j C_j(x,t)dV = \text{the rate at which group-}j \text{ precursor nuclei undergo}$$
$$\text{radioactive decay in } dV \text{ about } x \text{ at time } t. \tag{41}$$

On the other hand,

$$\beta_j(E')v\Sigma_f(E')\psi(x,\Omega',E',t)dVd\Omega' dE'$$
$$= \text{the rate at which group-}j \text{ precursor nuclei are produced}$$
$$\text{by neutrons in } dVd\Omega' dE' \text{ about } (x,\Omega',E') \text{ at time } t.$$

Integrating over $\boldsymbol{\Omega}'$ and E', we get the total rate of gain of the group-j precursor nuclei:

$$\left[\int_0^\infty \int_{4\pi} \beta_j(E') v \Sigma_f(E') \psi(\boldsymbol{x}, \boldsymbol{\Omega}', E', t) d\Omega' dE' \right] dV$$

$$= \text{the rate at which group-}j \text{ precursor nuclei}$$

$$\text{are produced in } dV \text{ about } \boldsymbol{x} \text{ at time } t. \qquad (42)$$

After some rearrangement, (40–42) give for $1 \leq j \leq 6$ the following equations for the precursor densities:

$$\frac{\partial C_j}{\partial t}(\boldsymbol{x}, t) + \lambda_j C_j(\boldsymbol{x}, t) = \int_0^\infty \int_{4\pi} \beta_j(E') v \Sigma_f(E') \psi(\boldsymbol{x}, \boldsymbol{\Omega}', E', t) d\Omega' dE'. \qquad (43)$$

As with the transport equation, each term in these equations describes a physical process that causes a gain or loss of group-j neutron precursor nuclei.

Equation (43) must be solved jointly with the neutron transport equation (39). In addition, ψ must satisfy the boundary condition:

$$\psi(\boldsymbol{x}, \boldsymbol{\Omega}, E, t) = \psi^b(\boldsymbol{x}, \boldsymbol{\Omega}, E, t), \quad \boldsymbol{x} \in \partial V, \quad \boldsymbol{\Omega} \cdot \boldsymbol{n} < 0, \quad 0 < E < \infty, \quad 0 < t, \qquad (44)$$

and ψ and C_j must satisfy the initial conditions:

$$\psi(\boldsymbol{x}, \boldsymbol{\Omega}, E, 0) = \psi^i(\boldsymbol{x}, \boldsymbol{\Omega}, E), \quad \boldsymbol{x} \in V, \quad \boldsymbol{\Omega} \in 4\pi, \quad 0 < E < \infty, \qquad (45a)$$

$$C_j(\boldsymbol{x}, 0) = C_j^i(\boldsymbol{x}), \quad \boldsymbol{x} \in V, \qquad (45b)$$

where ψ^b, ψ^i, and C_j^i are specified.

In full generality, the neutron angular flux $\psi(\boldsymbol{x}, \boldsymbol{\Omega}, E, t)$ and the precursor densities $C_j(\boldsymbol{x}, t)$ are obtained by solving (39) and (43), subject to the boundary condition stated in (44) and the initial conditions stated in (45). The subject of *nuclear reactor kinetics* is based on this system of equations.

2.6   Time-Dependent Neutron Transport Without Delayed Neutrons

In some time-dependent problems, the relatively small value of β (≈ 0.01) justifies the neglect of the delayed neutron terms. In such problems one can set $\beta_j = C_j = 0$ in (39). The resulting single transport equation for ψ:

$$\frac{1}{v} \frac{\partial \psi}{\partial t}(\boldsymbol{x}, \boldsymbol{\Omega}, E, t) + \boldsymbol{\Omega} \cdot \nabla \psi(\boldsymbol{x}, \boldsymbol{\Omega}, E, t) + \Sigma_t(E) \psi(\boldsymbol{x}, \boldsymbol{\Omega}, E, t)$$

$$= \int_0^\infty \int_{4\pi} \Sigma_s(\boldsymbol{\Omega}' \cdot \boldsymbol{\Omega}, E' \to E) \psi(\boldsymbol{x}, \boldsymbol{\Omega}', E', t) \, d\Omega' dE'$$

$$+ \frac{\chi_p(E)}{4\pi} \int_0^\infty \int_{4\pi} v \Sigma_f(E') \psi(\boldsymbol{x}, \boldsymbol{\Omega}', E', t) \, d\Omega' dE' + \frac{1}{4\pi} Q(\boldsymbol{x}, E, t), \qquad (46a)$$

is solved subject to the boundary condition (44) and initial condition (45a):

$$\psi(\boldsymbol{x}, \boldsymbol{\Omega}, E, t) = \psi^b(\boldsymbol{x}, \boldsymbol{\Omega}, E, t), \quad \boldsymbol{x} \in \partial V, \quad \boldsymbol{\Omega} \cdot \boldsymbol{n} < 0, \quad 0 < E < \infty, \quad 0 < t, \tag{46b}$$

$$\psi(\boldsymbol{x}, \boldsymbol{\Omega}, E, 0) = \psi^i(\boldsymbol{x}, \boldsymbol{\Omega}, E), \quad \boldsymbol{x} \in V, \quad \boldsymbol{\Omega} \in 4\pi, \quad 0 < E < \infty. \tag{46c}$$

2.7   The Steady-State Neutron Transport Equation

In steady-state problems, the precursor densities can be eliminated to obtain a single equation for ψ. Setting $\partial C_j / \partial t = 0$, in (43), we get:

$$\lambda_j C_j(\boldsymbol{x}) = \int_0^\infty \int_{4\pi} \beta_j(E') \nu \Sigma_f(E') \psi(\boldsymbol{x}, \boldsymbol{\Omega}', E') \, d\Omega' dE',$$

and introducing these expressions into the steady-state equation (39), we obtain:

$$\begin{aligned}
\boldsymbol{\Omega} \cdot &\nabla \psi(\boldsymbol{x}, \boldsymbol{\Omega}, E) + \Sigma_t(E) \psi(\boldsymbol{x}, \boldsymbol{\Omega}, E) \\
&= \int_0^\infty \int_{4\pi} \Sigma_s(\boldsymbol{\Omega}' \cdot \boldsymbol{\Omega}, E' \to E) \psi(\boldsymbol{x}, \boldsymbol{\Omega}', E') d\Omega' dE' \\
&\quad + \frac{\chi_p(E)}{4\pi} \int_0^\infty \int_{4\pi} [1 - \beta(E')] \nu \Sigma_f(E') \psi(\boldsymbol{x}, \boldsymbol{\Omega}', E') d\Omega' dE' \\
&\quad + \frac{1}{4\pi} \sum_{j=1}^6 \chi_j(E) \int_0^\infty \int_{4\pi} \beta_j(E') \nu \Sigma_f(E') \psi(\boldsymbol{x}, \boldsymbol{\Omega}', E') d\Omega' dE' + \frac{1}{4\pi} Q(\boldsymbol{x}, E).
\end{aligned} \tag{47}$$

Since $\beta = \sum \beta_j \approx 0.01$, it is often acceptable to set $\beta_j = 0$. In this case, (47) simplifies to:

$$\begin{aligned}
\boldsymbol{\Omega} \cdot &\nabla \psi(\boldsymbol{x}, \boldsymbol{\Omega}, E) + \Sigma_t(E) \psi(\boldsymbol{x}, \boldsymbol{\Omega}, E) \\
&= \int_0^\infty \int_{4\pi} \Sigma_s(\boldsymbol{\Omega}' \cdot \boldsymbol{\Omega}, E' \to E) \psi(\boldsymbol{x}, \boldsymbol{\Omega}', E') d\Omega' dE' \\
&\quad + \frac{\chi_p(E)}{4\pi} \int_0^\infty \int_{4\pi} \nu \Sigma_f(E') \psi(\boldsymbol{x}, \boldsymbol{\Omega}', E') d\Omega' dE' \\
&\quad + \frac{1}{4\pi} Q(\boldsymbol{x}, E), \quad \boldsymbol{x} \in V, \quad \boldsymbol{\Omega} \in 4\pi, \quad 0 < E < \infty.
\end{aligned} \tag{48a}$$

The first term on the right side of this equation is often called the *scattering source*. The second term is the *fission source*; this is isotropic and *separable* in space and energy – it is the product of a (known) function of energy and an (unknown) function only of space. (This separable form of the fission source is useful in developing strategies to solve [48a].) The third term is the specified *internal source*.

Equation (48a) must be solved subject to the steady-state boundary condition:

$$\psi(\boldsymbol{x}, \boldsymbol{\Omega}, E) = \psi^b(\boldsymbol{x}, \boldsymbol{\Omega}, E), \quad \boldsymbol{x} \in \partial V, \quad \boldsymbol{\Omega} \cdot \boldsymbol{n} < 0, \quad 0 < E < \infty, \tag{48b}$$

which is obtained from (44). As before, if the specified incident boundary flux $\psi^b = 0$, then ∂V is called a *vacuum boundary*.

2.8 *k*-Eigenvalue Problems

In steady-state reactor calculations, one often sees the following version of (48) in which the inhomogeneous source Q and the boundary source ψ^b are set to zero, and the fission source is modified by a constant factor $1/k$:

$$\boldsymbol{\Omega} \cdot \nabla \psi(\boldsymbol{x}, \boldsymbol{\Omega}, E) + \Sigma_t(E)\psi(\boldsymbol{x}, \boldsymbol{\Omega}, E) = \int_0^\infty \int_{4\pi} \Sigma_s(\boldsymbol{\Omega}' \cdot \boldsymbol{\Omega}, E' \to E)\psi(\boldsymbol{x}, \boldsymbol{\Omega}', E')d\boldsymbol{\Omega}'dE'$$

$$+ \frac{\chi_p(E)}{4\pi k} \int_0^\infty \int_{4\pi} \nu\Sigma_f(E')\psi(\boldsymbol{x}, \boldsymbol{\Omega}', E')d\boldsymbol{\Omega}'dE',$$

$$\boldsymbol{x} \in V, \ \boldsymbol{\Omega} \in 4\pi, \ 0 < E < \infty, \tag{49a}$$

$$\psi(\boldsymbol{x}, \boldsymbol{\Omega}, E) = 0, \ \ \boldsymbol{x} \in \partial V, \ \boldsymbol{\Omega} \cdot \boldsymbol{n} < 0, \ 0 < E < \infty. \tag{49b}$$

These equations always have the zero solution: $\psi = 0$. The goal is to find the *largest* value of k such that a nonzero solution ψ exists. This k is called the *criticality* (or *criticality eigenvalue*) of the system V; the corresponding ψ is called the *eigenfunction* or *fundamental mode*.

If a system V has a fissile region, then it can be shown that the criticality eigenvalue k always exists, and the corresponding eigenfunction ψ is unique (up to a multiplicative constant) and positive. (If V has no fissile region, then we adopt the convention that $k = 0$.)

The motivation for defining k in the above manner is as follows. In any system V with fission, neutrons are lost due to capture and leakage, and are produced by fission. If the production of neutrons due to fission exactly balances the loss of neutrons due to capture and leakage, then a nonzero, steady-state neutron flux is possible. (This concept underlies a steady-state power reactor.) By adjusting the magnitude of the fission source through the eigenvalue k, one can make this exact balance occur. If $k < 1$, the fission source must be increased for a steady-state solution to exist; this implies that capture and leakage dominate fission, and the reactor is *sub-critical*. If $k > 1$, the fission source must be decreased for a steady-state solution to exist; this implies that fission dominates capture and leakage, and the reactor is *supercritical*. If $k = 1$, capture and leakage exactly balance fission, and the reactor is *critical*. The calculation of k for differing reactor configurations is one of the most important and ubiquitous calculations in the design and operation of nuclear reactors.

In some problems (in particular, the field of reactor kinetics), the criticality k is replaced by the *reactivity* ρ, defined by

$$\frac{1}{k} = 1 - \rho. \tag{50}$$

A reactor is subcritical if $\rho < 0$, critical if $\rho = 0$, and supercritical if $\rho > 0$.

2.9 The Monoenergetic Neutron Transport Equation

A common simplifying assumption is to ignore energy dependence altogether, giving the so-called *one-speed* or *monoenergetic* form of the transport equation. Despite an apparently drastic approximation of the physics, this equation has been, and continues to be, the subject of much investigation, for several reasons. Under certain circumstances, the absence of the energy variable promotes a rigorous mathematical analysis of the transport equation, in

particular the establishment of existence, uniqueness, and completeness theorems for elementary solutions of the transport equation. Also, in special geometries, it is sometimes possible to construct analytic solutions to the one-speed transport equation. These solutions serve as benchmarks against which approximation methods and numerical solution techniques can be evaluated, and they provide insight into the nature of the transport process. In addition, in the widely used *multigroup* treatment of the energy variable in numerical work, the group-wise equations for the group-averaged angular fluxes are of one-speed form. Neutron transfers into a given energy group from all other groups appear only as sources in that group. Thus, methods developed for the solution of the one-speed transport equation can be applicable even when the energy variable is retained.

The monoenergetic transport equation can be derived from first principles, as we did above for the energy-dependent case, but with the one-speed assumption introduced at the outset. Alternatively, the energy-dependent transport equation (48a), in the steady-state case, can be manipulated to obtain the same result. We do this next.

The restriction of (48a) to single-energy neutrons requires the following assumptions:

1. The angular deflection of neutrons during scattering occurs without energy loss. In this case the differential cross section given in (11) can be expressed as:

$$\Sigma_s(\boldsymbol{\Omega} \cdot \boldsymbol{\Omega}', E \to E') = \Sigma_s(E', \boldsymbol{\Omega} \cdot \boldsymbol{\Omega}')\delta(E' - E). \tag{51a}$$

2. The internal and boundary sources are monoenergetic at some characteristic energy E_0:

$$Q(\boldsymbol{x}, E) = Q(\boldsymbol{x})\,\delta(E - E_0), \tag{51b}$$

$$\psi^b(\boldsymbol{x}, \boldsymbol{\Omega}, E) = \psi^b(\boldsymbol{x}, \boldsymbol{\Omega})\,\delta(E - E_0). \tag{51c}$$

3. All fission neutrons are born at the charateristic energy E_0:

$$\chi_P(E) = \delta(E - E_0). \tag{51d}$$

Then, since all neutrons are "born" with energy E_0 and cannot change their energy through scattering, the angular flux must contain only neutrons with energy E_0:

$$\psi(\boldsymbol{x}, \boldsymbol{\Omega}, E) = \psi(\boldsymbol{x}, \boldsymbol{\Omega})\,\delta(E - E_0). \tag{52}$$

Introducing (51–52) into (48a), we find that $\psi(\boldsymbol{x}, \boldsymbol{\Omega})$ satisfies the following energy-independent equation:

$$\boldsymbol{\Omega} \cdot \nabla\psi(\boldsymbol{x}, \boldsymbol{\Omega}) + \Sigma_t(E_0)\psi(\boldsymbol{x}, \boldsymbol{\Omega}) = \int_{4\pi} \Sigma_s(E_0, \boldsymbol{\Omega}' \cdot \boldsymbol{\Omega})\psi(\boldsymbol{x}, \boldsymbol{\Omega}')d\Omega'$$
$$+ \frac{\nu\Sigma_f(E_0)}{4\pi} \int_{4\pi} \psi(\boldsymbol{x}, \boldsymbol{\Omega}')d\Omega' + \frac{Q(\boldsymbol{x})}{4\pi}, \quad \boldsymbol{x} \in V, \ \boldsymbol{\Omega} \in 4\pi, \tag{53}$$

with boundary condition:

$$\psi(\boldsymbol{x}, \boldsymbol{\Omega}) = \psi^b(\boldsymbol{x}, \boldsymbol{\Omega}), \quad \boldsymbol{x} \in \partial V, \ \boldsymbol{\Omega} \cdot \boldsymbol{n} < 0. \tag{54}$$

The energy variable appears here only as a parameter, serving to fix the numerical values of the scattering, fission, and total cross section.

Further simplification ensues when scattering is isotropic in the laboratory frame, for then the differential cross section in (53) can be written as:

$$\Sigma_s(E_0, \boldsymbol{\Omega}' \cdot \boldsymbol{\Omega}) \equiv \Sigma_s(E_0)p(E_0, \boldsymbol{\Omega}' \cdot \boldsymbol{\Omega}) = \frac{\Sigma_s(E_0)}{4\pi}, \tag{55}$$

and (53) becomes:

$$\boldsymbol{\Omega} \cdot \nabla \psi(\boldsymbol{x}, \boldsymbol{\Omega}) + \Sigma_t \psi(\boldsymbol{x}, \boldsymbol{\Omega}) = \frac{(\Sigma_s + \nu \Sigma_f)}{4\pi} \int_{4\pi} \psi(\boldsymbol{x}, \boldsymbol{\Omega}') d\Omega' + \frac{Q(\boldsymbol{x})}{4\pi}. \tag{56}$$

Finally, when the system is *homogeneous* (the cross sections are independent of $\boldsymbol{x}$) and the dimensionless *optical depth* variable is introduced:

$$\boldsymbol{\tau} = \boldsymbol{x} \, \Sigma_t, \tag{57}$$

then distance becomes measured in units of mean free paths and (56) assumes the following simpler form:

$$\boldsymbol{\Omega} \cdot \nabla \psi(\boldsymbol{\tau}, \boldsymbol{\Omega}) + \psi(\boldsymbol{\tau}, \boldsymbol{\Omega}) = \frac{c}{4\pi} \int_{4\pi} \psi(\boldsymbol{\tau}, \boldsymbol{\Omega}') d\Omega' + \frac{Q_0(\boldsymbol{\tau})}{4\pi}. \tag{58}$$

Here, $Q_0 = Q/\Sigma_t$ and c is the *mean number of secondary neutrons produced per collision*:

$$c = \frac{(\Sigma_s + \nu \Sigma_f)}{\Sigma_t}. \tag{59}$$

If $\nu \sigma_f = 0$, then $c = \Sigma_s/\Sigma_t$ is also called the *scattering ratio*.

Monoenergetic eigenvalue problems can be formulated by setting $\psi^b = 0$ in (54), $Q = 0$ in (56), and letting c be the eigenvalue. The k-eigenvalue is then given in terms of this eigenvalue, or *critical value of c*, by:

$$k = \frac{\nu \Sigma_f}{c \Sigma_t - \Sigma_s}.$$

2.10   Mathematical Issues

Next, we briefly discuss some fundamental (mathematical) questions. Specifically:

1. Do solutions $\psi(\boldsymbol{x}, \boldsymbol{\Omega}, E, t)$ and $C_j(\boldsymbol{x}, t)$ of the neutron transport equations exist?
2. Are the solutions unique?
3. Are the solutions nonnegative (as they should be, physically)?
4. What can be said about the *smoothness* of these solutions?

In our discussion of these questions, we make a few basic and practically relevant assumptions: the physical system V is specified and finite and has at most a finite number of subregions, each having its own material cross sections. (The cross sections are histogram functions of $\boldsymbol{x}$.) The prescribed internal source, the prescribed incident boundary fluxes, and the prescribed

neutron flux and precursor densities at the initial time ($t = 0$) are all specified and nonnegative. The eigenvalue k of V has been calculated (see ❯ sect. 2.5.4), and V is either subcritical ($0 \leq k < 1$), critical ($k = 1$), or supercritical ($k > 1$). In the following, we attempt to state the basic results with a minimum of mathematical detail.

2.10.1 Existence, Uniqueness, and Nonnegativity of Transport Solutions

Briefly, each time-dependent neutron transport problem, with or without precursor densities, *always* has a unique nonnegative solution. Steady-state neutron transport problems (in which precursor densities are neglected) do not always have a unique nonnegative solution, but when they do not, there is a physical explanation. (A classic theoretical discussion of the existence of solutions of time-dependent transport problems is given in Case and Zweifel (1967).)

To discuss the connection between solutions of time-dependent and steady-state neutron transport problems, we consider time-dependent and steady-state problems without precursor densities in which the internal source and the prescribed incident boundary fluxes are nonnegative and independent of t. We then have:

1. If V is subcritical ($k < 1$), the time-dependent neutron flux limits as $t \to \infty$ to a steady-state neutron flux, which is the (unique, nonnegative) solution of the steady-state neutron transport problem.
2. If V is critical ($k = 1$) and the internal source and prescribed incident boundary fluxes are *nonzero*, the time-dependent neutron flux grows linearly in t as $t \to \infty$. In this situation, no limiting ($t \to \infty$) steady-state solution of the time-dependent problem exists, and no solution of the corresponding steady-state neutron transport problem exists.

   However, if the internal source and prescribed incident boundary fluxes are *zero*, then the time-dependent neutron flux limits as $t \to \infty$ to a steady-state neutron flux of the form:

$$\psi(\boldsymbol{x}, \boldsymbol{\Omega}, E, t) \approx C\Psi(\boldsymbol{x}, \boldsymbol{\Omega}, E) \quad \text{for} \quad t \approx \infty, \tag{60}$$

   where Ψ is the k-eigenfunction for the critical system and C is a constant that depends on the initial condition ψ^i of the time-dependent problem. In this situation, the steady-state neutron transport problem has an infinite number of solutions, all given by (60), with the constant C arbitrary.
3. If V is supercritical ($k > 1$), the time-dependent neutron flux grows exponentially in t as $t \to \infty$. If the internal source and prescribed incident boundary fluxes are nonzero, the corresponding steady-state neutron transport problem either has a unique nonpositive solution, or no solution exists.

   If the internal source and prescribed incident boundary fluxes are *zero*, then the steady-state neutron transport problem will either have the solution $\psi = 0$, or an infinite number of solutions of the form of (60), where Ψ is now some other (than the $k = 1$) eigenfunction of the system; this eigenfunction is nonpositive (nonphysical).

In all cases, a unique, positive solution of the time-dependent neutron transport problem exists. Also, a positive solution of the steady-state neutron transport problem exists if and only if the solution of a corresponding time-dependent problem has a steady-state limit as $t \to \infty$; and if the steady-state limit of the time-dependent problem does exist, it *is* a solution of the steady-state problem. Some of these issues are discussed in Case and Zweifel (1967).

2.10.2   The *n*th Collided Fluxes

The solution of source-driven neutron transport problems can be written in an advantageous way. To illustrate, let us consider the following monoenergetic steady-state problem with isotropic scattering:

$$\boldsymbol{\Omega} \cdot \nabla \psi(\boldsymbol{x}, \boldsymbol{\Omega}) + \Sigma_t(\boldsymbol{x}) \psi(\boldsymbol{x}, \boldsymbol{\Omega}) = \frac{\Sigma_s(\boldsymbol{x})}{4\pi} \int_{4\pi} \psi(\boldsymbol{x}, \boldsymbol{\Omega}') d\boldsymbol{\Omega}' + \frac{Q(\boldsymbol{x})}{4\pi}, \quad \boldsymbol{x} \in V, \ |\boldsymbol{\Omega}| = 1, \qquad (61a)$$

$$\psi(\boldsymbol{x}, \boldsymbol{\Omega}) = \psi^b(\boldsymbol{x}, \boldsymbol{\Omega}), \quad \boldsymbol{x} \in \partial V, \ \boldsymbol{\Omega} \cdot \boldsymbol{n} < 0. \qquad (61b)$$

If we define the following problem for $\psi_0(\boldsymbol{x}, \boldsymbol{\Omega})$:

$$\boldsymbol{\Omega} \cdot \nabla \psi_0(\boldsymbol{x}, \boldsymbol{\Omega}) + \Sigma_t(\boldsymbol{x}) \psi_0(\boldsymbol{x}, \boldsymbol{\Omega}) = \frac{Q(\boldsymbol{x})}{4\pi}, \quad \boldsymbol{x} \in V, \ |\boldsymbol{\Omega}| = 1, \qquad (62a)$$

$$\psi_0(\boldsymbol{x}, \boldsymbol{\Omega}) = \psi^b(\boldsymbol{x}, \boldsymbol{\Omega}), \quad \boldsymbol{x} \in \partial V, \ \boldsymbol{\Omega} \cdot \boldsymbol{n} < 0, \qquad (62b)$$

and for $1 \le n < \infty$ the following problems for $\psi_n(\boldsymbol{x}, \boldsymbol{\Omega})$:

$$\boldsymbol{\Omega} \cdot \nabla \psi_n(\boldsymbol{x}, \boldsymbol{\Omega}) + \Sigma_t(\boldsymbol{x}) \psi_n(\boldsymbol{x}, \boldsymbol{\Omega}) = \frac{\Sigma_s(\boldsymbol{x})}{4\pi} \int_{4\pi} \psi_{n-1}(\boldsymbol{x}, \boldsymbol{\Omega}') d\boldsymbol{\Omega}', \quad \boldsymbol{x} \in V, \ |\boldsymbol{\Omega}| = 1, \qquad (63a)$$

$$\psi_n(\boldsymbol{x}, \boldsymbol{\Omega}) = 0, \quad \boldsymbol{x} \in \partial V, \ \boldsymbol{\Omega} \cdot \boldsymbol{n} < 0, \qquad (63b)$$

then it is possible to interpret each ψ_n as a particular "component" of ψ.

First, in (62) for ψ_0, neutrons are *created* by the same internal and boundary sources and have the same mean free path as in (61); but when the neutrons in (62) experience a collision, they *die*. Thus, $\psi_0(\boldsymbol{x}, \boldsymbol{\Omega})$ describes the *uncollided* neutrons in problem (61) – the neutrons in V that have just been born and have yet to experience a collision in V or leak out of V.

Equation (63) for $n = 1$ have as their sole source the uncollided neutrons that scatter; when these (once-scattered) neutrons experience a collision, they die. Thus, $\psi_1(\boldsymbol{x}, \boldsymbol{\Omega})$ describes the *once-collided* neutron flux in problem (61) – the flux due to neutrons in V that have experienced exactly one scattering event and have yet to experience a second collision in V or leak out of V.

By continuing in this manner, we have for all $n \ge 0$,

$$\psi_n(\boldsymbol{x}, \boldsymbol{\Omega}) = \textit{the nth collided neutron flux}$$
$$= \text{the flux due to neutrons in } V \text{ that have experienced}$$
$$\text{exactly } n \text{ scattering events in } V. \qquad (64)$$

Also, if (62) and (63) are summed over $0 \le n < \infty$, it is easily seen that $\sum \psi_n$ satisfies (61) for ψ. Thus, the solution ψ of (61) can be written:

$$\psi(\boldsymbol{x}, \boldsymbol{\Omega}) = \sum_{n=0}^{\infty} \psi_n(\boldsymbol{x}, \boldsymbol{\Omega}). \qquad (65)$$

Therefore: at any instant in time, the neutron population consists of "newly born" neutrons, which have experienced only a few collisions (and have scattered in each), with "older" neutrons,

which have experienced many collisions (and have also scattered in each). Moreover, (62) and (63) show how to explicitly calculate, for each n, the flux of neutrons that have experienced exactly n collisions.

This view of neutron transport problems has practical benefits. For example, numerical methods for solving (61) are usually based on the *source iteration* algorithm, in which, effectively, (62) and (63) are solved recursively and the results added, as in (65). Source iteration converges rapidly for small, leaky systems, or systems with significant capture cross sections; here neutrons are unlikely to have long lives, so $\psi_n \to 0$ quickly. However, source iteration converges slowly for "diffusive" problems, which are many mean free paths in width (having small leakage rates) and scattering-dominated (having small neutron capture rates). For diffusive problems, neutrons can have long lives, so $\psi_n \to 0$ slowly.

A second benefit of (61–65) occurs in solving problems with localized or point sources. Here, $\psi_0(x, \Omega)$ [and to a lesser extent $\psi_1(x, \Omega)$] are strongly varying functions of x and Ω and are difficult to model numerically. A common strategy is to calculate the uncollided flux ψ_0 analytically and then calculate the collided fluxes ψ_n for $n \geq 1$ numerically. (In recent work, both ψ_0 and ψ_1 have been calculated analytically and the remaining ψ_n are calculated numerically.) This approach makes use of the fact that for point source problems, ψ_0 (and ψ_1) do not have to be treated by numerical methods that are likely to cause large errors.

A third practical benefit of (61–65) occurs in assessing the smoothness of solutions of (61). We briefly discuss this next and refer to Kellog (1974) for a more complete discussion.

2.10.3   Smoothness of the Angular Flux

This often poorly understood topic, dealing with the continuity and differentiability properties of the angular flux, has major implications in the accuracy of approximation schemes and numerical methods for simulating transport problems. It is not possible to discuss this subject fully here; instead we give some illustrative examples. (See Kellog (1974) for a more thorough discussion.) The basic facts are as follows:

1. Solutions of planar-geometry transport problems with vacuum boundaries and finite isotropic internal sources are *smooth* (continuous with continuous first derivatives) functions of x and μ, except at outer boundaries and material interfaces between regions with different cross sections and internal sources. At such interfaces, ψ is (i) continuous in x with a discontinuous first derivative, and (ii) discontinuous in μ at $\mu = 0$. This *boundary-layer* behavior occurs only at the interface between different material regions, and at the outer boundary of the system.

2. Angular flux solutions of multidimensional transport problems with vacuum boundaries exhibit the same boundary-layer behavior as described above at material interfaces and the outer boundary of the system. However, because of geometrical effects, multidimensional angular fluxes also lack smoothness away from boundary layers. Generally, multidimensional transport solutions are continuous functions of x and Ω but have discontinuous first derivatives. Occasionally, these solutions can even be discontinuous. Thus, multidimensional transport solutions are inherently not "smooth"; they lack even one continuous derivative in x and Ω. The lack of smoothness of the transport solution is an impediment to the calculation of accurate numerical solutions of multidimensional neutron transport problems.

3. Solutions of problems with nonzero but smooth prescribed incident boundary fluxes have the same smoothness properties as described above. However, if the incident boundary fluxes are not smooth, then the uncollided flux component of ψ can be nonsmooth throughout V. For example, an incident monodirectional (delta function) beam of neutrons on ∂V creates a delta function component of ψ that propagates entirely through V.

To illustrate the lack of smoothness for multidimensional problems (item 2 above), let us consider an infinite $(-\infty < x, y, z < \infty)$ purely absorbing $(\Sigma_s = 0)$ system with constant total cross section $\Sigma_t = \Sigma_y$, driven by an isotropic, spatially histogram internal source:

$$Q(x, y) = \begin{cases} Q_0, & |x| < X, \ |y| < Y, \\ 0, & \text{otherwise} . \end{cases} \tag{66}$$

Because of the lack of z-dependence in the geometry and sources, the angular flux ψ is independent of z. The neutron transport equation (see [56] and [2]) is:

$$\sqrt{1-\mu^2}\left(\cos\omega\frac{\partial\psi}{\partial x} + \sin\omega\frac{\partial\psi}{\partial y}\right) + \Sigma_t\psi(x, y, \mu, \omega) = \frac{Q(x, y)}{4\pi}. \tag{67}$$

Also, $\psi \to 0$ as $|x| \to \infty$ and $|y| \to \infty$.

The analytic solution, obtained by integrating (67) along the characteristic curve (the *flight path* of neutrons) $x(s) = x - s\cos\omega$, $y(s) = y - s\sin\omega$ for $0 < s < \infty$, can be written:

$$\psi(x, y, \mu, \omega) = \frac{1}{4\pi\sqrt{1-\mu^2}} \int_0^\infty Q(x - s\cos\omega, y - s\cos\omega)e^{-(\Sigma_t s/\sqrt{1-\mu^2})}ds. \tag{68}$$
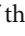
If the point (x, y) is outside the source region (which we henceforth assume) and the flight path does not intersect the source region, then $\psi = 0$.

If the flight path intersects the boundary of the source region, it does so for two values of s: $s_0(x, y, \omega) \leq s_1(x, y, \omega)$, as shown in ▶ *Fig. 17*. In this situation, we obtain explicitly from (68) and (66):

$$\psi(x, y, \mu, \omega) = \frac{1}{\sqrt{1-\mu^2}}\int_{s_0}^{s_1}\frac{Q_0}{4\pi}e^{-(\Sigma_t s/\sqrt{1-\mu^2})}ds$$

$$= \frac{Q_0}{4\pi\Sigma_t}\left(e^{-(\Sigma_t s_0(x,y,\omega)/\sqrt{1-\mu^2})} - e^{-(\Sigma_t s_1(x,y,\omega)/\sqrt{1-\mu^2})}\right). \tag{69}$$

This result can be extended to all points (x, y) outside the source region and all ω by simply defining $s_0 = s_1$ when the flight path does not intersect the source region.

For fixed x, y, and ω, it is evident that $\psi(x, y, \mu, \omega)$ is continuous and infinitely differentiable in the variable μ, with $\psi \to 0$ as $\mu \to \pm 1$.

Also, s_0 and s_1 are continuous and infinitely differentiable for most values of x, y, and ω. However, for each spatial point (x, y), there are generally four azimuthal angles ω for which the flight path passes through a corner of the source region (see ▶ *Fig. 18*). At one or two of these phase space points, $s_1(x, y, \omega)$ is a continuous function of x, y, and ω, but it has discontinuous first derivatives with respect to all three of these variables! Likewise, at zero or one of these phase space points, $s_0(x, y, \omega)$ is a continuous function of x, y, and ω, but it has discontinuous first derivatives with respect to all three of these variables. At all four of these phase space points,
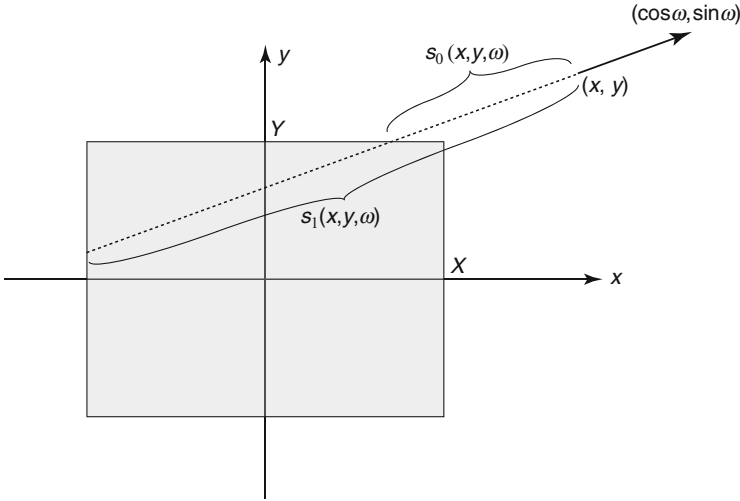
▣ Figure 17
$s_0(x, y, \omega)$ and $s_1(x, y, \omega)$
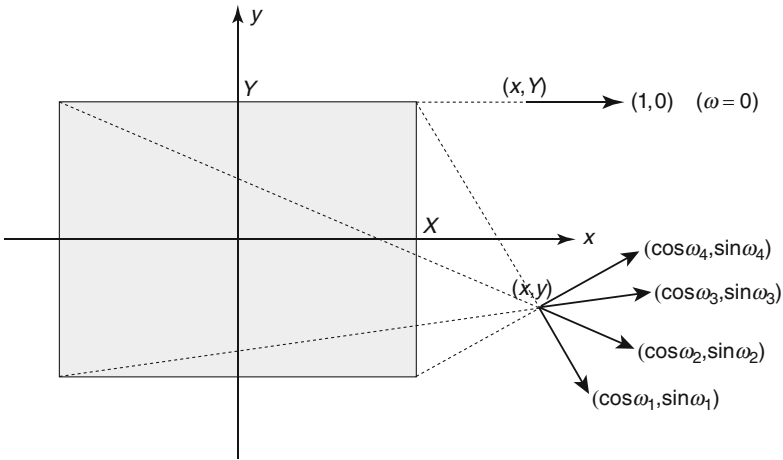
▣ Figure 18
$s_1(x, y, \omega)$ is not smooth at the indicated values of ω

$\psi(x, y, \mu, \omega)$ is a continuous function of x, y, and ω, but it has discontinuous first derivatives with respect to all three of these variables.

A more extreme situation occurs when the point (x, y) lies on a plane generated by an outer edge of the source region, and when the flight path traces along this outer edge of the source region. For example, from (68) we get for $x > X$, $y = Y$, $\omega = 0$, and any $\varepsilon > 0$ (see ❯ *Fig. 18*):

$$\psi(x, Y + \varepsilon, \mu, 0) = 0, \tag{70a}$$

$$\psi(x, Y - \varepsilon, \mu, 0) = \frac{Q_0}{4\pi\Sigma_t} \left(e^{-\Sigma_t(x-X)/\sqrt{1-\mu^2}} - e^{-\Sigma_t(x+X)/\sqrt{1-\mu^2}} \right). \tag{70b}$$

This implies that at the phase space point $(x, y, \mu, \omega) = (x, Y, \mu, 0)$, ψ is a discontinuous function of y. (And, a discontinuous function of ω.)

    This simple problem applies to the uncollided angular flux in any source-driven problem. In general, when the flight path $x - s\Omega$ passes through a "corner" of a source region, $\psi(x, \Omega, E)$ is continuous with a discontinuous derivative (with respect to x, y, or ω). When the flight path passes through a corner of a material region that does not contain a source, ψ has a weaker singularity (a continuous first derivative but a discontinuous second derivative). And, as we showed above, when the flight path traces along the planar edge of a source region, ψ is discontinuous. For problems with scattering, the statements in this paragraph hold for each nth collided flux ψ_n, and for ψ itself. For problems driven by boundary sources, similar results also follow.

    In general, for multidimensional, multiregion problems, ψ is generally a function with weak smoothness properties (Kellog 1974). This basic fact has not stopped practitioners from employing numerical methods that require the exact solution to be smoother than it actually is to achieve the theoretically optimal accuracy. However, the lack of smoothness of ψ negatively affects the accuracy and convergence rates of the resulting numerical solutions. For example, methods that would be second-order accurate if the solution is unrealistically smooth exhibit convergence rates that are less than second order when applied to realistic problems (Duo and Azmy 2007; Larsen 1982). (However, numerical experiments also show that certain integrals of the flux actually do converge with second-order accuracy (Larsen 1982).) The topic of the lack of smoothness of the angular flux and how this affects multidimensional numerical simulations is only qualitatively understood.

2.11   Generalizations of the Neutron Transport Equation

For simplicity, the transport equations and boundary conditions discussed above have not been written in the most general possible form. Here, we briefly describe some common generalizations.

2.11.1   Reflecting Boundaries

For physical systems V that possess a planar *symmetry boundary*, an equivalent transport problem can be formulated on a subregion of V using *symmetry* or *reflecting* boundary conditions. For example, the planar-geometry system $-Z \leq z \leq Z$ has a symmetry boundary at $z = 0$ if (i) the cross sections and internal source are even functions of z, e.g., $\Sigma_t(z, E) = \Sigma(-z, E)$, and (ii) the prescribed incident fluxes at $z = -Z$ and Z satisfy $\psi^b(-Z, \mu, E) = \psi^b(Z, -\mu, E)$ for $0 \leq \mu \leq 1$. In this case, symmetry considerations show that the angular flux must satisfy:

$$\psi(z, \mu, E) = \psi(-z, -\mu, E), \quad -Z < z < Z, \quad -1 \leq \mu \leq 1, \quad 0 < E < \infty. \tag{71a}$$

Here, one can formulate an equivalent planar-geometry transport problem on the half-system $0 \leq z \leq Z$. The transport equation on this half-system and the boundary condition at $z = Z$ are the same as before. The new *symmetry* or *reflecting* boundary condition at $z = 0$, obtained by setting $z = 0$ in (71a), is:

$$\psi(0, \mu, E) = \psi(0, -\mu, E), \quad 0 \leq \mu \leq 1, \quad 0 < E < \infty. \tag{71b}$$

If the transport problem on the half-system is solved, then the angular flux over the full system is obtained from (71a).

This strategy enables computer simulations to be performed more efficiently. In 1-D problems with a symmetry boundary, the savings is a factor of 2; in 2-D problems with two symmetry boundaries, the savings is a factor of 4; and in 3-D problems with three symmetry boundaries, the savings is a factor of 8.

2.11.2 Periodic Boundaries

Similarly, if a physical system is infinite with a *periodic* or *lattice* structure, and the angular flux itself is spatially periodic, then for obvious reasons it becomes imperative to formulate an equivalent problem on a single cell of the lattice. For example, if an infinite 1-D planar system $-\infty < z < \infty$ has spatially periodic cross sections and internal sources, e.g., $\Sigma_t(z) = \Sigma_t(z+Z)$, and if there are no sources at $z = \pm\infty$, then the angular flux is spatially periodic:

$$\psi(z, \mu, E) = \psi(z + Z, \mu, E). \tag{72a}$$

In this case, an equivalent transport problem can be formulated on a single cell $0 \le z \le Z$ with *periodic* boundary conditions obtained from (72a):

$$\psi(0, \mu, E) = \psi(Z, \mu, E), \quad -1 \le \mu \le 1, \quad 0 < E < \infty. \tag{72b}$$

If the transport problem on the single cell is solved, then the angular flux over the full system can be obtained from (72a).

2.11.3 Anisotropic Sources

Physically, internal neutron sources due to radioactive decay or spontaneous fission are isotropic – all directions of flight are equally probable. However, it is sometimes necessary to consider anisotropic internal sources $Q(x, \Omega, E)$ – for example, in calculating certain Green's functions, or in multigroup calculations, when including the source of neutrons that anisotropically scatter into a given energy group with the internal source for that group. (This latter topic will be discussed in detail in ▶ sect. 6.3). Overall, there is no mathematical reason why the internal neutron sources must be assumed to be isotropic; if appropriate, these sources can be taken to be anisotropic.

2.11.4 Coupled Neutron/Photon Transport

In reactor core calculations, the calculation of reaction rates relies on the determination of the neutron fluxes. However, in reactor shielding calculations, the calculation of dose rates relies on both the neutron fluxes and gamma-ray (photon) fluxes. The photons, which are produced by neutron absorption and inelastic neutron scattering, are more deeply penetrating than neutrons; the dose to humans on the far side of a reactor shield is due mostly to the transmitted

photons. To account for the photon transport in the shield, two coupled transport equations are formulated: one for the neutrons and one for the photons. When these are approximated using the multigroup approximation (discussed in ❯ sect. 6), the resulting two sets of multi-group equations can be merged into a single system of multigroup equations, with some groups describing neutrons and other groups describing photons.

2.11.5   Temperature-Dependent Cross Sections

Our derivation of the neutron transport equation ignores changes that occur in the macroscopic cross sections when temperature changes in the core occur due to an increase or decrease in the neutron flux (with a corresponding increase or decrease in reactor power). This approximation is generally valid when the reactor operates near a steady-state mode, but not when the reactor experiences significant transients in the neutron fluxes. To account for this, (i) an additional equation must be formulated yielding the temperature within the reactor $T(\boldsymbol{x}, t)$ as a function of space and time, with a source that depends on the reactor power, and (ii) the macroscopic cross sections in the reactor must be expressed as functions of $T(\boldsymbol{x}, t)$. The resulting equations are *nonlinear*: the neutron flux affects the temperature, which affects the macroscopic cross sections, which affects the flux. This is an extremely important topic in the fields of reactor kinetics and reactor safety.

2.11.6   Advection and Diffusion of Fission Products

Our derivation of the transport equation also ignores the spatial diffusion of fission products; delayed neutrons are assumed to be emitted at the site of the primary fission event. This is an excellent approximation for solid fuel reactors, but not when significant fuel motion is possible, as occurs, for instance, in liquid fuel reactors. The spatial motion of fission products can be accommodated by adding suitable advection or diffusion terms in the equations for the precursor densities. Then, in addition to the delayed emission in time, the delayed neutrons are emitted nonlocally in space.

2.12   Limitations of the Neutron Transport Equation

The neutron transport equation provides an extremely accurate description of the phase space neutron density in a nuclear reactor. In conjunction with appropriately formatted neutron–nucleus interaction data, this equation underlies the methods and codes used in the design of all existing nuclear reactors. However, the derivation of the transport equation has inherent approximations that limit the validity of the equation. Some of these approximations can be relaxed without significantly altering the mathematical structure of the equation. Other approximations are more fundamental and can only be relaxed at the expense of a much more complicated mathematical description. Some of the significant assumptions underlying the neutron transport equation are delineated below.

1. *The neutron is a point, structureless particle whose free motion between interactions can be described by classical mechanics.* Neutron properties requiring a quantum mechanical

description, such as spin and polarization, are assumed to influence only the interaction cross sections which, for the purpose of transport theory, are regarded as given. While the neutron phase space can be expanded to include internal states like spin and polarization, such effects are unimportant in most applications of neutron transport, but especially in reactor physics.

2. *The interaction centers, where neutrons collide with nuclei, are assumed to be randomly located with a Poisson distribution in the host medium, and collisions between neutrons and nuclei are well-defined isolated two-body interactions. Moreover, the probability of interaction with the target nuclei is assumed to depend only on the instantaneous state of the neutron and not on its prior interaction history.* In other words, the transport process is assumed to be *Markovian*, a statement that is encapsulated in the expression for the collision probability:

$$p(s)ds = \Sigma_t(\vec{x}, E, t)ds.$$

That is, the probability of an interaction in an incremental distance ds is proportional to ds and depends only on the neutron's current position and energy at the time of collision. The rate constant for the transition of state is just the macroscopic cross section. Also, the probability that the neutron can suffer more than one collision in ds is $o(ds)$, i.e., is negligible compared to ds. Corrections for non-Markovian effects have not been found necessary in the numerous applications of neutron transport theory. However, this may not be true in applications involving other types of particles. An example is low energy (~keV or less) atomic collision phenomena in solids, where isolated two-body collisions cannot be defined.

3. *The neutron transport equation, as derived in this section, describes the "expected" or "mean" neutron population in a medium.* Because of the statistical nature of neutron interactions and of the number of neutrons released per fission, the actual neutron number fluctuates about this mean value. However, the magnitude of the fluctuations depends on the population size. In power reactors, where the neutron number may be ~ 10^{15}, the deviation of the neutron population from the mean is small and the neutron transport equation for the expected density provides an accurate description of the transport process. However, for small neutron populations, such as encountered at start up in the presence of a weak source, the instantaneous neutron density will differ significantly and randomly from the mean density. This is because fission chains from a weak source are well separated, and some fission chains die prematurely, while others propagate for unusually long times. Therefore, a sufficiently strong overlap of chains does not occur for fluctuations to cancel out and a mean density to become established. Thus, although the neutron transport equation yields the correct mean neutron density, this is an incomplete characterization of the actual neutron population. Under these circumstances, a fully stochastic description of the neutron population is necessary. A generalization of the theory to explicitly account for stochastic effects in neutron transport is beyond the scope of this chapter but has been presented by Bell (1965).

4. *The neutron transport equation is a linear equation in which the macroscopic cross sections do not directly depend on the neutron density.* Two assumptions are necessary to ensure this independence:

   (a) *Neutron–neutron collisions are negligible.* In nuclear reactor applications, this is an excellent approximation because the density of target nuclei (10^{22} nuclei per cm^3) greatly exceeds the neutron density (<10^{15} neutrons per cm^3). In applications where interactions between moving particles is important, such as in the kinetic theory of gases, the collision operator becomes nonlinear and the appropriate transport equation becomes

the original (nonlinear) Boltzmann equation, which includes binary collisions between the particles.

(b) *The neutron reaction rate density is sufficiently small so as to not appreciably modify the isotopic makeup of the host medium, except during very long timescales.* This is also an excellent approximation in nuclear reactor applications. Since changes in material properties due to fuel burnup (density, thermal conductivity, poison accumulation, etc.) occur over much longer timescales than the timescale over which the neutron distribution relaxes, these effects can be treated by performing static transport calculations over various snapshots of the medium.

2.13 Discussion

We have (i) described the basic physical processes that underlie neutron transport, (ii) derived the mathematical equations that describe this process for time-dependent and steady-state nuclear reactor calculations, (iii) discussed some basic properties of the solutions of these equations, and (iv) discussed the conditions of validity of the equation. The neutron transport and precursor density equations form the basis for practical neutron (and photon) transport calculations in nuclear reactors and shields.

3 The Transport Equation in Special Geometries

Phase space for general neutron transport problems is 7-D: there are three spatial dimensions, two angular (*direction-of-flight*) dimensions, one energy dimension, and one temporal dimension. This is problematic for calculating deterministic numerical solutions of realistic problems; if each of the seven independent variables is discretized on a grid with a modest 10^2 cells, the resulting discrete problem will have 10^{14} unknowns! Problems of this magnitude will be beyond the capacity of the world's largest and fastest supercomputers for many years to come.

To formulate practical methods for solving realistic neutron transport problems, the size of phase space must be reduced as much as possible. For 3-D problems that have special space-angle symmetries, this can be done by reducing the number of spatial (and possibly angular) independent variables. In particular, one can formulate and solve a mathematically equivalent neutron transport equation with fewer than three independent spatial variables and possibly one rather than two angular variables. These special geometries are extremely important; for many years it was only possible to obtain practical numerical solutions of spatially 1-D and 2-D transport problems. In recent years, 3-D codes for practical problems have become available, but they are so costly to run that the great majority of neutron transport simulations remain 1-D and 2-D.

In the remainder of this chapter, we discuss the most important special geometries for which the transport equation can be formulated using one or two independent spatial variables. In each situation, we describe the geometry and derive the appropriate form of the transport equation.

To begin, we define a general 3-D problem for steady-state, monoenergetic, anisotropically scattering neutron transport in a prescribed convex spatial region V. This problem is driven by an internal isotropic source $Q(x)$, which is prescribed for all points x in V, and an incident

flux $\psi^b(x, \Omega)$, which is prescribed for all points x on the outer boundary ∂V of V and for all incident directions of flight Ω at x. The three restrictions of this problem: (i) steady-state, (ii) no fission, and (iii) monoenergetic transport, are made for simplicity only and can easily be relaxed. The problem is:

$$\Omega \cdot \nabla \psi(x, \Omega) + \Sigma_t(x)\psi(x, \Omega) = \int_{4\pi} \Sigma_s(x, \Omega \cdot \Omega')\psi(x, \Omega')d\Omega'$$

$$+ \frac{Q(x)}{4\pi}, \quad x \in V, \ \Omega \in 4\pi, \tag{73a}$$

$$\psi(x, \Omega) = \psi^b(x, \Omega), \quad x \in \partial V, \ \Omega \cdot n < 0. \tag{73b}$$

In the various geometries considered below, two terms in (73a) will change form: the *leakage* term $\Omega \cdot \nabla \psi$ on the left side, and the *scattering integral* $\int \Sigma_s \psi d\Omega'$ on the right side.

To begin, we formulate the above problem using standard 3-D Cartesian spatial variables and spherical harmonic functions to expand the scattering integral. Then, we describe the problem for two simpler Cartesian geometries: (1-D) planar geometry and (2-D) x, y-geometry. After this, we formulate the transport problem in the following *curvilinear* geometries: 1-D spherical geometry, 3-D (r, ϑ, z)-geometry, 2-D (r, z)-geometry, and 1-D cylindrical geometry. The 2-D (r, z)- and 1-D cylindrical-geometry transport equations are special cases of the 3-D (r, ϑ, z)-geometry equation. The most widely used geometries in practical 2-D applications are (x, y) and (r, z).

3.1 3-D Cartesian Geometry

For a standard 3-D Cartesian (x, y, z)-coordinate system (❯ *Fig. 19*) with θ = polar angle, ω = azimuthal angle, and $\mu = \cos\theta$ = polar cosine, we have:

$$x = xi + yj + zk, \tag{74a}$$

$$\Omega = \Omega_x i + \Omega_y j + \Omega_z k$$

$$= \sqrt{1 - \mu^2} \, (\cos\omega \, i + \sin\omega \, j) + \mu k, \tag{74b}$$

$$\mu = \cos\theta, \tag{74c}$$

$$d\Omega = d\mu \, d\omega. \tag{74d}$$

In this geometry,

$$\psi(x, \Omega) = \Psi(x, y, z, \mu, \omega), \tag{75}$$

and the leakage term in the transport equation can be written:

$$\Omega \cdot \nabla \psi(x, \Omega) = \left(\Omega_x \frac{\partial}{\partial x} + \Omega_y \frac{\partial}{\partial y} + \Omega_z \frac{\partial}{\partial z} \right) \Psi(x, y, z, \mu, \omega)$$

$$= \left[\sqrt{1 - \mu^2} \left(\cos\omega \frac{\partial}{\partial x} + \sin\omega \frac{\partial}{\partial y} \right) + \mu \frac{\partial}{\partial z} \right] \Psi(x, y, z, \mu, \omega). \tag{76}$$
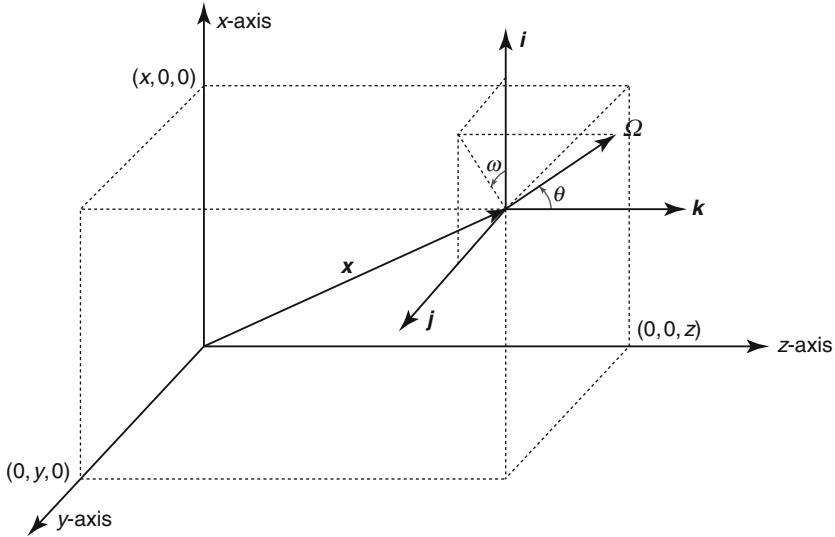
◼ Figure 19
3-D Cartesian geometry

Thus, the leakage operator depends explicitly on all the spatial and angular variables. (*Note*: In this discussion, ψ denotes the angular flux as a *general* function of space x and direction Ω; Ψ denotes the angular flux as a function of angular and direction variables that correspond to *specific* coordinate systems.)

To express the scattering integral, we use the fact that scattering is rotationally invariant. Thus, the differential scattering cross section is a function of the scattering cosine $\mu_0 = \Omega \cdot \Omega'$ and can be written as a Legendre polynomial expansion:

$$\Sigma_s(x, \Omega \cdot \Omega') = \sum_{n=0}^{N} \frac{2n+1}{4\pi} \Sigma_{s,n}(x) P_n(\Omega \cdot \Omega'), \tag{77}$$

where $P_n(\mu_0)$ is the nth Legendre polynomial (Duderstadt and Hamilton 1976). The *order N* of this expansion is generally infinite, but in applications the series is truncated and N is taken to be finite. If $N = 0$ (or 1), scattering is said to be *isotropic* (or *linearly anisotropic*).

The Legendre polynomials satisfy the *addition theorem*:

$$P_n(\Omega \cdot \Omega') = \frac{4\pi}{2n+1} \sum_{m=-n}^{n} Y_{n,m}(\Omega) Y_{n,m}^*(\Omega'), \tag{78}$$

where for $0 \le |m| \le n < \infty$, $Y_{n,m}(\Omega)$ is a *spherical harmonic* function:

$$Y_{n,m}(\Omega) = Y_{n,m}(\mu, \omega) = a_{n,m} P_n^{|m|}(\mu) e^{im\omega}, \tag{79a}$$

$$P_n^{|m|}(\mu) = \left(1 - \mu^2\right)^{|m|/2} \left(\frac{d}{d\mu}\right)^{|m|} P_n(\mu)$$

$$= \text{Associated Legendre function,} \tag{79b}$$

$$a_{n,m} = (-1)^{(m+|m|)/2} \left[\frac{2n+1}{4\pi} \frac{(n-|m|)!}{(n+|m|)!}\right]^{1/2}. \tag{79c}$$

Here * denotes complex conjugate, and $0! = 1$.

Introducing (78) into (77), we obtain:

$$\Sigma_s(\boldsymbol{x}, \boldsymbol{\Omega} \cdot \boldsymbol{\Omega}') = \sum_{n=0}^{N} \sum_{m=-n}^{n} \Sigma_{s,n}(\boldsymbol{x}) Y_{n,m}(\boldsymbol{\Omega}) Y_{n,m}^*(\boldsymbol{\Omega}'). \tag{80}$$

Thus, the scattering integral in (73a) can be written:

$$\int_{4\pi} \Sigma_s(\boldsymbol{x}, \boldsymbol{\Omega} \cdot \boldsymbol{\Omega}') \psi(\boldsymbol{x}, \boldsymbol{\Omega}') d\Omega'$$

$$= \sum_{n=0}^{N} \sum_{m=-n}^{n} \Sigma_{s,n}(\boldsymbol{x}) Y_{n,m}(\mu, \omega) \int_{-1}^{1} \int_{0}^{2\pi} Y_{n,m}^*(\mu', \omega') \Psi(x, y, z, \mu', \omega') d\omega' d\mu'. \tag{81}$$

Introducing (76) and (81) into (73a), we obtain the following 3-D Cartesian-geometry transport equation:

$$\left[\sqrt{1 - \mu^2} \left(\cos \omega \frac{\partial}{\partial x} + \sin \omega \frac{\partial}{\partial y}\right) + \mu \frac{\partial}{\partial z}\right] \psi(\boldsymbol{x}, \boldsymbol{\Omega}) + \Sigma_t(\boldsymbol{x}) \psi(\boldsymbol{x}, \boldsymbol{\Omega})$$

$$= \sum_{n=0}^{N} \sum_{m=-n}^{n} \Sigma_{s,n}(\boldsymbol{x}) Y_{n,m}(\boldsymbol{\Omega}) \int_{4\pi} Y_{n,m}^*(\boldsymbol{\Omega}') \psi(\boldsymbol{x}, \boldsymbol{\Omega}') d\Omega' + \frac{Q(\boldsymbol{x})}{4\pi}. \tag{82}$$

In (82), the shorthand notations of (75) and (79a) have been used. Equation (82) holds for all spatial points $\boldsymbol{x} \in V$ and all unit vectors $\boldsymbol{\Omega}$ ($-1 \le \mu \le 1$ and $0 \le \omega < 2\pi$). To determine ψ, (82) must be solved subject to the boundary condition expressed in (73b).

3.2   1-D Planar Geometry

In problems with 1-D planar symmetry,

1. The physical system is a planar "slab" consisting of spatial points (x, y, z) with $-\infty < x, y < \infty$ and $0 < z < Z$. Thus, the system is infinite in the (*transverse*) x- and y-directions and finite or possibly infinite in the (*depth*) z-direction.
2. The cross sections, isotropic internal source, and prescribed incident boundary fluxes are independent of the transverse variables x and y.

Because the problem geometry and neutron sources are independent of x and y, the angular flux itself is independent of x and y:

$$\psi(\boldsymbol{x}, \boldsymbol{\Omega}) = \Psi(z, \boldsymbol{\Omega}) = \Psi(z, \mu, \omega). \tag{83a}$$

In these circumstances, (82) immediately reduces to:

$$\mu \frac{\partial \Psi}{\partial z}(z, \boldsymbol{\Omega}) + \Sigma_t(z)\Psi(z, \boldsymbol{\Omega}) = \sum_{n=0}^{N} \sum_{m=-n}^{n} \Sigma_{s,n}(z) Y_{n,m}(\boldsymbol{\Omega}) \int_{4\pi} Y^*_{n,m}(\boldsymbol{\Omega}')\Psi(z, \boldsymbol{\Omega}')d\Omega'$$

$$+ \frac{Q(z)}{4\pi}, \quad 0 < z < Z, \quad \boldsymbol{\Omega} \in 4\pi. \tag{83b}$$

The boundary conditions prescribe the incident angular fluxes on the left and right edges of the slab:

$$\Psi(0, \mu, \omega) = \psi^b(\mu, \omega), \quad 0 < \mu \le 1, \ 0 \le \omega < 2\pi, \tag{83c}$$

$$\Psi(Z, \mu, \omega) = \psi^b(\mu, \omega), \quad -1 \le \mu < 0, \ 0 \le \omega < 2\pi. \tag{83d}$$

Equations (83) describe planar-geometry neutron transport *without azimuthal symmetry*.

The azimuthal angle can be eliminated by integrating the equations over $0 \le \omega < 2\pi$. If we define the *azimuthally integrated angular flux*:

$$\Psi(z, \mu) = \int_0^{2\pi} \Psi(z, \mu, \omega)d\omega, \tag{84}$$

then upon integration over ω, (83b) yields:

$$\mu \frac{\partial \Psi}{\partial z}(z, \mu) + \Sigma_t(z)\Psi(z, \mu)$$

$$= \sum_{n=0}^{N} \sum_{m=-n}^{n} \Sigma_{s,n}(z) \left(\int_0^{2\pi} Y_{n,m}(\boldsymbol{\Omega})d\omega \right) \int_{4\pi} Y^*_{n,m}(\boldsymbol{\Omega}')\Psi(z, \boldsymbol{\Omega}')d\Omega'$$

$$+ \frac{Q(z)}{2}, \quad 0 < z < Z, \ -1 \le \mu \le 1. \tag{85a}$$

However, (79) imply:

$$\int_0^{2\pi} Y_{n,m}(\boldsymbol{\Omega})d\omega = 2\pi\delta_{m,0} \left(\frac{2n+1}{4\pi} \right)^{1/2} P_n(\mu), \tag{85b}$$

and:

$$\int_{4\pi} Y^*_{n,0}(\boldsymbol{\Omega}')\Psi(z, \boldsymbol{\Omega}')d\Omega' = \int_{-1}^{1} \int_0^{2\pi} \left(\frac{2n+1}{4\pi} \right)^{1/2} P_n(\mu')\Psi(z, \mu', \omega')d\omega'd\mu'$$

$$= \left(\frac{2n+1}{4\pi} \right)^{1/2} \int_{-1}^{1} P_n(\mu')\Psi(z, \mu')d\mu'. \tag{85c}$$

Introducing these results into (85a), we obtain the following simpler equation for $\Psi(z, \mu)$:

$$\mu \frac{\partial \Psi}{\partial z}(z, \mu) + \Sigma_t(z)\Psi(z, \mu) = \sum_{n=0}^{N} \left(\frac{2n+1}{2} \right) \Sigma_{s,n}(z) P_n(\mu) \int_{-1}^{1} P_n(\mu')\Psi(z, \mu')d\mu'$$

$$+ \frac{Q(z)}{2}, \quad 0 < z < Z, \ -1 \le \mu \le 1. \tag{86a}$$

Also, integrating the boundary conditions (83c) and (83d) over ω, we obtain:

$$\Psi(0, \mu) = \psi^b(\mu) = \int_0^{2\pi} \psi^b(\mu, \omega)d\omega, \quad 0 < \mu \leq 1, \tag{86b}$$

$$\Psi(Z, \mu) = \psi^b(\mu) = \int_0^{2\pi} \psi^b(\mu, \omega)d\omega, \quad -1 \leq \mu < 0. \tag{86c}$$

Equation (86a) describe *azimuthally integrated planar-geometry neutron transport*.

To determine $\Psi(z, \mu)$, (86) must be solved. By (84), this solution is the azimuthally integrated angular flux of the original problem.

3.3   2-D (X,Y)-Geometry

In problems with 2-D (x, y)-symmetry (❯ *Fig. 20*),

1. The physical system is an infinite "cylinder," consisting of spatial points (x, y, z) with $(x, y) \in D$ (a convex region in the (x, y)-plane) and $-\infty < z < \infty$.
2. The cross sections, isotropic internal source, and prescribed incident boundary fluxes are independent of z.
3. The prescribed incident boundary fluxes are even functions of $\mu = \boldsymbol{\Omega} \cdot \boldsymbol{k}$:

$$\psi^b(x, y, \boldsymbol{\Omega}) = \psi^b(x, y, \boldsymbol{\Omega}_r), \quad (x, y) \in \partial D, \ \boldsymbol{\Omega} \cdot \boldsymbol{n} < 0, \tag{87a}$$

where:

$$\boldsymbol{\Omega} = \sqrt{1 - \mu^2} \cos \omega \, \boldsymbol{i} + \sqrt{1 - \mu^2} \sin \omega \, \boldsymbol{j} + \mu \boldsymbol{k}$$
$$= \eta \boldsymbol{i} + \xi \boldsymbol{j} + \mu \boldsymbol{k}, \tag{87b}$$
$$\boldsymbol{\Omega}_r = \eta \boldsymbol{i} + \xi \boldsymbol{j} - \mu \boldsymbol{k},$$
$$= \text{Reflection of } \boldsymbol{\Omega} \text{ across the } (x, y)\text{-plane.} \tag{87c}$$
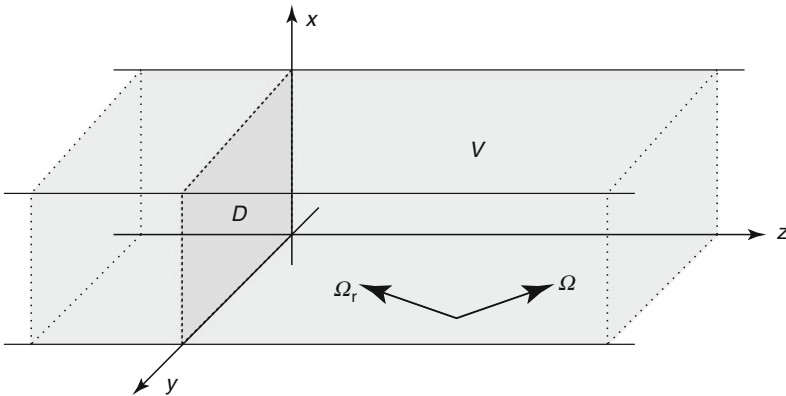
◼ Figure 20
2-D (x, y)-geometry
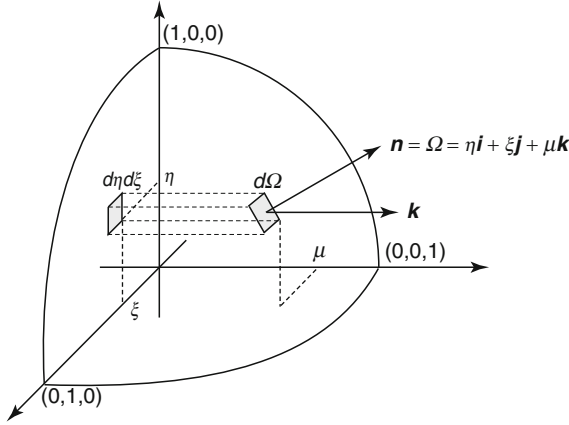
◘ Figure 21
dηdξ and *dΩ*

Because the problem geometry is independent of z and the neutron sources are even functions of μ, the neutron angular is also independent of z and an even function of μ: $\psi(x, \Omega) = \Psi(x, y, \mu, \omega) = \Psi(x, y, -\mu, \omega)$.

If we define:

$$\eta = \Omega_x = \sqrt{1 - \mu^2} \, \cos \omega, \tag{88a}$$

$$\xi = \Omega_y = \sqrt{1 - \mu^2} \, \sin \omega, \tag{88b}$$

then $|\Omega| = 1$ implies that for each value of η and ξ, there are two values of μ: $\mu^\pm = \pm\sqrt{1 - \eta^2 - \xi^2}$. Thus, if a function $f(\Omega)$ is an even function of μ, i.e., if for each η and ξ it has the same value at μ^+ and μ^-, then we can write:

$$f(\Omega) = g(\eta, \xi), \quad \eta^2 + \xi^2 \leq 1. \tag{89}$$

Also, from ❯ *Fig. 21*, we have:

$$d\Omega = \left(\frac{d\Omega}{d\eta d\xi} \right) d\eta d\xi = \frac{1}{|\mathbf{n} \cdot \mathbf{k}|} d\eta d\xi = \frac{d\eta d\xi}{|\mu|} = \frac{d\eta d\xi}{\sqrt{1 - \eta^2 - \xi^2}},$$

which implies:

$$\int_{4\pi} f(\Omega) d\Omega = 2 \int_{\eta^2 + \xi^2 \leq 1} \frac{g(\eta, \xi)}{\sqrt{1 - \eta^2 - \xi^2}} \, d\eta d\xi. \tag{90}$$

(The factor 2 occurs because the integral over $\eta^2 + \xi^2 \leq 1$ accounts for integration over only one hemisphere.)

From the above considerations, we can write:

$$\psi(\boldsymbol{x}, \boldsymbol{\Omega}) = \frac{1}{2}\Psi(x, y, \eta, \xi). \tag{91}$$

Using (91) and (88) in (76), we immediately get:

$$\boldsymbol{\Omega} \cdot \nabla\psi(\boldsymbol{x}, \boldsymbol{\Omega}) = \frac{1}{2}\left(\eta\frac{\partial}{\partial x} + \xi\frac{\partial}{\partial y}\right)\Psi(x, y, \eta, \xi). \tag{92}$$

Also, the spherical harmonic functions $Y_{n,m}(\boldsymbol{\Omega}) = Y_{n,m}(\mu, \omega)$ are even functions of μ for $n + m =$ even, and odd functions of μ for $n + m =$ odd (see [79]). Therefore,

$$\int_{4\pi} Y_{n,m}^*(\boldsymbol{\Omega}')\psi(\boldsymbol{x}, \boldsymbol{\Omega}')d\Omega' = \frac{1 + (-1)^{n+m}}{2}\int_{4\pi} Y_{n,m}^*(\boldsymbol{\Omega}')\psi(\boldsymbol{x}, \boldsymbol{\Omega}')d\Omega'$$

$$= \frac{1 + (-1)^{n+m}}{2}\int_{(\eta')^2 + (\xi')^2 \leq 1} \frac{Y_{n,m}^*(\eta', \xi')\Psi(x, y, \eta', \xi')}{\sqrt{1 - (\eta')^2 - (\xi')^2}}d\eta'd\xi'. \tag{93}$$

Introducing (92) and (93) into (82), we obtain the following (x, y)-*geometry neutron transport equation*:

$$\left(\eta\frac{\partial}{\partial x} + \xi\frac{\partial}{\partial y}\right)\Psi(x, y, \eta, \xi) + \Sigma_t(x, y)\Psi(x, y, \eta, \xi)$$

$$= \sum_{n=0}^{n}\sum_{m=-n}^{n}\left[1 + (-1)^{n+m}\right]\Sigma_{s,n}(x, y)Y_{n,m}(\eta, \xi)$$

$$\times \int_{(\eta')^2 + (\xi')^2 \leq 1} \frac{Y_{n,m}^*(\eta', \xi')\Psi(x, y, \eta', \xi')}{\sqrt{1 - (\eta')^2 - (\xi')^2}}d\eta'd\xi'$$

$$+ \frac{Q(x, y)}{2\pi}, \quad (x, y) \in D, \quad \eta^2 + \xi^2 \leq 1. \tag{94}$$

The (x, y)-geometry boundary condition prescribes the incident neutron flux for spatial points $(x, y) \in \partial D$ and for inward-pointing directions of flight $\boldsymbol{\Omega}$:

$$\Psi(x, y, \eta, \xi) = \Psi^b(x, y, \eta, \xi) = 2\psi^b(x, y, \eta, \xi, \mu^+),$$
$$(x, y) \in \partial D, \quad (\eta\boldsymbol{i} + \xi\boldsymbol{j}) \cdot \boldsymbol{n} < 0. \tag{95}$$

To determine $\Psi(x, y, \eta, \xi)$, (94) must be solved subject to the boundary conditions equation (95). The angular flux is then given by (91).

3.4   1-D Spherical Geometry

In problems with 1-D spherical symmetry (❯ *Fig. 22*),

The physical system is a sphere of radius R. (In the following, we take the center of the sphere to be the origin of the Cartesian coordinate system.)
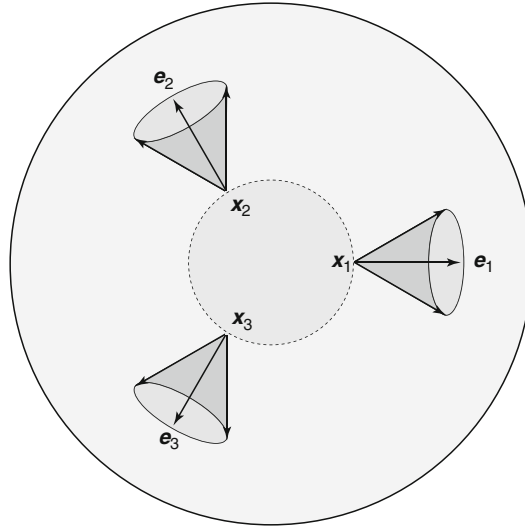
◘ Figure 22
1-D spherical symmetry. The angular flux is constant for: (i) spatial points x equally distant from the center of the sphere and (ii) directions of flight Ω that make an equal angle with $e = x/r$

The cross sections and internal source are functions only of the radial variable

$$r = \left(x^2 + y^2 + z^2 \right)^{1/2}. \tag{96}$$

For spatial points on the surface of the sphere ($|x| = r = R$) and for inward-pointing directions of flight ($\Omega \cdot x < 0$), the incident boundary fluxes are functions only of:

$$\mu = \Omega \cdot (x/r)$$
$$= \text{ Cosine of the angle between the direction of flight } \Omega$$
$$\text{and the radially outward direction } e = x/r. \tag{97}$$

In these circumstances, the angular flux should be a function only of r and μ:

$$\psi(x, \Omega) = \frac{1}{2\pi} \Psi(r, \mu). \tag{98}$$

[The factor 2π is included so that, as in planar geometry,

$$\int_{4\pi} \psi(x, \Omega) d\Omega = \int_{-1}^{1} \Psi(r, \mu) d\mu.] \tag{99}$$

Equation (98) implies:

$$\Omega \cdot \nabla \psi(x, \Omega) = \frac{1}{2\pi} \left(\frac{\partial \Psi}{\partial r} \Omega \cdot \nabla r + \frac{\partial \Psi}{\partial \mu} \Omega \cdot \nabla \mu \right),$$

where, using (96) and (97), we have:

$$\boldsymbol{\Omega} \cdot \nabla r = \left(\Omega_x \frac{\partial}{\partial x} + \Omega_y \frac{\partial}{\partial y} + \Omega_z \frac{\partial}{\partial z} \right) r = \Omega_x \frac{x}{r} + \Omega_y \frac{y}{r} + \Omega_z \frac{z}{r} = \mu,$$

$$\boldsymbol{\Omega} \cdot \nabla \mu = \left(\Omega_x \frac{\partial}{\partial x} + \Omega_y \frac{\partial}{\partial y} + \Omega_z \frac{\partial}{\partial z} \right) \left(\frac{\Omega_x x + \Omega_y y + \Omega_z z}{r} \right) = \cdots = \frac{1 - \mu^2}{r}.$$

Therefore,

$$\boldsymbol{\Omega} \cdot \nabla \psi(\boldsymbol{x}, \boldsymbol{\Omega}) = \frac{1}{2\pi} \left(\mu \frac{\partial}{\partial r} + \frac{1 - \mu^2}{r} \frac{\partial}{\partial \mu} \right) \Psi(r, \mu). \tag{100}$$

Also, defining the polar cosine μ locally (at each point) by (97) and letting ω be any consistently defined azimuthal angle, it is evident that Ψ is independent of ω. Thus, (85b) and (85c) hold, with $\Sigma_{s,n}(z)$ and $\Psi(z, \mu)$ replaced by $\Sigma_{s,n}(r)$ and $\Psi(r, \mu)$. Using this and (100) in (83b), we obtain the following *1-D spherical-geometry transport equation*:

$$\left(\mu \frac{\partial}{\partial r} + \frac{1 - \mu^2}{r} \frac{\partial}{\partial \mu} \right) \Psi(r, \mu) + \Sigma_t(r) \Psi(r, \mu)$$

$$= \sum_{n=0}^{N} \left(\frac{2n + 1}{2} \right) \Sigma_{s,n}(r) P_n(\mu) \int_{-1}^{1} P_n(\mu') \Psi(r, \mu') d\mu' + \frac{Q(r)}{2},$$

$$0 \le r \le R, \quad -1 \le \mu \le 1. \tag{101}$$

The spherical-geometry boundary condition prescribes the incident fluxes on the outer boundary of the sphere:

$$\Psi(R, \mu) = \Psi^b(\mu) = 2\pi \psi^b(R, \mu), \quad -1 \le \mu < 0. \tag{102}$$

To determine $\Psi(r, \mu)$, (101) must be solved subject to the boundary condition (102). The angular flux is then given by (98).

3.5 3-D (r, ϑ, z)-Geometry

To derive the 2-D (r, z) and the 1-D cylindrical transport equations, we first derive the 3-D transport equation expressed in terms of cylindrical variables: the *radial spatial variable* $r = \sqrt{x^2 + y^2}$ and the *azimuthal spatial angle* $\vartheta = \tan^{-1}(y/x)$. We also replace the azimuthal directional angle ω by the angular deflection γ from the spatial azimuthal angle ϑ. γ ranges over $-\pi \le \gamma \le \pi$. Directions satisfying $|\gamma| < \pi/2$ are *outgoing* and describe flow away from $r = 0$. Directions satisfying $|\gamma| > \pi/2$ are *incoming* and describe flow toward $r = 0$. The spatial variable z and the polar cosine μ retain their Cartesian geometry interpretations (see ❯ *Fig. 23*).
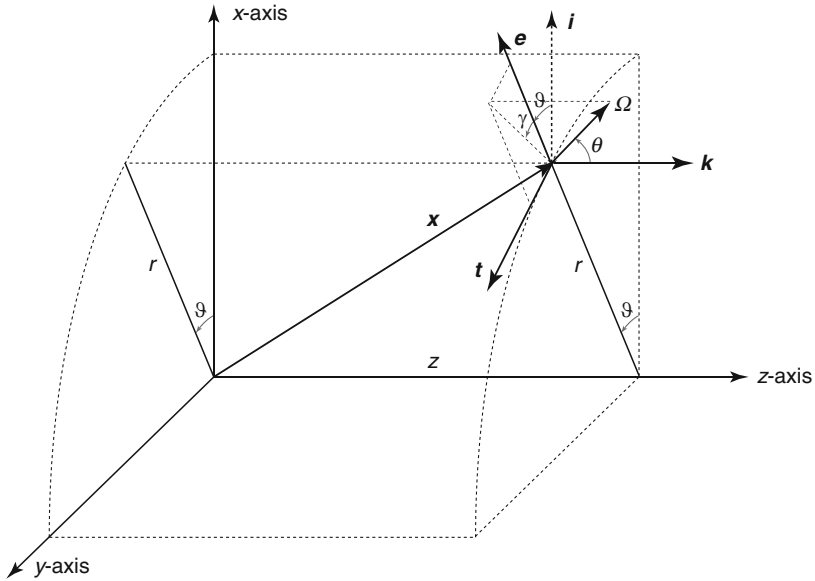
◘ Figure 23
3-D (r, ϑ, z) variables

The Cartesian spatial variables x and y, and the azimuthal angular variable ω are expressed in terms of the *curvilinear* variables r and ϑ, and the azimuthal angular variable γ by:

$$x = r \cos \vartheta, \tag{103a}$$

$$y = r \sin \vartheta, \tag{103b}$$

$$\omega = \vartheta + \gamma. \tag{103c}$$

Then, defining the unit vectors (see ❯ *Fig. 23*):

$$e = \frac{x}{r} \, i + \frac{y}{r} \, j = \cos \vartheta \, i + \sin \vartheta \, j, \tag{104a}$$

$$t = -\frac{y}{r} \, i + \frac{x}{r} \, j = -\sin \vartheta \, i + \cos \vartheta \, j, \tag{104b}$$

we have:

$$\tilde{x} = r e + z k, \tag{105a}$$

$$\tilde{\Omega} = \sqrt{1 - \mu^2} \, (\cos \gamma \, e + \sin \gamma \, t) + \mu k, \tag{105b}$$

$$d\tilde{\Omega} = d\mu \, d\gamma = d\mu d\omega = d\Omega. \tag{105c}$$

(A tilde signifies that $\tilde{x}$ is expressed in terms of r, ϑ, and z rather than x, y, and z, and that $\tilde{\Omega}$ is expressed in terms of γ and μ rather than ω and μ. We note that $\tilde{x} = x$ and $\tilde{\Omega} = \Omega$.) The angular flux is now expressed in terms of the new variables:

$$\psi(x, \Omega) = \psi(x, y, z, \mu, \omega) = \psi(r \cos \vartheta, r \sin \vartheta, z, \mu, \vartheta + \gamma)$$
$$\equiv \Psi(r, \vartheta, z, \mu, \gamma) = \Psi(\tilde{x}, \tilde{\Omega}). \tag{106}$$

The following identities can easily be shown:

$$\Omega \cdot \nabla r = \cos \gamma \sqrt{1 - \mu^2}, \tag{107a}$$

$$\Omega \cdot \nabla \vartheta = \frac{\sin \gamma}{r} \sqrt{1 - \mu^2}, \tag{107b}$$

$$\Omega \cdot \nabla z = \mu, \tag{107c}$$

$$\Omega \cdot \nabla \mu = 0, \tag{107d}$$

$$\Omega \cdot \nabla \gamma = -\frac{\sin \gamma}{r} \sqrt{1 - \mu^2}. \tag{107e}$$

Equations (106) and (107) then give:

$$\Omega \cdot \nabla \psi = \mu \frac{\partial \Psi}{\partial z} + \cos \gamma \sqrt{1 - \mu^2} \frac{\partial \Psi}{\partial r} + \frac{\sin \gamma}{r} \sqrt{1 - \mu^2} \left(\frac{\partial \Psi}{\partial \vartheta} - \frac{\partial \Psi}{\partial \gamma} \right). \tag{108}$$

We also have the identity:

$$\mu_0 = \Omega \cdot \Omega' = \sqrt{1 - \mu^2} \sqrt{1 - (\mu')^2} \left(\cos \omega \cos \omega' + \sin \omega \sin \omega' \right) + \mu \mu'$$
$$= \sqrt{1 - \mu^2} \sqrt{1 - (\mu')^2} \cos \left(\omega - \omega' \right) + \mu \mu'$$
$$= \sqrt{1 - \mu^2} \sqrt{1 - (\mu')^2} \cos \left(\gamma - \gamma' \right) + \mu \mu'$$
$$= \sqrt{1 - \mu^2} \sqrt{1 - (\mu')^2} \left(\cos \gamma \cos \gamma' + \sin \gamma \sin \gamma' \right) + \mu \mu'$$
$$= \tilde{\Omega} \cdot \tilde{\Omega}' = \tilde{\mu}_0. \tag{109}$$

We may define:

$$\Sigma_t(x) = \Sigma_t(x, y, z) = \Sigma_t(r \cos \vartheta, r \sin \vartheta, z)$$
$$\equiv \tilde{\Sigma}_t(r, \vartheta, z) = \tilde{\Sigma}_t(\tilde{x}), \tag{110a}$$
$$\Sigma_s(x, \mu_0) = \Sigma_s(x, y, z, \mu_0) = \Sigma_s(r \cos \vartheta, r \sin \vartheta, z, \mu_0)$$
$$\equiv \tilde{\Sigma}_s(r, \vartheta, z, \tilde{\mu}_0) = \tilde{\Sigma}_s(\tilde{x}, \tilde{\mu}_0), \tag{110b}$$
$$Q(x) = Q(x, y, z) = Q(r \cos \vartheta, r \sin \vartheta, z)$$
$$\equiv \tilde{Q}(r, \vartheta, z) = \tilde{Q}(\tilde{x}). \tag{110c}$$

From (81), the scattering integral becomes:

$$\int_{4\pi} \Sigma_s(x, \Omega \cdot \Omega') \psi(x, \Omega') d\Omega'$$
$$= \sum_{n=0}^{N} \sum_{m=-n}^{n} \tilde{\Sigma}_{s,n}(\tilde{x}) Y_{n,m}(\mu, \gamma) \int_{-1}^{1} \int_{-\pi}^{\pi} Y_{n,m}^*(\mu', \gamma') \Psi(r, \vartheta, z, \mu', \gamma') d\gamma' d\mu'. \tag{111}$$

5

Using (109) and (111) in (73a), we obtain the following (r, ϑ, z)-geometry transport equation:

$$\sqrt{1-\mu^2}\left[\cos\gamma\,\frac{\partial\Psi}{\partial r}(\tilde{\boldsymbol{x}},\tilde{\boldsymbol{\Omega}}) + \frac{\sin\gamma}{r}\left(\frac{\partial\Psi}{\partial\vartheta}(\tilde{\boldsymbol{x}},\tilde{\boldsymbol{\Omega}}) - \frac{\partial\Psi}{\partial\gamma}(\tilde{\boldsymbol{x}},\tilde{\boldsymbol{\Omega}})\right)\right] + \mu\frac{\partial\Psi}{\partial z}(\tilde{\boldsymbol{x}},\tilde{\boldsymbol{\Omega}}) + \tilde{\Sigma}_t(\tilde{\boldsymbol{x}})\Psi(\tilde{\boldsymbol{x}},\tilde{\boldsymbol{\Omega}})$$

$$= \sum_{n=0}^{N}\sum_{m=-n}^{n}\tilde{\Sigma}_{s,n}(\tilde{\boldsymbol{x}})Y_{n,m}(\tilde{\boldsymbol{\Omega}})\int_{4\pi}Y_{n,m}^*(\tilde{\boldsymbol{\Omega}}')\Psi(r,\vartheta,z,\tilde{\boldsymbol{\Omega}}')d\tilde{\boldsymbol{\Omega}}' + \frac{\tilde{Q}(\tilde{\boldsymbol{x}})}{4\pi}. \tag{112a}$$

This equation describes 3-D neutron transport in, e.g., a finite cylindrical system of radius R and length Z. The spatial and angular variables then vary over:

$$0 < r \le R, \quad -\pi \le \vartheta \le \pi, \quad 0 \le z \le Z, \quad -1 \le \mu \le 1, \quad -\pi \le \gamma \le \pi. \tag{112b}$$

In addition to (112), we must prescribe the incident angular flux on the outer boundary of the cylinder. First, on the outer "cylindrical" surface, we have:

$$\Psi(R,\vartheta,z,\mu,\gamma) = \Psi^b(\vartheta,z,\mu,\gamma), \quad 0 \le z \le Z, -\pi \le \vartheta \le \pi, \; -1 \le \mu \le 1, \; |\gamma| > \frac{\pi}{2}. \tag{113a}$$

At the circular "cap" at $z = 0$, we have:

$$\Psi(r,\vartheta,0,\mu,\gamma) = \Psi^b(r,\vartheta,\mu,\gamma), \quad 0 < r \le R, -\pi \le \vartheta \le \pi, \; 0 < \mu \le 1, \; -\pi \le \gamma \le \pi. \tag{113b}$$

At the other circular "cap" at $z = Z$, we have:

$$\Psi(r,\vartheta,Z,\mu,\gamma) = \Psi^b(r,\vartheta,\mu,\gamma), \quad 0 < r \le R, -\pi \le \vartheta \le \pi, \; -1 \le \mu < 0, \; -\pi \le \gamma \le \pi. \tag{113c}$$

Equations (112) and (113) describe 3-D neutron transport in the finite cylindrical system depicted in ❯ *Fig. 24*.
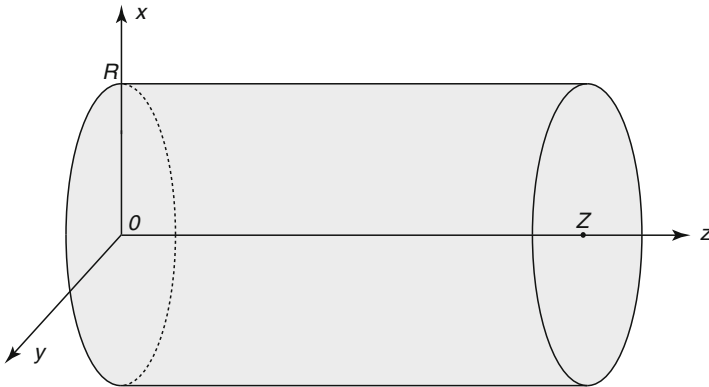
◨ **Figure 24**
Finite cylindrical system

3.6   2-D (r, z)-Geometry

In problems with 2-D (r, z)-symmetry,

1. The physical system is typically a finite cylinder consisting of spatial points (r, ϑ, z) with $0 \le r \le R, -\pi \le \vartheta \le \pi$, and $0 \le z \le Z$ (see ❯ *Fig. 24*).
2. The cross sections, internal isotropic source, and prescribed boundary conditions are independent of ϑ.
3. The prescribed incident boundary conditions are arbitrary functions of z, μ, and γ.

Thus, the system is symmetric through rotations of the spatial azimuthal angle ϑ (about the z-axis). The neutron angular flux will also have this symmetry, i.e., will be independent of ϑ:

$$\psi(\boldsymbol{x}, \boldsymbol{\Omega}) = \Psi(r, z, \mu, \gamma). \tag{114}$$

The (r, z)-*geometry transport equation* (and boundary conditions) can be obtained as a special case of the (r, ϑ, z)-geometry transport equations in which all quantities are independent of ϑ. Equations (112) and (113) yield:

$$\mu \frac{\partial \Psi}{\partial z}(r, z, \tilde{\boldsymbol{\Omega}}) + \sqrt{1 - \mu^2} \left(\cos \gamma \, \frac{\partial \Psi}{\partial r}(r, z, \tilde{\boldsymbol{\Omega}}) - \frac{\sin \gamma}{r} \frac{\partial \Psi}{\partial \gamma}(r, z, \tilde{\boldsymbol{\Omega}}) \right) + \tilde{\Sigma}_t(r, z) \Psi(r, z, \tilde{\boldsymbol{\Omega}})$$

$$= \int_{4\pi} \tilde{\Sigma}_s(r, z, \tilde{\boldsymbol{\Omega}} \cdot \tilde{\boldsymbol{\Omega}}') \Psi(r, z, \tilde{\boldsymbol{\Omega}}') \, d\tilde{\boldsymbol{\Omega}}' + \frac{\tilde{Q}(r, z)}{4\pi}, \quad 0 < r \le R, \ 0 \le z \le Z,$$
$$-1 \le \mu \le 1, \ -\pi \le \gamma \le \pi, \tag{115}$$

and:

$$\Psi(R, z, \mu, \gamma) = \Psi^b(z, \mu, \gamma), \ \ 0 \le z \le Z, \ -1 \le \mu \le 1, \ |\gamma| > \frac{\pi}{2}, \tag{116a}$$

$$\Psi(r, 0, \mu, \gamma) = \Psi^b(r, \mu, \gamma), \ \ 0 < r \le R, \ 0 < \mu \le 1, \ -\pi \le \gamma \le \pi, \tag{116b}$$

$$\Psi(r, Z, \mu, \gamma) = \Psi^b(r, \mu, \gamma), \ \ 0 < r \le R, \ -1 \le \mu < 0, \ -\pi \le \gamma \le \pi. \tag{116c}$$

The scattering integral in (115) can be written as in (111) or (112).

Equations (115) and (116) describe neutron transport in a finite cylindrical system with rotational symmetry.

3.7   1-D Cylindrical Geometry

In problems with 1-D cylindrical symmetry,

1. The physical system is an infinite cylinder consisting of spatial points (r, ϑ, z) with $0 \le r \le R$, $-\pi \le \vartheta \le \pi$, and $-\infty < z < \infty$.
2. The cross sections, internal isotropic source, and prescribed boundary conditions are independent of ϑ and z.
3. The prescribed incident boundary conditions are arbitrary functions of μ and γ.

Because the system is independent of ϑ and z, the neutron flux will also be independent of these variables:

$$\psi(\mathbf{x}, \mathbf{\Omega}) = \Psi(r, \mu, \gamma) = \Psi(r, \tilde{\mathbf{\Omega}}). \tag{117}$$

The *1-D cylindrical-geometry transport equation* (and boundary conditions) is a special case of the (r, z)-geometry transport equations in which all quantities are independent of z. Equations (115) and (116) yield:

$$\sqrt{1 - \mu^2} \left(\cos \gamma \frac{\partial \Psi}{\partial r}(r, \tilde{\mathbf{\Omega}}) - \frac{\sin \gamma}{r} \frac{\partial \Psi}{\partial \gamma}(r, \tilde{\mathbf{\Omega}}) \right) + \tilde{\Sigma}_t(r) \Psi(r, \tilde{\mathbf{\Omega}})$$

$$= \int_{4\pi} \tilde{\Sigma}_s(r, \tilde{\mathbf{\Omega}} \cdot \tilde{\mathbf{\Omega}}') \Psi(r, \tilde{\mathbf{\Omega}}') \, d\tilde{\Omega}' + \frac{\tilde{Q}(r)}{4\pi}, \quad 0 < r \le R, \quad -1 \le \mu \le 1, \quad -\pi \le \gamma \le \pi, \tag{118}$$

and:

$$\Psi(R, \mu, \gamma) = \Psi^b(\mu, \gamma), \quad -1 \le \mu \le 1, \quad |\gamma| > \frac{\pi}{2}. \tag{119}$$

The scattering integral in (118) can be written as in (111) or (112).

Equations (118) and (119) describe neutron transport in an infinite cylindrical system with rotational symmetry and no axial (z-) dependence. The equations have one spatial variable (r) and two angular variables (μ and γ). In contrast, the 1-D planar and 1-D spherical-geometry transport equations have one spatial variable and only one angular variable.

3.8 Discussion

We have derived several forms of the neutron transport equation for 3-D problems in which geometric symmetries cause the angular flux to depend on fewer than three independent spatial variables. This has been done only for the most widely used 2-D geometries: (x, y) and (r, z). Less important 2-D geometries, which are not treated here, are the two 2-D spherical geometries, cylindrical (ϑ, z)-geometry, and 2-D *helical* geometry (Larsen 2007). Also, we have not treated 3-D spherical geometry.

In the preceding derivations, we assumed for simplicity monoenergetic transport, no time-dependence, and no fission. However, it is straightforward to include these extra features.

We also assumed that in each geometry, the prescribed internal source Q is isotropic. This can immediately be relaxed to allow an internal anisotropic source whose spatial and angular dependences are the same as those allowed for the angular flux. For instance, in 1-D spherical geometry the angular flux is a function of r and μ, and one can include an internal anisotropic source, which is also a function of r and μ. Such sources arise naturally in multigroup problems, in which all the group angular fluxes have the same space-angle symmetry, and thus the source of neutrons that scatter into each group also share this symmetry.

In our derivations, we have not always stated the most general possible allowed geometric form of the spatial region V. For example, in 1-D spherical geometry, the physical system V was assumed to be the interior of a sphere of radius R. However, R could also be the *exterior* of a sphere of radius R, or, more generally, a *shell* consisting of points (r, ϑ, z) satisfying $R_0 \le r \le R_1$.

In these new cases, boundary conditions that prescribe the incident flux must be imposed on *all* physical boundaries.

Also, *reflecting* boundary conditions can be used along planes of geometric symmetry, and *periodic* boundary conditions are used to model one cell of an infinite periodic lattice. These and other types of boundary conditions are often employed in applications.

In all curvilinear geometries, the angular variables are expressed locally in space and change their value continuously as neutrons stream along flight paths. This gives rise to *angular derivative* terms in the neutron transport equation that significantly complicate the derivation of accurate numerical solutions (Lewis and Miller 1984). For example, the 1-D spherical-geometry transport equation (101) contains partial derivatives with respect to both r and μ. Mathematically, this leakage operator is a 2-D partial differential operator. Nonetheless, the historical tradition in the nuclear engineering community is to count only the spatial variables when describing a transport operator as 1-D, 2-D, or 3-D. Thus, the spherical-geometry transport equation is *called* a 1-D transport equation, even though it is has partial derivatives with respect to two independent variables.

4 Integral Equation for Neutron Transport

In this section, we derive the integral form of the transport equation (Bell and Glasstone 1970; Case and Zweifel 1967; Williams 1971), an alternate but equivalent description of the transport process embodied in the integrodifferential form that we have been discussing thus far. The integral transport equation can be derived using first flight kernels to relate the angular flux in an element of phase space to the neutron emission rate due to fixed, scattering, and fission sources everywhere in the medium, and to sources on the boundary. Here, though, we proceed directly from the differential part of the integrodifferential transport equation by noting that it is formally a linear first-order partial differential operator that can be inverted using standard techniques. The result is not an explicit solution for the angular flux, because the right side of the equation contains the scattering and fission sources, but is an alternate form of the Boltzmann equation, which has the form of an integral equation.

4.1 Integral Equation for the Angular Flux

We begin by compactly expressing the time- and energy-dependent general-geometry transport equation (46a) as:

$$\frac{1}{v}\frac{\partial\psi}{\partial t}(\boldsymbol{x},\boldsymbol{\Omega},E,t) + \boldsymbol{\Omega}\cdot\nabla\psi(\boldsymbol{x},\boldsymbol{\Omega},E,t) + \Sigma_t(\boldsymbol{x},E,t)\psi(\boldsymbol{x},\boldsymbol{\Omega},E,t) = Q(\boldsymbol{x},\boldsymbol{\Omega},E,t), \quad \boldsymbol{x}\in V,$$

$$(120a)$$

with the boundary condition (44) and initial condition (45a):

$$\psi(\boldsymbol{x},\boldsymbol{\Omega},E,t) = \psi^b(\boldsymbol{x},\boldsymbol{\Omega},E,t), \quad \boldsymbol{x}\in\partial V, \ \boldsymbol{\Omega}\cdot\boldsymbol{n} < 0, \ 0 < E < \infty, \ 0 < t, \qquad (120b)$$

$$\psi(\boldsymbol{x},\boldsymbol{\Omega},E,0) = \psi^i(\boldsymbol{x},\boldsymbol{\Omega},E), \quad \boldsymbol{x}\in V, \ \boldsymbol{\Omega}\in 4\pi, \ 0 < E < \infty. \qquad (120c)$$

The source Q in (120a), now including neutrons arising from inscatter and fission, is given by:

$$Q(\boldsymbol{x}, \boldsymbol{\Omega}, E, t) = \int_0^\infty \int_{4\pi} \Sigma_s(\boldsymbol{\Omega}' \cdot \boldsymbol{\Omega}, E' \to E)\psi(\boldsymbol{x}, \boldsymbol{\Omega}', E', t)\, d\Omega' dE'$$
$$+ \frac{\chi_p(E)}{4\pi} \int_0^\infty \int_{4\pi} \nu\Sigma_f(E')\psi(\boldsymbol{x}, \boldsymbol{\Omega}', E', t)\, d\Omega' dE' + \frac{1}{4\pi}Q(\boldsymbol{x}, E, t). \quad (121)$$
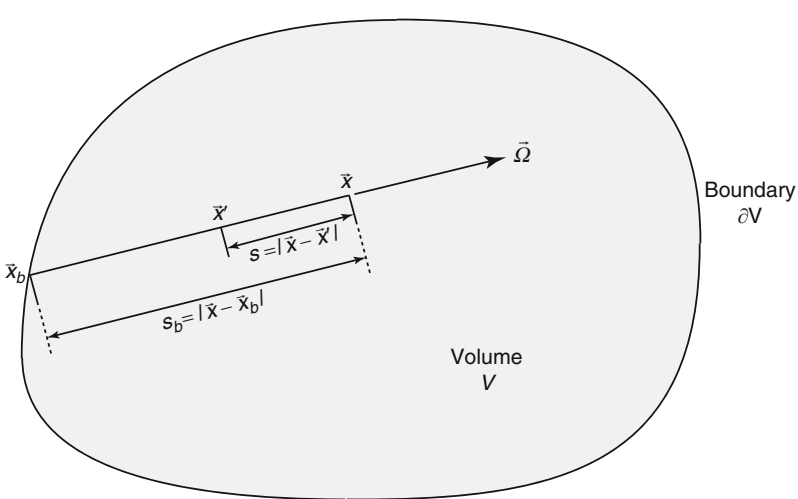
We ignore for the moment the fact that this source depends on the unknown angular flux and view (120) as a transport equation in a purely absorbing medium with a distributed source, and we seek an exact solution for the angular flux. To proceed in the general case, it is convenient to incorporate the initial condition as a source in the transport equation. Equation (120a) then reads:

$$\frac{1}{v}\frac{\partial\psi}{\partial t}(\boldsymbol{x}, \boldsymbol{\Omega}, E, t) + \boldsymbol{\Omega} \cdot \nabla\psi(\boldsymbol{x}, \boldsymbol{\Omega}, E, t) + \Sigma_t(\boldsymbol{x}, E, t)\psi(\boldsymbol{x}, \boldsymbol{\Omega}, E, t) = \widehat{Q}(\boldsymbol{x}, \boldsymbol{\Omega}, E, t), \quad \boldsymbol{x} \in V,$$
$$(122)$$

where:

$$\widehat{Q}(\boldsymbol{x}, \boldsymbol{\Omega}, E, t) = Q(\boldsymbol{x}, \boldsymbol{\Omega}, E, t) + \frac{1}{v}\delta(t)\psi^i(\boldsymbol{x}, \boldsymbol{\Omega}, E), \quad (123)$$

where $\widehat{Q}(\boldsymbol{x}, E, \boldsymbol{\Omega}, t) = \psi(\boldsymbol{x}, \boldsymbol{\Omega}, E, t) = 0$ for $t < 0$. The boundary condition remains as given by (120b).

We consider a point $\boldsymbol{x}' \in V$ that lies a distance s from $\boldsymbol{x} \in V$ along the direction $-\boldsymbol{\Omega}$, which intersects the boundary ∂V at a point $\boldsymbol{x}_b$, as shown in ❯ *Fig. 25*:
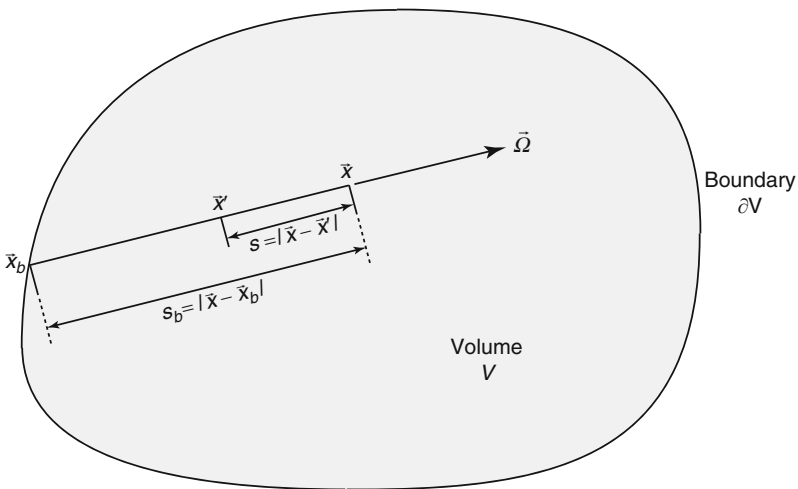
❒ **Figure 25**
Coordinates for the integral transport equation

Straightforward vector addition gives:

$$x' = x - s\Omega, \tag{124a}$$

$$x_b = x - s_b\Omega, \tag{124b}$$

where s_b is the distance from x to the boundary along the direction $-\Omega$. Similarly, if t is the time at which the neutron traveling along Ω is found at position x, then the neutron passed through position x' at the earlier time t' given by:

$$t' = t - \frac{s}{v}. \tag{125}$$

We now write (122) with respect to the independent variables (x', Ω, E, t'):

$$\frac{1}{v}\frac{\partial \psi}{\partial t'}(x', \Omega, E, t') + \Omega \cdot \nabla \psi(x', \Omega, E, t') + \Sigma_t(x', E, t')\psi(x', \Omega, E, t') = \widehat{Q}(x', \Omega, E, t'), \quad x' \in V, \tag{126}$$

where ∇ now operates on x', and we consider the derivative of the angular flux with respect to s:

$$
\begin{aligned}
-\frac{d}{ds}\psi(x', \Omega, E, t') &= -\frac{d}{ds}\psi\left(x - s\Omega, \Omega, E, t - \frac{s}{v}\right) \\
&= -\left[\frac{\partial t'}{\partial s}\frac{\partial \psi}{\partial t'} + \frac{\partial x'}{\partial s} \cdot \nabla \psi\right] \\
&= -\left[\frac{\partial \left(t - \frac{s}{v}\right)}{\partial s}\frac{\partial \psi}{\partial t'} + \frac{\partial (x - s\Omega)}{\partial s} \cdot \nabla \psi\right] \\
&= \frac{1}{v}\frac{\partial \psi}{\partial t'} + \Omega \cdot \nabla \psi.
\end{aligned}
\tag{127}
$$

Thus, the streaming operator in (126) is the total derivative or directional derivative along the path of the neutron. We can then rewrite (126) as:

$$-\frac{d\psi}{ds}\left(x - s\Omega, \Omega, E, t - \frac{s}{v}\right) + \Sigma_t\left(x - s\Omega, E, t - \frac{s}{v}\right)\psi\left(x - s\Omega, \Omega, E, t - \frac{s}{v}\right)$$
$$= \widehat{Q}\left(x - s\Omega, \Omega, E, t - \frac{s}{v}\right), \quad 0 \le s \le s_b, \tag{128}$$

where:

$$\widehat{Q}\left(x - s\Omega, \Omega, E, t - \frac{s}{v}\right) = Q\left(x - s\Omega, \Omega, E, t - \frac{s}{v}\right) + \frac{1}{v}\delta\left(t - \frac{s}{v}\right)\psi^i(x - s\Omega, \Omega, E). \tag{129}$$

Equation (128) is a first-order ordinary differential equation in s, which can be solved using the integrating factor method. Multiplying (128) by the integrating factor:

$$\exp\left[-\int_0^s \Sigma_t\left(x - s''\Omega, E, t - \frac{s''}{v}\right)ds''\right]$$

and manipulating the resulting equation in the usual way gives:

$$
\frac{d}{ds}\left[\exp\left(-\int_0^s \Sigma_t\left(x - s''\boldsymbol{\Omega}, E, t - \frac{s''}{v}\right) ds''\right)\psi\left(x - s\boldsymbol{\Omega}, \boldsymbol{\Omega}, E, t - \frac{s}{v}\right)\right]
$$

$$
= -\widehat{Q}\left(x - s\boldsymbol{\Omega}, \boldsymbol{\Omega}, E, t - \frac{s}{v}\right)\exp\left[-\int_0^s \Sigma_t\left(x - s''\boldsymbol{\Omega}, E, t - \frac{s''}{v}\right) ds''\right]. \tag{130}
$$

Integrating (130) between 0 and s and reorganizing terms yields, after a bit of algebra:

$$
\psi(x, \boldsymbol{\Omega}, E, t) = \exp\left(-\int_0^s \Sigma_t\left(x - s''\boldsymbol{\Omega}, E, t - \frac{s''}{v}\right) ds''\right)\psi\left(x - s\boldsymbol{\Omega}, \boldsymbol{\Omega}, E, t - \frac{s}{v}\right)
$$

$$
+ \int_0^s \widehat{Q}\left(x - s'\boldsymbol{\Omega}, \boldsymbol{\Omega}, E, t - \frac{s'}{v}\right)\exp\left[-\int_0^{s'} \Sigma_t\left(x - s''\boldsymbol{\Omega}, E, t - \frac{s''}{v}\right) ds''\right] ds'. \tag{131}
$$

Evaluating (131) at the boundary point $s = s_b$ and noting that:

$$
\psi\left(x - s_b\boldsymbol{\Omega}, \boldsymbol{\Omega}, E, t - \frac{s_b}{v}\right) = \psi\left(x_b, \boldsymbol{\Omega}, E, t - \frac{s_b}{v}\right),
$$

$$
= \psi^b\left(x_b, \boldsymbol{\Omega}, E, t - \frac{s_b}{v}\right) U(vt - s_b), \tag{132}
$$

where $U(\cdot)$ is the Heaviside unit step function, we obtain:

$$
\psi(x, \boldsymbol{\Omega}, E, t) = \exp\left(-\int_0^{s_b} \Sigma_t\left(x - s''\boldsymbol{\Omega}, E, t - \frac{s''}{v}\right) ds''\right)\psi^b\left(x_b, \boldsymbol{\Omega}, E, t - \frac{s_b}{v}\right) U(vt - s_b)
$$

$$
+ \int_0^{s_b} \widehat{Q}\left(x - s'\boldsymbol{\Omega}, \boldsymbol{\Omega}, E, t - \frac{s'}{v}\right)\exp\left[-\int_0^{s'} \Sigma_t\left(x - s''\boldsymbol{\Omega}, E, t - \frac{s''}{v}\right) ds''\right] ds'. \tag{133}
$$

The Heaviside function $U(vt - s_b)$ in (133) accounts for the finite neutron speed; a source neutron originating at the boundary and traveling at speed v cannot stream a distance s_b to arrive at position x at time t if $vt < s_b$.

Next, we note that the integral over s' in (133) for the initial condition part of the source $\widehat{Q}$ can be explicitly carried out to give:

$$
\int_0^{s_b} \frac{1}{v}\delta\left(t - \frac{s'}{v}\right)\psi^i(x - s'\boldsymbol{\Omega}, \boldsymbol{\Omega}, E)\exp\left[-\int_0^{s'} \Sigma_t\left(x - s''\boldsymbol{\Omega}, E, t - \frac{s''}{v}\right) ds''\right] ds'
$$

$$
= \psi^i(x - vt\boldsymbol{\Omega}, \boldsymbol{\Omega}, E)\exp\left[-\int_0^{vt} \Sigma_t\left(x - s''\boldsymbol{\Omega}, E, t - \frac{s''}{v}\right) ds''\right] U(s_b - vt), \tag{134}
$$

where well-known properties of the delta function have been used. Isolating this term in (133) and noting from (124a) and (124b) that:

$$
s_b = |x - x_b|, \tag{135}
$$

we obtain:

$$
\psi(\boldsymbol{x}, \boldsymbol{\Omega}, E, t) = \psi^b\left(\boldsymbol{x}_b, \boldsymbol{\Omega}, E, t - \frac{|\boldsymbol{x} - \boldsymbol{x}_b|}{v}\right) \exp\left(-\int_0^{|\boldsymbol{x}-\boldsymbol{x}_b|} \Sigma_t\left(\boldsymbol{x} - s''\boldsymbol{\Omega}, E, t - \frac{s''}{v}\right) ds''\right)
$$

$$
\times\, U(vt - |\boldsymbol{x} - \boldsymbol{x}_b|) + \psi^i(\boldsymbol{x} - vt\boldsymbol{\Omega}, \boldsymbol{\Omega}, E) \exp\left(-\int_0^{vt} \Sigma_t\left(\boldsymbol{x} - s''\boldsymbol{\Omega}, E, t - \frac{s''}{v}\right) ds''\right)
$$

$$
\times\, U(|\boldsymbol{x} - \boldsymbol{x}_b| - vt) + \int_0^{|\boldsymbol{x}-\boldsymbol{x}_b|} Q\left(\boldsymbol{x} - s'\boldsymbol{\Omega}, \boldsymbol{\Omega}, E, t - \frac{s'}{v}\right)
$$

$$
\times\, \exp\left(-\int_0^{s'} \Sigma_t\left(\boldsymbol{x} - s''\boldsymbol{\Omega}, E, t - \frac{s''}{v}\right) ds''\right) ds'. \tag{136}
$$

To obtain the final result, we transform the line integral in the last term in (136) to a volume integral. To effect this transformation, we first introduce an angular direction variable $\boldsymbol{\Omega}'$ and express this term as:

$$
\int_{4\pi} \int_0^{|\boldsymbol{x}-\boldsymbol{x}_b|} \delta(\boldsymbol{\Omega} - \boldsymbol{\Omega}') Q\left(\boldsymbol{x} - s'\boldsymbol{\Omega}', \boldsymbol{\Omega}', E, t - \frac{s'}{v}\right)
$$

$$
\times \exp\left(-\int_0^{s'} \Sigma_t\left(\boldsymbol{x} - s''\boldsymbol{\Omega}', E, t - \frac{s''}{v}\right) ds''\right) ds' d\boldsymbol{\Omega}'. \tag{137}
$$

Defining the intermediate position vector:

$$
\boldsymbol{x}' = \boldsymbol{x} - s'\boldsymbol{\Omega}', \tag{138}
$$

we note that an elementary volume about $\boldsymbol{x}'$ can be written as:

$$
dV' = (s'd\theta')(s'\sin\theta' d\phi')ds' = s'^2 ds' \sin\theta' d\theta' d\phi' = s'^2 ds' d\boldsymbol{\Omega}'. \tag{139}
$$

Further, noting from (138) that $s' = |\boldsymbol{x} - \boldsymbol{x}'|$, (139) yields:

$$
ds' d\boldsymbol{\Omega}' = \frac{dV'}{s'^2} = \frac{dV'}{|\boldsymbol{x} - \boldsymbol{x}'|^2}. \tag{140}
$$

Introducing these results into (136), we obtain:

$$
\psi(\boldsymbol{x}, \boldsymbol{\Omega}, E, t) = \psi^b\left(\boldsymbol{x}_b, \boldsymbol{\Omega}, E, t - \frac{|\boldsymbol{x} - \boldsymbol{x}_b|}{v}\right) \exp\left(-\int_0^{|\boldsymbol{x}-\boldsymbol{x}_b|} \Sigma_t\left(\boldsymbol{x} - s''\boldsymbol{\Omega}, E, t - \frac{s''}{v}\right) ds''\right)
$$

$$
\times\, U(vt - |\boldsymbol{x} - \boldsymbol{x}_b|) + \psi^i(\boldsymbol{x} - vt\boldsymbol{\Omega}, \boldsymbol{\Omega}, E) \exp\left(-\int_0^{vt} \Sigma_t\left(\boldsymbol{x} - s''\boldsymbol{\Omega}, E, t - \frac{s''}{v}\right) ds''\right)
$$

$$
\times\, U(|\boldsymbol{x} - \boldsymbol{x}_b| - vt) + \int_V Q\left(\boldsymbol{x}', \boldsymbol{\Omega}', E, t - \frac{|\boldsymbol{x} - \boldsymbol{x}'|}{v}\right)
$$

$$
\times\, \frac{\exp\left[-\int_0^{|\boldsymbol{x}-\boldsymbol{x}'|} \Sigma_t\left(\boldsymbol{x} - s''\boldsymbol{\Omega}', E, t - \frac{s''}{v}\right) ds''\right]}{|\boldsymbol{x} - \boldsymbol{x}'|^2} \delta(\boldsymbol{\Omega} - \boldsymbol{\Omega}') dV', \tag{141}
$$

where we have noted that the integration domain $[0, s_b] \times [0, \pi] \times [0, 2\pi]$ is just the volume V of the medium.

Equation (141), with the source given by (121), represents the most general form of the integral transport equation for the angular flux. It is valid for an arbitrary boundary source, initial condition, and fixed source. Although complicated in appearance, the terms in this equation each have a simple physical interpretation. To see this, we first note that the integral:

$$\tau(\boldsymbol{x}, \boldsymbol{x}', \boldsymbol{\Omega}, E, t) = \int_0^{|\boldsymbol{x}-\boldsymbol{x}'|} \Sigma_t\left(\boldsymbol{x} - s''\boldsymbol{\Omega}, E, t - \frac{s''}{v}\right) ds'', \tag{142}$$

is the *optical distance* (the number of mean free paths) that a neutron with energy E experiences while traveling from $\boldsymbol{x}'$ (at time $t' = t - |\boldsymbol{x} - \boldsymbol{x}'|/v$) to $\boldsymbol{x}$ (at time t) in the direction of flight $\boldsymbol{\Omega} = (\boldsymbol{x} - \boldsymbol{x}')/|\boldsymbol{x} - \boldsymbol{x}'|$. The exponential factor $\exp[-\tau(\cdots)]$ appearing in (141) is the probability that a neutron will not suffer a collision over this distance, while $\exp[-\tau(\cdots)]/|\boldsymbol{x}-\boldsymbol{x}'|^2$ is the free flight kernel that additionally accounts for geometric spreading of a point source of neutrons. Thus, the first term in (141) describes the contribution to the angular flux at $(\boldsymbol{x}, \boldsymbol{\Omega}, E, t)$ from neutrons that orginated at the boundary $\boldsymbol{x}_b$ with energy E and direction $\boldsymbol{\Omega}$ at an earlier time $|\boldsymbol{x} - \boldsymbol{x}_b|/v$ and arrive at $\boldsymbol{x}$ without suffering any collisions. The second term describes neutrons from the initial distribution with energy E and direction $\boldsymbol{\Omega}$ that are initially located at $\boldsymbol{x} - vt\boldsymbol{\Omega}$ and experience no collisions during the subsequent time interval t while streaming to $\boldsymbol{x}$. The third term accounts for source neutrons, as well as neutrons born in scattering and fission collisions with energy E and direction $\boldsymbol{\Omega}$ over the entire medium at an earlier time $|\boldsymbol{x} - \boldsymbol{x}_b|/v$ that subsequently arrive at $\boldsymbol{x}$ unattenuated.

4.2   The Integral Equation for the Scalar Flux

The complexity of the integral equation is greatly reduced, and its utility greatly enhanced, when scattering is isotropic and a steady state is assumed. Under these conditions, (141) can be reduced without approximation to an integral equation for the scalar flux. To show this, we observe that the source Q given by (121) becomes independent of $\boldsymbol{\Omega}$ and simplifies to:

$$Q(\boldsymbol{x}, \boldsymbol{\Omega}, E) = \frac{1}{4\pi} \int_0^\infty \Sigma_s(E' \to E)\phi(\boldsymbol{x}, E')\, dE'$$
$$+ \frac{\chi_p(E)}{4\pi} \int_0^\infty v\Sigma_f(E')\phi(\boldsymbol{x}, E')\, dE' + \frac{1}{4\pi} Q(\boldsymbol{x}, E). \tag{143}$$

Further, assuming a free surface condition, i.e., $\psi^b = 0$ and a homogeneous medium, the integral equation (141) becomes:

$$\psi(\boldsymbol{x}, \boldsymbol{\Omega}, E) = \int_V \frac{\exp\left(-\Sigma_t(E)|\boldsymbol{x} - \boldsymbol{x}'|\right)}{|\boldsymbol{x} - \boldsymbol{x}'|^2} Q(\boldsymbol{x}', E)\, \delta(\boldsymbol{\Omega} - \boldsymbol{\Omega}')dV'. \tag{144}$$

Integrating (144) over $\boldsymbol{\Omega}$ and substituting (143) into (144), we obtain the final result:

$$\phi(\boldsymbol{x}, E) = \int_V \frac{\exp\left(-\Sigma_t(E)|\boldsymbol{x} - \boldsymbol{x}'|\right)}{4\pi|\boldsymbol{x} - \boldsymbol{x}'|^2} \int_0^\infty dE'\left[\Sigma_s(E' \to E) + \chi_p(E)v\Sigma_f(E')\right]$$
$$\times \phi(\boldsymbol{x}', E')dV' + \int_V \frac{\exp\left(-\Sigma_t(E)|\boldsymbol{x} - \boldsymbol{x}'|\right)}{4\pi|\boldsymbol{x} - \boldsymbol{x}'|^2} Q(\boldsymbol{x}', E)dV'. \tag{145}$$

This form of the integral equation, which has the scalar flux as the unknown, is known as *Peierls' equation*. Although stated above for a homogeneous medium with a free surface, it is apparent from the foregoing that Peierls' equation can be modified to account for boundary sources and material inhomogeneities.

4.3   Discussion

Peierls' equation is used in reactor physics for computing collision and escape probabilities in the context of fuel assembly homogenization. *Peierls' equation* has the advantage that the angular part of the flux is exactly treated, so that quadrature approximations of angular integrals are not necessary in numerical work. Moreover, boundary conditions are explicitly incorporated into the equation and therefore are not affected by numerical schemes devised to approximate the integral operator. However, unlike the integrodifferential transport equation, the integral equation is spatially nonlocal, which makes it less efficient for numerical solution.

At a more mathematical level, the integral equation is used in establishing the existence and uniqueness of solutions to the integrodifferential equation and, when expressed in terms of the collision density, in establishing rigorous results for convergence of the Monte Carlo method. Finally, we note that (145) can be reduced to the familiar forms of Peierls' equation appropriate in slab, spherically symmetric, and cylindrically symmetric geometries by suitable reductions of the free flight kernel.

5   The Adjoint Neutron Transport Equation

The transport operator is *non-self-adjoint*, and in many circumstances it is useful to formulate and solve the *adjoint transport equation*. This "dual" description is a powerful and enriching feature of the theory of linear operators and has been effectively exploited in reactor physics and neutron transport theory (Bell and Glasstone 1970; Case and Zweifel 1967; Henry 1975; Weinberg and Wigner 1958). Moreover, although the adjoint flux is a mathematical artifice, it can be interpreted physically as an "importance function" that quantifies the relative contribution of neutrons to a desired physical quantity (Lewins 1965). Adjoint formulations underlie the development of perturbation theory and variational methods (Bell and Glasstone 1970; Lewins 1968; Pomraning 1967a,b; Stacey 1974), sensitivity and uncertainty analysis (Cacuci 2003), and play a prominent role in the construction of a priori error estimates in the deterministic numerical solution of the transport equation. Also, neutron importance maps generated from the adjoint flux can be used to develop efficient variance reduction techniques that can result in dramatic improvements in the efficiency of Monte Carlo simulation methods (Van Riper et al. 1997). Finally, in criticality problems, the adjoint fundamental eigenfunction is pivotal in developing a rigorous basis for reduced-order models, such as the point kinetics equations.

In this section, we derive the equation that is the mathematical adjoint of the general integrodifferential transport equation given by (46). For reasons that will become apparent below, we refer to the latter as the *forward transport equation*. We show how adjoint boundary and initial conditions can be assigned that are consistent with the importance interpretation of the adjoint angular flux, and we close with a presentation on forward and adjoint Green's functions.

A rigorous development of the theory of adjoint operators would rely heavily on techniques from functional analysis, a level of abstraction that is beyond the scope of this book. Instead, we adopt a more pedestrian approach that relies on explicit construction and emphasizes physical interpretation over mathematical rigor.

5.1 Definitions

We begin by defining the inner product, also known as the scalar product, of two real functions u and w of the phase space and time coordinates $(\vec{x}, \Omega, E, t)$ as:

$$\langle u, w \rangle = \int_0^T \int_0^\infty \int_R \int_{4\pi} u(\vec{x}, \Omega, E, t)\, w(\vec{x}.\Omega, E, t)\, d\Omega dV dE dt. \tag{146}$$

The integration domain is the phase space covering the volume of the body, the surface of the unit sphere, an allowable range of energies, and a time span which in principle can be infinite. The restriction to real functions is not unreasonable, since the functions encountered in neutronics applications, such as cross sections, sources, neutron number, angular flux, neutron importance, etc., are real and have well-defined physical interpretations. Moreover, the operators that act on these functions are also real. Smoothness and continuity of all functions and sufficient orders of their derivatives is tacitly assumed, and all mathematical operations employed are assumed to be valid. Useful properties of the inner product that follow, and which will be applied repeatedly in the ensuing, include symmetry, linearity, and homogeneity. These properties are encapsulated in the following statements:

$$\langle u, w \rangle = \langle w, u \rangle, \tag{147}$$

$$\langle \alpha_1 u_1 + \alpha_2 u_2, \alpha_3 w \rangle = \alpha_1 \alpha_3 \langle u_1, w \rangle + \alpha_2 \alpha_3 \langle u_2, w \rangle, \tag{148}$$

where α_1, α_2, and α_3 are real scalars. These properties of the inner product must be modified if the functions of interest are not real.

Given a linear operator $\mathcal{L}$, which may be differential, integral, or integro-differential, two real functions u and w, and an inner product, the *adjoint* of this operator, denoted by $\mathcal{L}^\dagger$, is defined by the inner-product identity:

$$\langle w, \mathcal{L}u \rangle = \langle u, \mathcal{L}^\dagger w \rangle. \tag{149}$$

Besides serving as a formal definition of an adjoint operator, this identity also defines an algorithm for the explicit construction of $\mathcal{L}^\dagger$. In this context, it is understood that all necessary elementary operations from calculus (differentiation rules, integration by parts, switching orders of integration, manipulating dummy variables) are applied until the function u stands freely under the inner product while w is acted upon by an operator. The latter operator is the adjoint operator. If $\mathcal{L}$ is either entirely or partially differential in form, boundary terms will arise during this process, and these must be dealt with to complete the adjoint formulation. Strictly

speaking, $\mathcal{L}^\dagger$ without regard to the boundary terms is referred to as the *formal adjoint* of $\mathcal{L}$, and the identity equation (149) is more precisely expressed as:

$$\langle w, \mathcal{L}u \rangle = P[u, w] + \langle u, \mathcal{L}^\dagger w \rangle, \tag{150}$$

where P denotes a boundary functional, also known as the bilinear concomitant. When $\mathcal{L}^\dagger = \mathcal{L}$, we say that the operator $\mathcal{L}$ is *formally self-adjoint*. As we shall be treating all boundary terms explicitly, we drop the qualifying "formal" and, in what follows, simply refer to $\mathcal{L}^\dagger$ as the adjoint operator.

5.2   Illustrative Example

Before proceeding with the derivation of the adjoint of the transport operator, it is instructive to apply the process to a 1-D second-order differential operator. Although this is done here for illustrative purposes, it is worth pointing out that the diffusion approximation to the transport equation and heavy gas models in neutron thermalization are described by second-order differential operators in spatial and energy variables, respectively. Thus, let us consider $\mathcal{L}$ to be defined by:

$$\mathcal{L}u = a_2(x)\frac{d^2u(x)}{dx^2} + a_1(x)\frac{du(x)}{dx} + a_0(x)u(x); \quad x \in [a, b], \tag{151}$$

with the inner product:

$$\langle u, w \rangle = \int_a^b u(x)w(x)dx. \tag{152}$$

Suitable boundary conditions on $u(x)$ are presumed prescribed at $x = a$ and $x = b$, and the coefficients a_0, a_1, and a_2 are specified functions of x. Proceeding, we multiply (151) by another function $w(x)$ and integrate over the domain of x. Noting the linearity of the inner product, the resulting expression may be written as a sum of inner products of w with the individual components of $\mathcal{L}$:

$$\begin{aligned} \langle w, \mathcal{L}u \rangle &= \langle w, \mathcal{L}_2 u \rangle + \langle w, \mathcal{L}_1 u \rangle + \langle w, \mathcal{L}_0 u \rangle \\ &= \int_a^b w(x)\, a_2(x)\frac{d^2u(x)}{dx^2}dx + \int_a^b w(x)\, a_1(x)\frac{du(x)}{dx}dx \\ &\quad + \int_a^b w(x)\, a_0(x)u(x)dx. \end{aligned} \tag{153}$$

We consider each term independently and manipulate the integrands such that $u(x)$ is freestanding. Beginning with the last term on the right, we note that since multiplication is a commutative operation, we can write simply:

$$\begin{aligned} \langle w, \mathcal{L}_0 u \rangle &= \int_a^b w(x)\, a_0(x)u(x)dx \\ &= \int_a^b u(x)\, a_0(x)w(x)dx \\ &= \left\langle u, \mathcal{L}_0^\dagger w \right\rangle \equiv \langle u, \mathcal{L}_0 w \rangle. \end{aligned} \tag{154a}$$

This shows that the operation of multiplication is self-adjoint. Next, we consider the term involving the first derivative of u and integrate by parts:

$$
\begin{aligned}
\langle w, \mathcal{L}_1 u \rangle &= \int_a^b w(x)\, a_1(x) \frac{du(x)}{dx}\, dx \\
&= \left[w(x) a_1(x) u(x) \right]_a^b - \int_a^b u(x)\, \frac{d}{dx}\left[a_1(x) w(x) \right] dx \\
&= \left[w(x) a_1(x) u(x) \right]_a^b + \int_a^b u(x) \left\{ -\frac{d}{dx}\left[a_1(x) w(x) \right] \right\} dx \\
&= \left[w(x) a_1(x) u(x) \right]_a^b + \left\langle u, \mathcal{L}_1^\dagger w \right\rangle.
\end{aligned}
\tag{154b}
$$

This shows that a first-order differential operator is non-self-adjoint. However, when $a_1 = $ constant, i.e., when $\mathcal{L}_1$ is a pure first derivative, we have the simple relationship $\mathcal{L}_1^\dagger = -\mathcal{L}_1$. We consider finally the term involving the second derivative of u and integrate by parts twice:

$$
\begin{aligned}
\langle w, \mathcal{L}_2 u \rangle &= \int_a^b w(x)\, a_2(x) \frac{d^2 u(x)}{dx^2}\, dx \\
&= \left[w(x) a_2(x) \frac{du(x)}{dx} \right]_a^b - \int_a^b \frac{du(x)}{dx} \frac{d}{dx}\left[a_2(x) w(x) \right] dx \\
&= \left[w(x) a_2(x) \frac{du(x)}{dx} - u(x) \frac{d}{dx}\left[a_2(x) w(x) \right] \right]_a^b + \int_a^b u(x) \frac{d^2}{dx^2}\left[a_2(x) w(x) \right] dx \\
&= \left[w(x) a_2(x) \frac{du(x)}{dx} - u(x) \frac{d}{dx}\left[a_2(x) w(x) \right] \right]_a^b + \left\langle u, \mathcal{L}_2^\dagger w \right\rangle.
\end{aligned}
\tag{154c}
$$

This shows that, in general, a second-order differential operator is non-self-adjoint. However, there are two circumstances under which $\mathcal{L}_2$ is self-adjoint: (i) when $a_2 = $ constant, i.e., when $\mathcal{L}_2$ is a pure second derivative, and (ii) when the second-order differential operator appears in the symmetric form:

$$
\mathcal{L}_2 u = \frac{d}{dx}\left[a_2(x) \frac{du(x)}{dx} \right].
\tag{155}
$$

Combining (154) and inserting them into (153), we obtain for the adjoint of a general second-order ordinary differential operator:

$$
\mathcal{L}^\dagger w = \frac{d^2}{dx^2}\left[a_2(x) w(x) \right] - \frac{d}{dx}\left[a_1(x) w(x) \right] + a_0(x) w(x); \quad x \in [a, b].
\tag{156}
$$

We remlark that although the operator defined by (151) is non-self-adjoint, it is well known and readily verified that any second-order differential operator can be converted into the self-adjoint form:

$$
\mathcal{L} u = \frac{d}{dx}\left[p(x) \frac{du(x)}{dx} \right] + r(x)\, u(x),
\tag{157}
$$

by a suitable transformation of the coefficients. To complete this illustration, it is necessary to comment on the boundary functional associated with $\mathcal{L}$, which is given by:

$$P[u, w] = \left[w(x) a_2(x) \frac{du(x)}{dx} - u(x) \left(\frac{d}{dx} [a_2(x)w(x)] - a_1(x)w(x) \right) \right]_a^b. \quad (158)$$

Since u represents a physical quantity (such as the neutron scalar flux, chemical concentration, or temperature) that satisfies a well-posed mathematical model, a sufficient number of boundary conditions are presumably available. In the above example, these may take the form of u and/or its first derivative being specified at one or the other boundary $x = a$ and $x = b$. However, the adjoint function w is an arbitrary function (assumed sufficiently smooth) with no apparent physical attribute on which to base the assignment of boundary conditions. It will be shown below that a consistent set of boundary conditions can be obtained by requiring the boundary functional $P[u, w]$ to vanish. Thus, in the above example, if u satisfies:

$$u(a) = 0, \quad (159a)$$

$$u(b) = 0, \quad (159b)$$

then, $P[u, w]$ will vanish if:

$$w(a) = 0, \quad (160a)$$

$$w(b) = 0. \quad (160b)$$

On the other hand, if u satisfies:

$$\frac{du}{dx}\Big|_a = 0, \quad (161a)$$

$$\frac{du}{dx}\Big|_b = 0, \quad (161b)$$

then for $P[u, w]$ to vanish, w must satisfy the mixed boundary conditions:

$$\frac{d}{dx} [a_2(x)w(x)]_a - a_1(a)w(a) = 0, \quad (162a)$$

$$\frac{d}{dx} [a_2(x)w(x)]_b - a_1(b)w(b) = 0. \quad (162b)$$

Similarly, mixed boundary conditions on u, i.e., a linear combination of (159a, 159b) and (161a, 162b), yield mixed boundary conditions on w. Inhomogeneous boundary conditions and inhomogeneous terms (sources) can also be accommodated, as is demonstrated below for the adjoint neutron transport equation. Finally, if the operator is self-adjoint and the boundary conditions for u and w are identical, the problem is said to be self-adjoint, otherwise it is non-self-adjoint.

We close by remarking that the adjoints of 2-D and 3-D second-order differential operators can be similarly derived, employing Green's identities in lieu of integration by parts.

5.3   The Adjoint Transport Equation

We now apply the procedure developed above to derive the adjoint of the time-dependent forward transport equation, which we recall from (46) is:

$$
\frac{1}{v}\frac{\partial \psi}{\partial t}(x, \Omega, E, t) + \Omega \cdot \nabla \psi(x, \Omega, E, t) + \Sigma_t(E)\psi(x, \Omega, E, t)
$$

$$
= \int_0^\infty \int_{4\pi} \Sigma_s(\Omega' \cdot \Omega, E' \to E)\psi(x, \Omega', E', t)\, d\Omega' dE'
$$

$$
+ \frac{\chi_p(E)}{4\pi}\int_0^\infty \int_{4\pi} v\Sigma_f(E')\psi(x, \Omega', E', t)\, d\Omega' dE' + \frac{1}{4\pi}Q(x, E, t), \tag{163a}
$$

subject to the boundary condition and initial conditions:

$$
\psi(x, \Omega, E, t) = \psi^b(x, \Omega, E, t), \quad x \in \partial V, \ \Omega \cdot n < 0, \ 0 < E < \infty, \ 0 < t < T, \tag{163b}
$$

$$
\psi(x, \Omega, E, 0) = \psi^i(x, \Omega, E), \quad x \in V, \ \Omega \in 4\pi, \ 0 < E < \infty. \tag{163c}
$$

It is convenient to express (163a) in the compact form:

$$
\mathcal{L}\psi = \mathcal{L}_t\psi + \mathcal{L}_l\psi + \mathcal{L}_r\psi - \mathcal{L}_s\psi - \mathcal{L}_f\psi = Q, \tag{164}
$$

where components of $\mathcal{L}$ symbolically describe time evolution, free streaming or leakage, removal (outscatter and absorption), inscatter, and fission operators, respectively, and Q is the fixed source. Proceeding as outlined earlier, we take the inner product of an auxilliary function $\psi^\dagger(x, \Omega, E, t)$ with $\mathcal{L}\psi$ and define the adjoint operator $\mathcal{L}^\dagger$ through the inner-product identity:

$$
\langle \psi^\dagger, \mathcal{L}\psi \rangle = P\left[\psi, \psi^\dagger\right] + \langle \psi, \mathcal{L}^\dagger\psi^\dagger \rangle, \tag{165}
$$

where we have explicitly noted that boundary terms arise from the differential components of the transport operator. Inserting (164) into (165) and noting the linearity of $\mathcal{L}$, we can write:

$$
\langle \psi^\dagger, \mathcal{L}\psi \rangle = \left\langle \psi, \mathcal{L}_t^\dagger\psi^\dagger \right\rangle + \left\langle \psi, \mathcal{L}_l^\dagger\psi^\dagger \right\rangle + \left\langle \psi, \mathcal{L}_r^\dagger\psi^\dagger \right\rangle - \left\langle \psi, \mathcal{L}_s^\dagger\psi^\dagger \right\rangle - \left\langle \psi, \mathcal{L}_f^\dagger\psi^\dagger \right\rangle. \tag{166}
$$

We begin our treatment with the simplest term, namely, the removal term:

$$
\langle \psi^\dagger, \mathcal{L}_r\psi \rangle = \int_0^T dt \int_0^\infty dE \int_{4\pi} d\Omega \int_V dV\, \psi^\dagger(x, \Omega, E, t)\Sigma_t(E)\psi(x, \Omega, E, t)
$$

$$
= \int_0^T dt \int_0^\infty dE \int_{4\pi} d\Omega \int_V dV\, \psi(x, \Omega, E, t)\Sigma_t(E)\psi^\dagger(x, \Omega, E, t)
$$

$$
= \left\langle \psi, \mathcal{L}_r^\dagger\psi^\dagger \right\rangle = \left\langle \psi, \mathcal{L}_r\psi^\dagger \right\rangle. \tag{167a}
$$

Thus, the removal term is trivially self-adjoint. Next, we consider the time evolution term and integrate by parts:

$$
\begin{aligned}
\langle \psi^\dagger, \mathcal{L}_t \psi \rangle &= \int_0^\infty dE \int_{4\pi} d\Omega \int_V dV \int_0^T dt\, \psi^\dagger(x,\Omega,E,t) \frac{1}{v} \frac{\partial \psi}{\partial t}(x,\Omega,E,t) \\
&= \int_0^\infty dE \int_{4\pi} d\Omega \int_V dV \left[\frac{1}{v} \psi^\dagger(x,\Omega,E,t)\psi(x,\Omega,E,t) \right]_0^T \\
&\quad + \int_0^T dt \int_0^\infty dE \int_{4\pi} d\Omega \int_V dV \psi^\dagger(x,\Omega,E,t) \left[-\frac{1}{v}\frac{\partial \psi^\dagger}{\partial t}(x,\Omega,E,t) \right] \\
&= P_t[\psi,\psi^\dagger] + \left\langle \psi, \mathcal{L}_t^\dagger \psi^\dagger \right\rangle.
\end{aligned}
\tag{167b}
$$

The boundary functional P_t denotes a restricted inner product, wherein the time variable is constrained to take its initial and final values only. Being a first-order differential operator, the time evolution operator is non-self-adjoint. Proceeding likewise for the streaming operator, we first note the vector identity:

$$
\psi^\dagger \mathcal{L}_l \psi = \psi^\dagger \Omega \cdot \nabla \psi = \nabla \cdot \left(\Omega \psi \psi^\dagger \right) - \psi \Omega \cdot \nabla \psi^\dagger
$$

and apply the divergence theorem to get:

$$
\begin{aligned}
\langle \psi^\dagger, \mathcal{L}_l \psi \rangle &= \int_0^T dt \int_0^\infty dE \int_{4\pi} d\Omega \int_V dV \left[\nabla \cdot \left(\Omega \psi \psi^\dagger \right) - \psi \Omega \cdot \nabla \psi^\dagger \right] \\
&= \int_0^T dt \int_0^\infty dE \int_{4\pi} d\Omega \int_{\partial V} dA\, n \cdot \Omega\, \psi(x,\Omega,E,t)\, \psi^\dagger(x,\Omega,E,t) \\
&\quad + \int_0^T dt \int_0^\infty dE \int_{4\pi} d\Omega \int_V dV \psi(x,\Omega,E,t) \left[-\Omega \cdot \nabla \psi^\dagger \right] \\
&= P_l[\psi,\psi^\dagger] + \left\langle \psi, \mathcal{L}_l^\dagger \psi^\dagger \right\rangle.
\end{aligned}
\tag{167c}
$$

The boundary functional P_l denotes a restricted inner product, wherein the spatial variable is constrained to lie on the surface of the body. We observe that the streaming operator is also non-self-adjoint.

We consider now the adjoint of the inscatter operator, which is an integral operator. The significance of this is that boundary terms will not arise. Thus:

$$
\begin{aligned}
\langle \psi^\dagger, \mathcal{L}_s \psi \rangle &= \int_0^T dt \int_V dV \int_0^\infty dE \int_{4\pi} d\Omega \\
&\quad \psi^\dagger(x,\Omega,E,t) \int_0^\infty dE' \int_{4\pi} d\Omega'\, \Sigma_s(\Omega' \cdot \Omega, E' \to E)\psi(x,\Omega',E',t) \\
&= \int_0^T dt \int_V dV \int_0^\infty dE' \int_{4\pi} d\Omega' \\
&\quad \int_0^\infty dE \int_{4\pi} d\Omega\, \psi^\dagger(x,\Omega,E,t)\Sigma_s(\Omega' \cdot \Omega, E' \to E)\psi(x,\Omega',E',t)
\end{aligned}
$$

$$
= \int_0^T dt \int_V dV \int_0^\infty dE \int_{4\pi} d\Omega
$$
$$
\int_0^\infty dE' \int_{4\pi} d\Omega' \, \psi(\boldsymbol{x}, \boldsymbol{\Omega}, E, t) \Sigma_s(\boldsymbol{\Omega} \cdot \boldsymbol{\Omega}', E \to E') \psi^\dagger(\boldsymbol{x}, \boldsymbol{\Omega}', E', t)
$$
$$
= \int_0^T dt \int_V dV \int_0^\infty dE \int_{4\pi} d\Omega
$$
$$
\psi(\boldsymbol{x}, \boldsymbol{\Omega}, E, t) \int_0^\infty dE' \int_{4\pi} d\Omega' \, \Sigma_s(\boldsymbol{\Omega} \cdot \boldsymbol{\Omega}', E \to E') \psi^\dagger(\boldsymbol{x}, \boldsymbol{\Omega}', E', t)
$$
$$
= \left\langle \psi, \mathcal{L}_s^\dagger \psi^\dagger \right\rangle, \tag{167d}
$$

where in the first step, the orders of integration for the pre- and post-collision energies were switched, as were the corresponding directions, and in the second step, the dummy variables for pre- and post-collision energies were interchanged, as were those of the corresponding directions. We notice that the adjoint of the inscatter operator is obtained simply by reversing the orders of the pre- and post-collision arguments in the scattering kernel. Since scattering is rotationally symmetric, this affects only the energy loss part of the kernel. In other words, the scattering operator for coherent scattering (i.e., scattering without energy loss) is self-adjoint.

Manipulating the fission operator in the same manner as the scattering operator, we get:

$$
\langle \psi^\dagger, \mathcal{L}_f \psi \rangle = \int_0^T dt \int_V dV \int_0^\infty dE \int_{4\pi} d\Omega
$$
$$
\psi^\dagger(\boldsymbol{x}, \boldsymbol{\Omega}, E, t) \frac{\chi_p(E)}{4\pi} \int_0^\infty dE' \int_{4\pi} d\Omega' \nu \Sigma_f(E') \psi(\boldsymbol{x}, \boldsymbol{\Omega}', E', t)
$$
$$
= \int_0^T dt \int_V dV \int_0^\infty dE' \int_{4\pi} d\Omega'
$$
$$
\int_0^\infty dE \int_{4\pi} d\Omega \frac{\chi_p(E)}{4\pi} \psi^\dagger(\boldsymbol{x}, \boldsymbol{\Omega}, E, t) \nu \Sigma_f(E') \psi(\boldsymbol{x}, \boldsymbol{\Omega}', E', t)
$$
$$
= \int_0^T dt \int_V dV \int_0^\infty dE \int_{4\pi} d\Omega
$$
$$
\int_0^\infty dE' \int_{4\pi} d\Omega' \frac{\chi_p(E')}{4\pi} \psi(\boldsymbol{x}, \boldsymbol{\Omega}, E, t) \nu \Sigma_f(E) \psi^\dagger(\boldsymbol{x}, \boldsymbol{\Omega}', E', t)
$$
$$
= \int_0^T dt \int_V dV \int_0^\infty dE \int_{4\pi} d\Omega
$$
$$
\psi(\boldsymbol{x}, \boldsymbol{\Omega}, E, t) \, \nu \Sigma_f(E) \int_0^\infty dE' \int_{4\pi} d\Omega' \frac{\chi_p(E')}{4\pi} \psi^\dagger(\boldsymbol{x}, \boldsymbol{\Omega}', E', t)
$$
$$
= \left\langle \psi, \mathcal{L}_f^\dagger \psi^\dagger \right\rangle. \tag{167e}
$$

The fission operator is non-self-adjoint with respect to the energy variable, the angular distribution being isotropic. It becomes self-adjoint when the fission cross section is energy independent and all fission neutrons are born with the same energy, i.e., in the one-speed approximation.

Finally, substituting (167a—167e) into (166) yields:

$$
\langle \psi^\dagger, \mathcal{L} \psi \rangle = P_t \left[\psi, \psi^\dagger \right] + P_l \left[\psi, \psi^\dagger \right] + \langle \psi, \mathcal{L}^\dagger \psi^\dagger \rangle, \tag{168}
$$

and thus for the adjoint transport operator:

$$\mathcal{L}^\dagger \psi^\dagger = -\frac{1}{v}\frac{\partial \psi^\dagger}{\partial t}(\boldsymbol{x}, \boldsymbol{\Omega}, E, t) - \boldsymbol{\Omega} \cdot \nabla \psi^\dagger(\boldsymbol{x}, \boldsymbol{\Omega}, E, t) + \Sigma_t(E)\psi^\dagger(\boldsymbol{x}, \boldsymbol{\Omega}, E, t)$$
$$- \int_0^\infty \int_{4\pi} \Sigma_s(\boldsymbol{\Omega} \cdot \boldsymbol{\Omega}', E \to E')\psi^\dagger(\boldsymbol{x}, \boldsymbol{\Omega}', E', t)\, d\boldsymbol{\Omega}' dE'$$
$$- v\Sigma_f(E) \int_0^\infty \int_{4\pi} \frac{\chi_p(E')}{4\pi}\psi^\dagger(\boldsymbol{x}, \boldsymbol{\Omega}', E', t)\, d\boldsymbol{\Omega}' dE'. \tag{169}$$

Although $\psi^\dagger(\boldsymbol{x}, \boldsymbol{\Omega}, E, t)$ is referred to as the *adjoint angular flux*, the physical interpretation of this quantity (hence its units) can only be established when it is related to some functional of the forward angular flux $\psi(\boldsymbol{x}, \boldsymbol{\Omega}, E, t)$, which, moreover, will dictate the choice of the adjoint source and adjoint boundary-initial conditions. This will be demonstrated shortly below, but first we make some general observations on the adjoint transport process.

An adjoint problem is defined such that the adjoint angular flux $\psi^\dagger(\boldsymbol{x}, \boldsymbol{\Omega}, E, t)$ is a solution of the following adjoint transport equation:

$$-\frac{1}{v}\frac{\partial \psi^\dagger}{\partial t}(\boldsymbol{x}, \boldsymbol{\Omega}, E, t) - \boldsymbol{\Omega} \cdot \nabla \psi^\dagger(\boldsymbol{x}, \boldsymbol{\Omega}, E, t) + \Sigma_t(E)\psi^\dagger(\boldsymbol{x}, \boldsymbol{\Omega}, E, t)$$
$$= \int_0^\infty \int_{4\pi} \Sigma_s(\boldsymbol{\Omega} \cdot \boldsymbol{\Omega}', E \to E')\psi^\dagger(\boldsymbol{x}, \boldsymbol{\Omega}', E', t)\, d\boldsymbol{\Omega}' dE'$$
$$+ v\Sigma_f(E) \int_0^\infty \int_{4\pi} \frac{\chi_p(E')}{4\pi}\psi^\dagger(\boldsymbol{x}, \boldsymbol{\Omega}', E', t)\, d\boldsymbol{\Omega}' dE' + Q^\dagger(\boldsymbol{x}, \boldsymbol{\Omega}, E, t), \tag{170}$$

for a given source adjoint $Q^\dagger$ and given adjoint boundary and initial conditions. The adjoint flux represents the flow of pseudo-particles, or adjoint particles (sometimes also referred to as "adjunctons"), which, like neutrons, are created, destroyed, and redistributed in phase space. However, the adjoint transport process is fundamentally different. Adjoint particles:

- Are born in the medium distributed in phase space according to the adjoint source, but beginning at some *final* or *terminal* time
- Stream in *reverse* time to earlier times and travel in *reverse* directions
- *Gain* energy in scattering collisions, but the inscattering and outscattering terms do not balance when integrated over all energies and directions, i.e., the energy-dependent adjoint scattering operator is *nonconservative*
- Are isotropically emitted in fission reactions, but the energy-dependence of the adjoint fission cross section is proportional to the neutron fission spectrum while the energy spectrum of the resulting adjoint fission particles is proportional to the neutron fission cross section.

In other words, the adjoint equation is a *backward* transport equation, the adjoint angular flux satisfying a final or terminal condition in time instead of an initial condition, and a boundary condition which is specified for outgoing directions instead of incoming directions. To emphasize this distinction between the two approaches, the neutron transport equation is referred to as a *forward* transport equation.

Like the forward transport equation, the adjoint transport equation has a unique solution for subcritical systems with fixed sources, while adjoint k-eigenvalue and adjoint α-eigenvalue problems can be defined for multiplying systems. For both types of eigenvalue problems, it can

be shown that the adjoint fundamental mode is positive and the dominant adjoint eigenvalue is identical to the dominant eigenvalue of the forward problem.

5.4   Adjoint Flux as an Importance Function

Adjoint transport problems lead to a natural physical interpretation of the adjoint flux and, under certain circumstances, an adjoint formulation results in a more efficient solution to a physical problem than the traditional forward approach. We demonstrate this next.

Expressing the forward and adjoint problems in condensed notation as:

$$\mathcal{L}\psi = Q, \tag{171}$$

$$\mathcal{L}^{\dagger}\psi^{\dagger} = Q^{\dagger}, \tag{172}$$

and then subtracting the inner product of ψ with (172) from the inner-product of $\psi^{\dagger}$ with (171), we obtain:

$$\langle \psi^{\dagger}, \mathcal{L}\psi \rangle - \langle \psi, \mathcal{L}^{\dagger}\psi^{\dagger} \rangle = \langle \psi^{\dagger}, Q \rangle - \langle \psi, Q^{\dagger} \rangle. \tag{173}$$

Noting the definition of the adjoint operator as expressed by the inner product identity equation (168), the left-hand side of (173) can be simplified to obtain:

$$P_t\left[\psi, \psi^{\dagger}\right] + P_l\left[\psi, \psi^{\dagger}\right] = \langle \psi^{\dagger}, Q \rangle - \langle \psi, Q^{\dagger} \rangle, \tag{174}$$

where P_t is given by:

$$P_t\left[\psi, \psi^{\dagger}\right] = \int_0^{\infty} dE \int_{4\pi} d\Omega \int_V dV \frac{1}{v}\psi^{\dagger}(\boldsymbol{x}, \boldsymbol{\Omega}, E, T)\psi(\boldsymbol{x}, \boldsymbol{\Omega}, E, T)$$
$$- \int_0^{\infty} dE \int_{4\pi} d\Omega \int_V dV \frac{1}{v}\psi^{\dagger}(\boldsymbol{x}, \boldsymbol{\Omega}, E, 0)\psi(\boldsymbol{x}, \boldsymbol{\Omega}, E, 0), \tag{175}$$

and P_l by:

$$P_l\left[\psi, \psi^{\dagger}\right] = \int_0^T dt \int_0^{\infty} dE \int_{4\pi} d\Omega \int_{\partial V} dA\, \boldsymbol{n}\cdot\boldsymbol{\Omega}\,\psi(\boldsymbol{x}, \boldsymbol{\Omega}, E, t)\,\psi^{\dagger}(\boldsymbol{x}, \boldsymbol{\Omega}, E, t)$$
$$= \int_0^T dt \int_0^{\infty} dE \int_{\boldsymbol{n}\cdot\boldsymbol{\Omega}>0} d\Omega \int_{\partial V} dA\, \boldsymbol{n}\cdot\boldsymbol{\Omega}\,\psi(\boldsymbol{x}, \boldsymbol{\Omega}, E, t)\,\psi^{\dagger}(\boldsymbol{x}, \boldsymbol{\Omega}, E, t)$$
$$- \int_0^T dt \int_0^{\infty} dE \int_{\boldsymbol{n}\cdot\boldsymbol{\Omega}<0} d\Omega \int_{\partial V} dA\,|\boldsymbol{n}\cdot\boldsymbol{\Omega}|\,\psi(\boldsymbol{x}, \boldsymbol{\Omega}, E, t)\,\psi^{\dagger}(\boldsymbol{x}, \boldsymbol{\Omega}, E, t). \tag{176}$$

The identity expressed by (174) is a key result in the adjoint-space formulation of transport problems. It relates functionals of the forward and adjoint angular fluxes at initial and final times and along incoming and outgoing directions at the surface of the body to the functionals of these fluxes in the interior of the body with fixed sources. This *generalized reciprocity relationship* enables transport problems to be posed using either forward or adjoint descriptions, provides a physical interpretation of the adjoint flux, and imposes consistent adjoint boundary and terminal conditions. While the class of such problems is wide, we highlight here so-called source-detector problems for subcritical systems at steady state, for which the adjoint formulation is extensively employed.

5.4.1   Source-Detector Problems

A classic forward problem is to determine a desired linear functional of the steady-state flux for a given interior source distribution and a free surface boundary condition. That is, we are interested in the solution of the forward transport equation:

$$\mathcal{L}\psi = Q, \tag{177a}$$

$$\psi = 0, \quad \boldsymbol{x} \in \partial V, \ \boldsymbol{\Omega} \cdot \boldsymbol{n} < 0, \ 0 < E < \infty, \tag{177b}$$

which is used to compute the functional:

$$\langle f, \psi \rangle = \int_0^\infty dE \int_{4\pi} d\Omega \int_R dV \, f(\boldsymbol{x}, \boldsymbol{\Omega}, E) \, \psi(\boldsymbol{x}, \boldsymbol{\Omega}, E), \tag{178}$$

where R is a subregion in the body and $f(\boldsymbol{x}, \boldsymbol{\Omega}, E)$ is a real function that makes the above functional a useful physical quantity. For instance, if it is desired to know the response of a detector to the local neutron flux, then f would be equated with the detector cross section $\Sigma_d(E)$, and subregion R would be the detector volume. If the detector is localized at some point $\boldsymbol{x}_0$ so that:

$$f(\boldsymbol{x}, \boldsymbol{\Omega}, E) = \Sigma_d(E) \, \delta(\boldsymbol{x} - \boldsymbol{x}_0), \tag{179}$$

then the desired functional gives the reaction rate at this point:

$$\begin{aligned}
\langle f, \psi \rangle &= \int_0^\infty dE \int_{4\pi} d\Omega \, \Sigma_d(E) \, \psi(\boldsymbol{x}_0, \boldsymbol{\Omega}, E) \\
&= \int_0^\infty dE \, \Sigma_d(E) \, \phi(\boldsymbol{x}_0, E), \tag{180}
\end{aligned}$$

where ϕ is the scalar flux at the detector. By choosing f appropriately, the functional can be generalized to yield energy and/or angle-dependent responses.

Since we are dealing with time-independent situations, the reciprocity condition, (174), reduces, upon substituting the vacuum boundary condition (177b), to:

$$\langle \psi^\dagger, Q \rangle - \langle \psi, Q^\dagger \rangle = \int_0^\infty dE \int_{\boldsymbol{n} \cdot \boldsymbol{\Omega} > 0} d\Omega \int_{\partial V} dA \, \boldsymbol{n} \cdot \boldsymbol{\Omega} \, \psi(\boldsymbol{x}, \boldsymbol{\Omega}, E) \, \psi^\dagger(\boldsymbol{x}, \boldsymbol{\Omega}, E), \tag{181}$$

where the right-hand side contains the outward-directed forward and adjoint angular fluxes at the boundary. If now $Q^\dagger$ is identified with f, a permissible operation because of the arbitrariness of the adjoint source, and moreover if we require the outward-directed adjoint flux at the boundary to vanish, (181) reduces to the particularly simple form:

$$\langle f, \psi \rangle = \langle \psi^\dagger, Q \rangle. \tag{182}$$

This result states that the desired functional of the forward flux can alternatively be obtained as the inner product of the adjoint flux with the physical source, where the adjoint flux now solves the *specific* adjoint transport problem:

$$\mathcal{L}^{\dagger}\psi^{\dagger} = f, \tag{183a}$$

$$\psi^{\dagger} = 0, \quad \boldsymbol{x} \in \partial V, \quad \boldsymbol{\Omega} \cdot \boldsymbol{n} > 0, \quad 0 < E < \infty. \tag{183b}$$

The significance of this adjoint formulation of a detector response is twofold. First, it will be observed that the adjoint problem given by (183a,b) is independent of the source Q in the forward problem. Thus, if a detector response is desired for multiple different sources, an adjoint computation would be more efficient than a forward computation. The latter would require multiple solutions of the forward transport equation, one for each source, followed by evaluation of the inner product $\langle f, \psi \rangle$ for each such solution. The adjoint approach, on the other hand, necessitates obtaining a single solution to the adjoint transport equation, followed by evaluation of the inner product $\langle \psi^{\dagger}, Q \rangle$ for each source. This is computationally far less laborious than solving the forward problem for each different source. If multiple generalized responses are of interest for the same forward source, the forward computation is preferred for precisely the same reasons.

Second, let us assume that the forward source corresponds to one particle injected into the system locally in phase space, at a specified point $\boldsymbol{x}_0$, direction of flight Ω_0, and energy E_0:

$$Q(\boldsymbol{x}, \boldsymbol{\Omega}, E) = \delta(\boldsymbol{x} - \boldsymbol{x}_0)\, \delta(\boldsymbol{\Omega} - \boldsymbol{\Omega}_0)\, \delta(E - E_0). \tag{184}$$

Then, from (182), the resulting detector response is given by:

$$\langle f, \psi \rangle = \psi^{\dagger}(\boldsymbol{x}_0, \boldsymbol{\Omega}_0, E_0). \tag{185}$$

This result indicates that the detector response is equal to the adjoint flux at the point of injection of the neutron. Thus, the adjoint flux is a direct measure of the *importance* of a locally injected neutron to the response of a detector. For this reason, the adjoint flux is commonly referred to as the *importance function*. Moreover, the boundary (and terminal) conditions assigned to the adjoint flux become physically reasonable and consistent with this notion of importance. For instance, in the above problem, a neutron leaving the body at the boundary cannot contribute to the detector response, and hence its importance is *zero*.

For external detector locations, measuring the importance of outgoing neutrons, the adjoint boundary conditions require modification. In this case, we take $Q^{\dagger} = 0$ and by way of illustration, consider a monodirectional and monoenergetic incident beam condition for the forward problem:

$$\psi(\boldsymbol{x}, \boldsymbol{\Omega}, E) = \delta(\boldsymbol{x} - \boldsymbol{x}_b)\, \delta(\boldsymbol{\Omega} - \boldsymbol{\Omega}_b)\, \delta(E - E_b), \quad \boldsymbol{x} \in \partial V, \quad \boldsymbol{\Omega} \cdot \boldsymbol{n} < 0, \quad 0 < E < \infty, \tag{186}$$

where $\boldsymbol{x}_b$ is the point on the boundary at which the beam of neutrons of energy E_b is incident along direction $\boldsymbol{\Omega}_b$. Note that since $\boldsymbol{x}$ is restricted to lie on the boundary, the delta function

$\delta\,(\pmb{x} - \pmb{x}_b)$ is 2-D. This then gives a source normalization of one incident particle per second. The reciprocity relationship equation (174) reduces in this case to:

$$\int_0^\infty dE \int_{\pmb{n}\cdot\pmb{\Omega}>0} d\Omega \int_{\partial V} dA\,\pmb{n}\cdot\pmb{\Omega}\,\psi(\pmb{x},\pmb{\Omega},E)\,\psi^\dagger(\pmb{x},\pmb{\Omega},E)$$

$$= |\pmb{n}\cdot\pmb{\Omega}_b|\,\psi^\dagger(\pmb{x}_b,\pmb{\Omega}_b,E_b), \quad \pmb{\Omega}_b\cdot\pmb{n}<0. \tag{187}$$

If the desired quantity is the total leakage from the body, we may assign:

$$\psi^\dagger(\pmb{x},\pmb{\Omega},E) = 1, \quad \pmb{x}\in\partial V,\ \ \pmb{\Omega}\cdot\pmb{n}>0,\ \ 0<E<\infty, \tag{188}$$

and (187) then becomes:

$$J^+ = \int_0^\infty dE \int_{\pmb{n}\cdot\pmb{\Omega}>0} d\Omega \int_{\partial V} dA\,\pmb{n}\cdot\pmb{\Omega}\,\psi(\pmb{x},\pmb{\Omega},E)$$

$$= |\pmb{n}\cdot\pmb{\Omega}_b|\,\psi^\dagger(\pmb{x}_b,\pmb{\Omega}_b,E_b), \quad \pmb{\Omega}_b\cdot\pmb{n}<0. \tag{189}$$

Thus, the total leakage from a body, given a monodirectional and monoenergetic incident beam, can be obtained by solving the homogeneous adjoint transport equation with unit outgoing adjoint flux at the boundary. In this case, the importance to the detector of neutrons *exiting* the medium will be the highest of any other group of neutrons. Since the forward problem involves singular functions at the boundary while the adjoint problem does not, numerical solution of the adjoint transport equation will be more efficient. With an appropriate choice of adjoint boundary condition in (187), it is evident that adjoint space formulation of surface energy spectra and/or angular distributions can be realized, with and without interior sources. This analysis can be further extended to show that the adjoint flux in a critical system measures the importance of a neutron injected at a particular phase space location in sustaining the fundamental mode.

From the considerations of this section, we observe that the adjoint problem cannot be considered independently of the forward problem. The identification of the adjoint source and assignment of adjoint boundary (and terminal) conditions makes the adjoint formulation (forward-) problem dependent. However, regardless of the application, the adjoint flux can always be imbued with an "importance" attribute, thereby rendering it a physically meaningful quantity.

5.5 Green's Functions

Finally, we consider a particularly interesting special case of the generalized reciprocity relationship given by (174). Let the forward and adjoint sources be completely localized in phase space and in time:

$$Q(\pmb{x},\pmb{\Omega},E,t) = \delta\,(\pmb{x}-\pmb{x}_0)\,\delta\,(\pmb{\Omega}-\pmb{\Omega}_0)\,\delta\,(E-E_0)\,\delta\,(t-t_0), \tag{190a}$$

$$Q^\dagger(\pmb{x},\pmb{\Omega},E,t) = \delta\,(\pmb{x}-\pmb{x}_1)\,\delta\,(\pmb{\Omega}-\pmb{\Omega}_1)\,\delta\,(E-E_1)\,\delta\,(t-t_1). \tag{190b}$$

The resulting solutions of the forward and adjoint transport equations with homogeneous boundary and initial/terminal conditions are the forward and adjoint volume Green's functions and are denoted by:

$$\psi(\boldsymbol{x}, \boldsymbol{\Omega}, E, t) \equiv G\left(\boldsymbol{x}, \boldsymbol{\Omega}, E, t \,;\, \boldsymbol{x}_0, \boldsymbol{\Omega}_0, E_0, t_0\right), \tag{191a}$$

$$\psi^\dagger(\boldsymbol{x}, \boldsymbol{\Omega}, E, t) \equiv G^\dagger\left(\boldsymbol{x}, \boldsymbol{\Omega}, E, t \,;\, \boldsymbol{x}_1, \boldsymbol{\Omega}_1, E_1, t_1\right). \tag{191b}$$

For these sources, the reciprocity condition equation (174) reduces to:

$$\langle G^\dagger, Q \rangle = \langle G, Q^\dagger \rangle, \tag{192}$$

which, upon inserting (190a) and (190b) then yields the result:

$$G^\dagger\left(\boldsymbol{x}_0, \boldsymbol{\Omega}_0, E_0, t_0 \,;\, \boldsymbol{x}_1, \boldsymbol{\Omega}_1, E_1, t_1\right) = G\left(\boldsymbol{x}_1, \boldsymbol{\Omega}_1, E_1, t_1 \,;\, \boldsymbol{x}_0, \boldsymbol{\Omega}_0, E_0, t_0\right), \tag{193}$$

where from causality we require that $t_1 > t_0$. The right-hand side of the above equation is the neutron angular flux at the phase space point $(\boldsymbol{x}_1, \boldsymbol{\Omega}_1, E_1)$ at time t_1, known as the field variables, resulting from the injection of a neutron at another phase space point $(\boldsymbol{x}_0, \boldsymbol{\Omega}_0, E_0)$ at an earlier time t_0, known as the source variables. Equation (193) shows that this is identical to the angular flux for the adjoint problem but with the source and field variables reversed. A similar relationship involving surface Green's functions may be derived by imposing an incident beam on the boundary:

$$\psi(\boldsymbol{x}, \boldsymbol{\Omega}, E, t) = \delta\left(\boldsymbol{x} - \boldsymbol{x}_0\right) \delta\left(\boldsymbol{\Omega} - \boldsymbol{\Omega}_0\right) \delta\left(E - E_0\right) \delta\left(t - t_0\right),$$
$$\boldsymbol{x} \in \partial V, \;\; \boldsymbol{\Omega} \cdot \boldsymbol{n} < 0, \;\; 0 < E < \infty, \tag{194a}$$

$$\psi^\dagger(\boldsymbol{x}, \boldsymbol{\Omega}, E, t) = \delta\left(\boldsymbol{x} - \boldsymbol{x}_1\right) \delta\left(\boldsymbol{\Omega} - \boldsymbol{\Omega}_1\right) \delta\left(E - E_1\right) \delta\left(t - t_1\right),$$
$$\boldsymbol{x} \in \partial V, \;\; \boldsymbol{\Omega} \cdot \boldsymbol{n} > 0, \;\; 0 < E < \infty, \tag{194b}$$

where $\boldsymbol{x}_0$ and $\boldsymbol{x}_1$ are two arbitrary points on boundary, and the source normalization is one particle (neutron and adjuncton) per second. Substituting these into (174) we obtain:

$$|\boldsymbol{n} \cdot \boldsymbol{\Omega}_0| \, G^\dagger\left(\boldsymbol{x}_0, \boldsymbol{\Omega}_0, E_0, t_0 \,;\, \boldsymbol{x}_1, \boldsymbol{\Omega}_1, E_1, t_1\right) = |\boldsymbol{n} \cdot \boldsymbol{\Omega}_1| \, G\left(\boldsymbol{x}_1, \boldsymbol{\Omega}_1, E_1, t_1 \,;\, \boldsymbol{x}_0, \boldsymbol{\Omega}_0, E_0, t_0\right), \tag{195}$$

subject to the causality constraint $t_1 > t_0$ and where again homogeneous initial and terminal conditions have been assumed.

These reciprocity relationships can be used to construct the angular flux for a distributed source from the corresponding Green's function. Let us consider a localized adjoint interior source, for which the adjoint angular flux is just the adjoint Green's function $G^\dagger$, and a distributed forward source, for which the solution is the forward angular flux ψ. The reciprocity condition for this problem reads:

$$\langle G^\dagger, Q \rangle = \langle \psi, Q^\dagger \rangle, \tag{196}$$

or, more explicitly:

$$\psi(\boldsymbol{x}, \boldsymbol{\Omega}, E, t)$$
$$= \int_0^t dt' \int_V dV' \int_0^\infty dE' \int_{4\pi} d\Omega' \, Q(\boldsymbol{x}', \boldsymbol{\Omega}', E', t') \, G^\dagger \left(\boldsymbol{x}', \boldsymbol{\Omega}', E', t'; \boldsymbol{x}, \boldsymbol{\Omega}, E, t \right). \quad (197)$$

Recalling (193), the adjoint Green's function in (197) can be replaced by the forward Green's function but with field and source variables reversed, to finally obtain:

$$\psi(\boldsymbol{x}, \boldsymbol{\Omega}, E, t)$$
$$= \int_0^t dt' \int_V dV' \int_0^\infty dE' \int_{4\pi} d\Omega' \, Q(\boldsymbol{x}', \boldsymbol{\Omega}', E', t') \, G \left(\boldsymbol{x}, \boldsymbol{\Omega}, E, t; \boldsymbol{x}', \boldsymbol{\Omega}', E', t' \right). \quad (198)$$

This result is a statement of the *superposition principle* for linear systems: the angular flux corresponding to a distributed source can be obtained by a superposition of angular fluxes for elementary sources. It is a direct consequence of the linearity of the transport operator.

5.6   Discussion

We have seen that neutron transport problems can be mathematically modeled using either a forward or an adjoint formulation. The adjoint operator is commonly derived using an inner-product identity, and the adjoint formulation always inherits physical relevance that is unique to the forward problem. The interpretation of the adjoint flux as an importance function makes it possible to derive the adjoint transport equation from first principles, using balance arguments akin to those employed in the derivation of the forward equation (Bell and Glasstone 1970; Henry 1975; Lewins 1965). For certain applications, adjoint formulations have clear computational advantages over forward formulations, while for other applications the reverse is true. Forward and adjoint functions taken collectively provide a means of generating highly accurate approximate solutions at reduced cost, as exemplified by their use in variational methods, perturbation theory, and Monte Carlo simulations.

The derivations and results of this section simplify considerably for neutron transport in the one-speed approximation. Under these conditions, the scattering and fission operators become self-adjoint, leaving only the time evolution and streaming operators as non-self-adjoint. However, upon reflecting the direction and time variables, i.e, setting $\boldsymbol{\Omega} \to -\boldsymbol{\Omega}$ and $t \to -t$, the one-speed adjoint transport equation becomes identical to the forward transport equation. The distinction between the two formulations then stems purely from the respective sources and boundary and initial/terminal conditions, but for criticality problems in particular, this consequence obviates the need to independently solve the adjoint transport equation – the adjoint angular flux is obtained by simply reflecting the direction variable in the forward angular flux. Moreover, in a critical system, where sources are absent and homogeneous boundary conditions are imposed, the adjoint scalar flux is identical to the forward scalar flux.

Finally, we remark that under certain restrictive conditions, a hybrid forward–backward formulation can be developed to describe linear transport processes. Although this approach has not found utility in reactor physics or neutron transport applications, it is nevertheless widely used in the theory of radiation damage and atomic sputtering (Prinja 1989; Sigmund 1969; Williams 1979).

6   The Multigroup and One-Speed Neutron Transport Equations

The *multigroup* approximation to the neutron transport equation is almost universally used to discretize the continuous-energy variable E (Duderstadt and Hamilton 1976; Henry 1975; Lewis and Miller 1993). The structure of the resulting multigroup transport equations is closely related to that of the original transport equation, the difference being that the energy variable is discrete rather than continuous. (Thus, integrals over E are replaced by sums over *energy groups*.) Several important identities of the original continuous-energy scattering operator are preserved in the multigroup approximation. Here, we derive the multigroup transport equations and discuss some of their properties.

6.1   The Continuous-Energy Problem

We consider a general, steady-state, 3-D neutron transport equation:

$$\boldsymbol{\Omega} \cdot \nabla \psi(\boldsymbol{x}, \boldsymbol{\Omega}, E) + \Sigma_t(\boldsymbol{x}, E)\psi(\boldsymbol{x}, \boldsymbol{\Omega}, E)$$
$$= \int_0^\infty \int_{4\pi} \Sigma_s(\boldsymbol{x}, \boldsymbol{\Omega}' \cdot \boldsymbol{\Omega}, E' \to E)\psi(\boldsymbol{x}, \boldsymbol{\Omega}', E')\, d\Omega' dE'$$
$$+ \frac{\chi(\boldsymbol{x}, E)}{4\pi} \int_0^\infty \int_{4\pi} \nu\Sigma_f(\boldsymbol{x}, E')\psi(\boldsymbol{x}, \boldsymbol{\Omega}', E')\, d\Omega' dE'$$
$$+ \frac{1}{4\pi} Q(\boldsymbol{x}, E), \quad \boldsymbol{x} \in V, \ \boldsymbol{\Omega} \in 4\pi, \ 0 < E < \infty, \tag{199a}$$

with the boundary condition:

$$\psi(\boldsymbol{x}, \boldsymbol{\Omega}, E) = \psi^b(\boldsymbol{x}, \boldsymbol{\Omega}, E), \quad \boldsymbol{x} \in \partial V, \ \boldsymbol{\Omega} \cdot \boldsymbol{n} < 0, \ 0 < E < \infty. \tag{199b}$$

The cross sections and fission spectrum in these equations satisfy the usual identities (see [8], [13b], [14b], and [77]):

$$\Sigma_t(E) = \Sigma_s(E) + \Sigma_\gamma(E) + \Sigma_f(E), \tag{200a}$$

$$\Sigma_s(E) = \int_0^\infty \int_{4\pi} \Sigma_s(\boldsymbol{\Omega} \cdot \boldsymbol{\Omega}', E \to E')\, d\Omega' dE' \tag{200b}$$

$$\int_0^\infty \chi(E)\, dE = 1, \tag{200c}$$

$$\Sigma_s(\boldsymbol{\Omega}' \cdot \boldsymbol{\Omega}, E' \to E) = \sum_{n=0}^N \frac{2n+1}{4\pi} \Sigma_{s,n}(E' \to E) P_n(\boldsymbol{\Omega}' \cdot \boldsymbol{\Omega}). \tag{200d}$$

6.2   The Multigroup Transport Equations

The multigroup approximation requires that a finite number G of energy bins or *groups* be chosen:

$$E_{min} = E_G < E_{G-1} < \cdots < E_g < E_{g-1} < \cdots < E_2 < E_1 = E_{max},$$

with E_{min} sufficiently small that neutrons with energies less than E_{min} are negligible, and with E_{max} sufficiently large that neutrons with energies greater than E_{max} are negligible. The energy range $E_g \le E < E_{g-1}$ is the gth *energy group*. It is customary to order the energy groups with

the group index g increasing as the energies decrease. Then the slowing down of fast fission neutrons occurs through energy groups with increasing indices.

For each $1 \leq g \leq G$, we define:

$$\psi_g(\boldsymbol{x}, \boldsymbol{\Omega}) = \int_{E_g}^{E_{g-1}} \psi(\boldsymbol{x}, \boldsymbol{\Omega}, E)dE$$

$$= \text{Angular flux for group } g, \tag{201a}$$

$$\chi_g(\boldsymbol{x}) = \int_{E_g}^{E_{g-1}} \chi(\boldsymbol{x}, E)dE$$

$$= \text{Multigroup fission spectrum for group } g, \tag{201b}$$

$$Q_g(\boldsymbol{x}) = \int_{E_g}^{E_{g-1}} Q(\boldsymbol{x}, E)dE$$

$$= \text{Internal multigroup source to group } g. \tag{201c}$$

Because these quantities are integrals over energy groups, the group fluxes have dimensions $\text{cm}^{-2}\ \text{s}^{-1}$, the multigroup fission spectrum is dimensionless, and the multigroup sources have dimensions $\text{cm}^{-3}\ \text{s}^{-1}$. Also, by the preceding definitions and (200c), the multigroup fission spectrum automatically satisfies:

$$\sum_{g=1}^{G} \chi_g(\boldsymbol{x}) = \sum_{g=1}^{G} \int_{E_g}^{E_{g-1}} \chi(\boldsymbol{x}, E)dE = \int_{E_{min}}^{E_{max}} \chi(\boldsymbol{x}, E)dE = 1. \tag{202}$$

To proceed, we integrate (199a) over the gth energy group, obtaining:

$$\boldsymbol{\Omega} \cdot \nabla \psi_g(\boldsymbol{x}, \boldsymbol{\Omega}) + \int_{E_g}^{E_{g-1}} \Sigma_t(\boldsymbol{x}, E)\psi(\boldsymbol{x}, \boldsymbol{\Omega}, E)dE$$

$$= \sum_{g'=1}^{G} \int_{E_g}^{E_{g-1}} \int_{E'_g}^{E_{g'-1}} \int_{4\pi} \Sigma_s(\boldsymbol{x}, E' \to E, \boldsymbol{\Omega}' \cdot \boldsymbol{\Omega})\psi(\boldsymbol{x}, \boldsymbol{\Omega}', E')d\boldsymbol{\Omega}'dE'dE$$

$$+ \frac{\chi_g(\boldsymbol{x})}{4\pi} \sum_{g'=1}^{G} \int_{E'_g}^{E_{g'-1}} \int_{4\pi} \nu\Sigma_f(\boldsymbol{x}, E')\psi(\boldsymbol{x}, \boldsymbol{\Omega}', E')d\boldsymbol{\Omega}'dE' + \frac{Q_g(\boldsymbol{x})}{4\pi}. \tag{203}$$

Equivalently,

$$\boldsymbol{\Omega} \cdot \nabla \psi_g(\boldsymbol{x}, \boldsymbol{\Omega}) + \left[\frac{\int_{E_g}^{E_{g-1}} \Sigma_t(\boldsymbol{x}, E)\psi(\boldsymbol{x}, \boldsymbol{\Omega}, E)dE}{\int_{E_g}^{E_{g-1}} \psi(\boldsymbol{x}, \boldsymbol{\Omega}, E)dE} \right] \psi_g(\boldsymbol{x}, \boldsymbol{\Omega})$$

$$= \sum_{g'=1}^{G} \int_{4\pi} \left[\frac{\int_{E_g}^{E_{g-1}} \int_{E_{g'}}^{E_{g'-1}} \Sigma_s(\boldsymbol{x}, E' \to E, \boldsymbol{\Omega}' \cdot \boldsymbol{\Omega})\psi(\boldsymbol{x}, \boldsymbol{\Omega}', E')dE'dE}{\int_{E_{g'}}^{E_{g'-1}} \psi(\boldsymbol{x}, \boldsymbol{\Omega}', E')dE'} \right] \psi_{g'}(\boldsymbol{x}, \boldsymbol{\Omega}')d\boldsymbol{\Omega}'$$

$$+ \frac{\chi_g(\boldsymbol{x})}{4\pi} \sum_{g'=1}^{G} \int_{4\pi} \left[\frac{\int_{E_{g'}}^{E_{g'-1}} \nu\Sigma_f(\boldsymbol{x}, E')\psi(\boldsymbol{x}, \boldsymbol{\Omega}', E')dE'}{\int_{E_{g'}}^{E_{g'-1}} \psi(\boldsymbol{x}, \boldsymbol{\Omega}', E')dE'} \right] \psi_{g'}(\boldsymbol{x}, \boldsymbol{\Omega}')d\boldsymbol{\Omega}'$$

$$+ \frac{Q_g(\boldsymbol{x})}{4\pi}, \tag{204}$$

or:

$$\boldsymbol{\Omega} \cdot \nabla \psi_g(\boldsymbol{x}, \boldsymbol{\Omega}) + \hat{\Sigma}_{t,g}(\boldsymbol{x}, \boldsymbol{\Omega})\psi_g(\boldsymbol{x}, \boldsymbol{\Omega}) = \sum_{g'=1}^{G} \int_{4\pi} \hat{\Sigma}_{s,g' \to g}(\boldsymbol{x}, \boldsymbol{\Omega}', \boldsymbol{\Omega})\psi_{g'}(\boldsymbol{x}, \boldsymbol{\Omega}')d\boldsymbol{\Omega}'$$

$$+ \frac{\chi_g(\boldsymbol{x})}{4\pi} \sum_{g'=1}^{G} \int_{4\pi} \hat{\nu}\hat{\Sigma}_{f,g}(\boldsymbol{x}, \boldsymbol{\Omega}')\psi_{g'}(\boldsymbol{x}, \boldsymbol{\Omega}')d\boldsymbol{\Omega}' + \frac{Q_g(\boldsymbol{x})}{4\pi}, \tag{205}$$

where:

$$\hat{\Sigma}_{t,g}(\boldsymbol{x}, \boldsymbol{\Omega}) = \left[\frac{\int_{E_g}^{E_{g-1}} \Sigma_t(\boldsymbol{x}, E)\psi(\boldsymbol{x}, \boldsymbol{\Omega}, E)dE}{\int_{E_g}^{E_{g-1}} \psi(\boldsymbol{x}, \boldsymbol{\Omega}, E)dE} \right], \tag{206a}$$

$$\hat{\Sigma}_{s,g' \to g}(\boldsymbol{x}, \boldsymbol{\Omega}', \boldsymbol{\Omega}) = \left[\frac{\int_{E_g}^{E_{g-1}} \int_{E_{g'}}^{E_{g'-1}} \Sigma_s(\boldsymbol{x}, E' \to E, \boldsymbol{\Omega}' \cdot \boldsymbol{\Omega})\psi(\boldsymbol{x}, \boldsymbol{\Omega}', E')dE'dE}{\int_{E_{g'}}^{E_{g'-1}} \psi(\boldsymbol{x}, \boldsymbol{\Omega}', E')dE'} \right], \tag{206b}$$

$$\hat{\nu}\hat{\Sigma}_{f,g}(\boldsymbol{x}, \boldsymbol{\Omega}') = \left[\frac{\int_{E_{g'}}^{E_{g'-1}} \nu\Sigma_f(\boldsymbol{x}, E')\psi(\boldsymbol{x}, \boldsymbol{\Omega}', E')dE'}{\int_{E_{g'}}^{E_{g'-1}} \psi(\boldsymbol{x}, \boldsymbol{\Omega}', E')dE'} \right]. \tag{206c}$$

Exact boundary conditions can be obtained by integrating (199b) over the energy groups:

$$\psi_g(\boldsymbol{x}, \boldsymbol{\Omega}) = \psi_g^b(\boldsymbol{x}, \boldsymbol{\Omega}) = \int_{E_g}^{E_{g-1}} \psi^b(\boldsymbol{x}, \boldsymbol{\Omega}, E)dE, \quad \boldsymbol{x} \in V, \ \boldsymbol{\Omega} \cdot \boldsymbol{n} < 0. \tag{207}$$

Equations (205–207) are an exact system of equations for the group fluxes. If the hatted coefficients in (205) were known, then (205) and (207) would, in the absence of spatial and angular discretizations, yield the exact group fluxes. However, by (206), the hatted coefficients depend on the solution of the continuous-energy problem and are not known.

In the multigroup approximation, an approximation for ψ is specified and introduced into the right sides of (206). The resulting approximate *multigroup cross sections* are then used in (205).

Specifically, in each of the bracketed terms in (206), we introduce the approximation:

$$\psi(\boldsymbol{x}, \boldsymbol{\Omega}, E) \approx \Psi(\boldsymbol{x}, E)f(\boldsymbol{x}, \boldsymbol{\Omega}), \tag{208}$$

where $\Psi(\boldsymbol{x}, E)$ is a specified *neutron spectrum*. The function $f(\boldsymbol{x}, \boldsymbol{\Omega})$ cancels out of each numerator and denominator, and (206) yield the *multigroup cross sections*:

$$\Sigma_{t,g}(\boldsymbol{x}) = \left[\frac{\int_{E_g}^{E_{g-1}} \Sigma_t(\boldsymbol{x}, E)\Psi(\boldsymbol{x}, E)dE}{\int_{E_g}^{E_{g-1}} \Psi(\boldsymbol{x}, E)dE} \right], \tag{209a}$$

$$\Sigma_{s,g' \to g}(\boldsymbol{x}, \boldsymbol{\Omega}' \cdot \boldsymbol{\Omega}) = \left[\frac{\int_{E_g}^{E_{g-1}} \int_{E_{g'}}^{E_{g'-1}} \Sigma_s(\boldsymbol{x}, E' \to E, \boldsymbol{\Omega}' \cdot \boldsymbol{\Omega})\Psi(\boldsymbol{x}, E')dE'dE}{\int_{E_{g'}}^{E_{g'-1}} \Psi(\boldsymbol{x}, E')dE'} \right], \tag{209b}$$

$$\nu\Sigma_{f,g}(\boldsymbol{x}) = \left[\frac{\int_{E_{g'}}^{E_{g'-1}} \nu\Sigma_f(\boldsymbol{x}, E')\Psi(\boldsymbol{x}, E')dE'}{\int_{E_{g'}}^{E_{g'-1}} \Psi(\boldsymbol{x}, E)dE'} \right]. \tag{209c}$$

Introducing these expressions into (205), we obtain the *multigroup transport equations* (Duderstadt and Hamilton 1976; Henry 1975; Lewis and Miller 1993):

$$\boldsymbol{\Omega} \cdot \nabla\psi_g(\boldsymbol{x}, \boldsymbol{\Omega}) + \Sigma_{t,g}(\boldsymbol{x})\psi_g(\boldsymbol{x}, \boldsymbol{\Omega}) = \sum_{g'=1}^{G} \int_{4\pi} \Sigma_{s,g'\to g}(\boldsymbol{x}, \boldsymbol{\Omega}' \cdot \boldsymbol{\Omega})\psi_{g'}(\boldsymbol{x}, \boldsymbol{\Omega}')d\Omega'$$

$$+ \frac{\chi_g(\boldsymbol{x})}{4\pi} \sum_{g'=1}^{G} \int_{4\pi} \nu\hat{\Sigma}_{f,g}(\boldsymbol{x})\psi_{g'}(\boldsymbol{x}, \boldsymbol{\Omega}')d\Omega' + \frac{Q_g(\boldsymbol{x})}{4\pi}, \quad \boldsymbol{x} \in V, \ \boldsymbol{\Omega} \in 4\pi, \ 1 \le g \le G. \tag{210}$$

The multigroup fluxes $\psi_g(\boldsymbol{x}, \boldsymbol{\Omega})$ are obtained by solving these equations with the *multigroup boundary conditions* (207).

To complete the multigroup approximation, the multigroup capture, fission, and scattering cross sections are defined analogous to (209):

$$\Sigma_{\gamma,g}(\boldsymbol{x}) = \left[\frac{\int_{E_g}^{E_{g-1}} \Sigma_\gamma(\boldsymbol{x}, E)\Psi(\boldsymbol{x}, E)dE}{\int_{E_g}^{E_{g-1}} \Psi(\boldsymbol{x}, E)dE} \right], \tag{211a}$$

$$\Sigma_{f,g}(\boldsymbol{x}) = \left[\frac{\int_{E_g}^{E_{g-1}} \Sigma_f(\boldsymbol{x}, E)\Psi(\boldsymbol{x}, E)dE}{\int_{E_g}^{E_{g-1}} \Psi(\boldsymbol{x}, E)dE} \right], \tag{211b}$$

$$\Sigma_{s,n,g'\to g}(\boldsymbol{x}) = \left[\frac{\int_{E_g}^{E_{g-1}} \int_{E_{g'}}^{E_{g'-1}} \Sigma_{s,n}(\boldsymbol{x}, E' \to E)\Psi(\boldsymbol{x}, E')dE'dE}{\int_{E_{g'}}^{E_{g'-1}} \Psi(\boldsymbol{x}, E')dE'} \right]. \tag{211c}$$

Then by (209), (211), and (200a), the following identities hold for all g and g':

$$\Sigma_{t,g}(\boldsymbol{x}) = \frac{\int_{E_g}^{E_{g-1}} \left[\Sigma_s(\boldsymbol{x}, E) + \Sigma_\gamma(\boldsymbol{x}, E) + \Sigma_f(\boldsymbol{x}, E) \right] \Psi(\boldsymbol{x}, E)dE}{\int_{E_g}^{E_{g-1}} \Psi(\boldsymbol{x}, E)dE}$$

$$= \Sigma_{s,g}(\boldsymbol{x}) + \Sigma_{\gamma,g}(\boldsymbol{x}) + \Sigma_{f,g}(\boldsymbol{x}), \tag{212a}$$

$$\Sigma_{s,g'\to g}(\boldsymbol{x}, \boldsymbol{\Omega}' \cdot \boldsymbol{\Omega}) = \frac{\int_{E_g}^{E_{g-1}} \int_{E_{g'}}^{E_{g'-1}} \left[\sum_{n=0}^{N} \frac{2n+1}{4\pi} \Sigma_{s,n}(E' \to E)P_n(\boldsymbol{\Omega}' \cdot \boldsymbol{\Omega}) \right] \Psi(\boldsymbol{x}, E')dE'dE}{\int_{E_{g'}}^{E_{g'-1}} \Psi(\boldsymbol{x}, E')dE'}$$

$$= \sum_{n=0}^{N} \frac{2n+1}{4\pi} \Sigma_{s,n,g'\to g} P_n(\boldsymbol{\Omega}' \cdot \boldsymbol{\Omega}), \tag{212b}$$

and:

$$\sum_{g'=1}^{G} \int_{4\pi} \Sigma_{s,g\to g'}(\boldsymbol{x}, \boldsymbol{\Omega}' \cdot \boldsymbol{\Omega}) d\Omega' = \sum_{g'=1}^{G} \int_{4\pi} \left[\sum_{n=0}^{N} \frac{2n+1}{4\pi} \Sigma_{s,n,g\to g'}(\boldsymbol{x}) P_n(\boldsymbol{\Omega}' \cdot \boldsymbol{\Omega}) \right] d\Omega'$$

$$= \sum_{g'=1}^{G} \left[\sum_{n=0}^{N} \frac{2n+1}{4\pi} \Sigma_{s,n,g\to g'}(\boldsymbol{x}) \int_{4\pi} P_n(\boldsymbol{\Omega}' \cdot \boldsymbol{\Omega}) d\Omega' \right]$$

$$= \sum_{g'=1}^{G} \left[\sum_{n=0}^{N} \frac{2n+1}{4\pi} \Sigma_{s,n,g\to g'}(\boldsymbol{x}) 4\pi \delta_{n,0} \right]$$

$$= \sum_{g'=1}^{G} \Sigma_{s,0,g\to g'}(\boldsymbol{x})$$

$$= \sum_{g'=1}^{G} \left[\frac{\int_{E_{g'}}^{E_{g'-1}} \int_{E_g}^{E_{g-1}} \Sigma_{s,0}(\boldsymbol{x}, E' \to E) \Psi(\boldsymbol{x}, E') dE' dE}{\int_{E_g}^{E_{g-1}} \Psi(\boldsymbol{x}, E') dE'} \right]$$

$$= \frac{\int_{E_{min}}^{E_{max}} \left[\int_{E_g}^{E_{g-1}} \Sigma_{s,0}(\boldsymbol{x}, E' \to E) \Psi(\boldsymbol{x}, E') dE' \right] dE}{\int_{E_g}^{E_{g-1}} \Psi(\boldsymbol{x}, E') dE'}$$

$$= \frac{\int_{E_g}^{E_{g-1}} \Sigma_s(\boldsymbol{x}, E') \Psi(\boldsymbol{x}, E') dE'}{\int_{E_g}^{E_{g-1}} \Psi(\boldsymbol{x}, E') dE'}$$

$$= \Sigma_{s,g}(\boldsymbol{x}). \tag{212c}$$

Equations (202) and (212) hold for any choice of $\Psi(\boldsymbol{x}, E)$; they are the multigroup analog of the continuous-energy identities (200). These identities have the following significance: (i) Equations (200a) and (212a) guarantee that the multigroup transport equations describe the same types of physical reactions between neutrons and nuclei as the continuous-energy transport equations. (ii) Equations (200b) and (212c) guarantee that the continuous-energy and multigroup scattering operators are *conservative* – they neither create nor destroy neutrons. (These operators only rearrange neutrons in $(\boldsymbol{\Omega}, E)$–space.) (iii) Equations (200c) and (201b) guarantee that the continuous-energy and multigroup fission spectra satisfy the same normalization. (iv) Equations (200d) and (212b) guarantee that the continuous-energy and multigroup differential scattering cross sections satisfy the same type of Legendre polynomial expansions.

We have noted that the structure of the multigroup transport equations is similar to that of the continuous-energy transport equation, the difference being that in the multigroup equations, the energy variable is discrete rather than continuous. From the above derivation, the only error in the multigroup equations occurs in replacing the "exact" multigroup cross sections (206) by the approximate multigroup cross sections (209). This replacement is exact in three hypothetical situations:

1. *The continuous-energy angular flux $\psi(\boldsymbol{x}, \boldsymbol{\Omega}, E)$ has the form of (208) and Ψ is known.* Unfortunately, (208) requires the angular flux to have the same energy spectrum for each direction of flight and the same direction-dependence for each energy. This occurs for an infinite homogeneous spatial medium where ψ is isotropic, but it does not generally occur otherwise.
2. *The continuous-energy cross sections are histograms in E and E' on the specified energy grid.* In this situation, the multigroup cross sections are independent of Ψ and equal to the
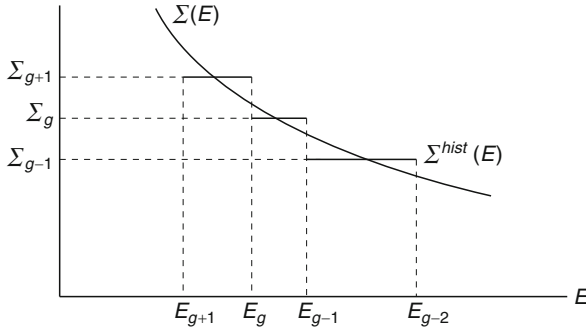
◘ Figure 26
Continuous-energy histogram cross sections

continuous-energy cross sections within each group (see❯ *Fig. 26*). Unfortunately, physical cross sections lack this simple histogram energy-dependence.

3. *The number of energy groups G becomes very large and the group widths* $\Delta E_g = E_{g-1} - E_g$ *become small.* In this limiting case, the multigroup cross sections become independent of Ψ and equal to the continuous-energy cross section evaluated at E_g (and $E_{g'}$).

Thus, the multigroup neutron transport equations are rarely exact for realistic neutron transport problems.

Nonetheless, item 2 in the preceding list suggests a useful way to interpret the multigroup transport equations: *they exactly represent a continuous-energy transport problem with cross sections that are histograms in energy.* If a multigroup approximation for a continuous-energy transport problem is developed, then the multigroup approximation yields the exact group fluxes for the continuous-energy transport problem whose (continuous-energy) cross sections $\Sigma^{hist}(E)$ are equal to the multigroup cross sections on each energy group:

$$\Sigma^{hist}(E) = \Sigma_g, \quad E_g \leq E < E_{g-1}, \ 1 \leq g \leq G.$$

Effectively, then, the multigroup approximation is an approximation to the continuous-energy cross sections. If the physical continuous-energy cross sections are approximated by histograms in energy, then the multigroup approximation will yield the exact group fluxes for the approximate problem with histogram cross sections.

This discussion makes it plausible that as the number of energy groups increases and the energy group widths decrease, the error in the multigroup approximation should decrease. In fact, this is seen in practice.

6.3 The Within-Group and One-Group Transport Equations

For each g, (210) can be written:

$$\boldsymbol{\Omega} \cdot \nabla \psi_g(\boldsymbol{x}, \boldsymbol{\Omega}) + \Sigma_{t,g}(\boldsymbol{x}) \psi_g(\boldsymbol{x}, \boldsymbol{\Omega}) = \int_{4\pi} \Sigma_{s,g \to g}(\boldsymbol{x}, \boldsymbol{\Omega}' \cdot \boldsymbol{\Omega}) \psi_g(\boldsymbol{x}, \boldsymbol{\Omega}') d\Omega'$$
$$+ \frac{\chi_g(\boldsymbol{x})}{4\pi} \int_{4\pi} v \hat{\Sigma}_{f,g}(\boldsymbol{x}) \psi_g(\boldsymbol{x}, \boldsymbol{\Omega}') d\Omega' + S_g(\boldsymbol{x}, \boldsymbol{\Omega}), \tag{213a}$$

where:

$$S_g(\boldsymbol{x}, \boldsymbol{\Omega}) = \frac{Q_g(\boldsymbol{x})}{4\pi} + \sum_{g' \neq g} \int_{4\pi} \Sigma_{s,g' \to g}(\boldsymbol{x}, \boldsymbol{\Omega}' \cdot \boldsymbol{\Omega}) \psi_{g'}(\boldsymbol{x}, \boldsymbol{\Omega}') d\boldsymbol{\Omega}'$$

$$+ \frac{\chi_g(\boldsymbol{x})}{4\pi} \sum_{g' \neq g} \int_{4\pi} \nu \hat{\Sigma}_{f,g}(\boldsymbol{x}) \psi_{g'}(\boldsymbol{x}, \boldsymbol{\Omega}') d\boldsymbol{\Omega}'. \tag{213b}$$

Equation (213a) is the *within-group* transport equation; it has the form of a monoenergetic transport equation, with an anisotropic *group-to-group source* S_g representing (i) the internal neutron source, (ii) the scattering source from groups g' to g, and (iii) the fission source from groups g' to g.

Equations (213) suggest an iterative strategy for solving multigroup transport problems. Specifically, estimates of $\psi_{g'}$ could be introduced into (213b) to obtain estimates of S_g. Then (213a) could be solved to obtain new estimates of ψ_g, and the process could be repeated. Variations on this idea are used in practical simulations (Lewis and Miller 1993).

6.4   Discussion

For obvious reasons, a practical goal is to make the number of energy groups G as small as possible and yet achieve sufficient accuracy. For this reason, great care is often taken in the derivation of the neutron spectrum $\Psi(\boldsymbol{x}, E)$ used to calculate multigroup cross sections. We cannot discuss here the various procedures used to calculate Ψ. However, we do note that different physical circumstances can lead to very different values of G.

For example, in light water reactor cores, where (208) is often a valid approximation, satisfactory numerical results can often be achieved with only $G = 2$ energy groups, group 1 representing the fast neutrons and group 2 representing the thermal neutrons. However, in shielding problems, where the neutron spectrum changes radically (and continuously) from one side of the shield to the other, often $G > 100$ energy groups are required to achieve accurate results.

A fundamental limitation with the conventional multigroup approximation presented here is the assumption (208) that at each spatial point, the energy spectrum is independent of direction $\boldsymbol{\Omega}$. This assumption is not valid at material interfaces between two materials with different capture cross sections. (If the material to the left of an interface has absorption resonances at different energies than the material to the right of the interface, then near the resonance, the neutrons traveling to the right will have an energy spectrum associated with the material on the left of the interface, and the neutrons traveling to the left will have a different energy spectrum associated with the material on the right of the interface.) At present, if highly accurate results are desired near material interfaces, the only option is to use a large number of energy groups G.

Another issue is that because neutron cross sections $\Sigma(E)$ can be extraordinarily complicated functions of E, the angular flux $\psi(\boldsymbol{x}, \boldsymbol{\Omega}, E)$ will also be a complicated function of E. In such cases, it is, as a practical matter, impossible to choose an energy group structure fine enough to "resolve" all the energy-dependent peaks and valleys of Σ and ψ. Hence, the calculation of suitable multigroup cross sections (i.e., the calculation of suitable neutron spectra to be used in [209] and [211]) becomes a problem-dependent, time-consuming, and yet essential

task. Because of this, the multigroup approximation is, although relatively simple to formulate, difficult to implement in detail for practical problems.

7   The Age and Wigner Approximations

In the classic Age and Wigner approximations to the neutron transport equation, the neutron scattering operator is approximated either directly (in the Age approximation) or indirectly (in the Wigner approximation) by a first-order differential operator (Larsen and Ahrens 2001; Weinberg and Wigner 1958). The resulting approximate equations are easier to solve numerically, and in certain problems, they can be solved analytically.

Conventional derivations of the Age and Wigner approximations from the infinite-medium neutron spectrum equation make use of a transformation of the equation from the energy variable E to the *lethargy* variable $u = \ln(E_0/E)$, where $E_0 \geq$ maximum neutron energy. After this transformation is made, the Age and Wigner approximations are derived, and then the results are converted back to E. (These derivations do not explain why the transformation from E to u is made to facilitate the approximations.) Here, the Age and Wigner approximations are derived directly from the scattering operator expressed in terms of E; we do not first transform the infinite-medium neutron spectrum equation from E to u. Thus, the derivations given here have a certain pedagogical advantage: they do not involve the lethargy variable.

However, after deriving the Age and Wigner approximations, we briefly discuss why the use of the lethargy variable has a certain practical advantage in the calculation of multigroup cross sections.

7.1   The Infinite-Medium Neutron Spectrum Equation

We consider the eigenvalue problem defined by (49), with the elastic differential scattering cross section defined by (10) and (11). (Equations (10) are valid for *epithermal* energies $E \gg kT =$ the mean thermal energy of the nuclei.) Integrating (49a) over $\boldsymbol{\Omega}$ and defining

$$\phi(\boldsymbol{x}, E) = \int_{4\pi} \psi(\boldsymbol{x}, \boldsymbol{\Omega}, E) d\Omega = \text{ scalar flux}, \tag{214a}$$

$$\boldsymbol{J}(\boldsymbol{x}, E) = \int_{4\pi} \boldsymbol{\Omega} \psi(\boldsymbol{x}, \boldsymbol{\Omega}, E) d\Omega = \text{ neutron current}, \tag{214b}$$

we obtain:

$$\nabla \cdot \boldsymbol{J}(\boldsymbol{x}, E) + \Sigma_t(E)\phi(\boldsymbol{x}, E) = \int_E^{E/\alpha} \frac{\Sigma_s(E')\phi(\boldsymbol{x}, E')}{(1-\alpha)E'} dE' + \frac{\chi_P(E)}{k} \int_0^\infty \nu\Sigma_f(E')\phi(\boldsymbol{x}, E') dE',$$

where:

$$\alpha = \left(\frac{A-1}{A+1}\right)^2.$$

For an infinite homogeneous medium, ϕ and $\boldsymbol{J}$ are independent of $\boldsymbol{x}$, and the previous equation can be written:

$$\Sigma_t(E)\phi(E) = \int_E^{E/\alpha} \frac{\Sigma_s(E')\phi(E')}{(1-\alpha)E'} dE' + Q(E), \tag{215a}$$

or:

$$\Sigma_a(E)\phi(E) = \mathcal{L}\phi(E) + Q(E), \tag{215b}$$

where $Q(E)$ is the fission source and $\mathcal{L}$ is the *elastic neutron scattering operator*:

$$Q(E) = \frac{\chi_p(E)}{k} \int_0^\infty \nu\Sigma_f(E')\phi(E')dE', \tag{215c}$$

$$\mathcal{L}\phi(E) = \int_E^{E/\alpha} \frac{\Sigma_s(E')\phi(E')}{(1-\alpha)E'}dE' - \Sigma_s(E)\phi(E). \tag{215d}$$

In the following, we assume that $Q(E) = C\chi_p(E)$, where the constant C is given.

For $A = 1$ (epithermal elastic neutron scattering off hydrogen nuclei), $\alpha = 0$ and (215) become:

$$\Sigma_t(E)\phi(E) = \int_E^\infty \frac{\Sigma_s(E')\phi(E')}{E'}dE' + Q(E). \tag{216}$$

This equation can be solved analytically. Differentiating it with respect to E, we get:

$$\frac{d}{dE}[\Sigma_t(E)\phi(E) - Q(E)] = -\frac{\Sigma_t(E)\phi(E)}{E}, \tag{217}$$

which is an easily solved first-order ordinary differential equation. Assuming $Q(E) = \phi(E) = 0$ for $E \geq E_0$, we obtain the analytic solution:

$$\phi(E) = \frac{1}{\Sigma_t(E)}\left[Q(E) + \int_E^{E_0} Q(E')\frac{\Sigma_s(E')}{\Sigma_t(E')E'}e^{\int_E^{E'}\frac{\Sigma_s(E'')}{\Sigma_t(E'')}\frac{dE''}{E''}}dE'\right]. \tag{218}$$

However,

$$\int_E^{E'}\frac{\Sigma_s(E'')}{\Sigma_t(E'')}\frac{dE''}{E''} = \int_E^{E'}\frac{\Sigma_t(E'')-\Sigma_a(E'')}{\Sigma_t(E'')}\frac{dE''}{E''} = \left(\ln\frac{E'}{E}\right) - \int_E^{E'}\frac{\Sigma_a(E'')}{\Sigma_t(E'')}\frac{dE''}{E''},$$

so (218) can be written in the equivalent and more common form:

$$\phi(E) = \frac{1}{\Sigma_t(E)}\left[Q(E) + \frac{1}{E}\int_E^{E_0} Q(E')\frac{\Sigma_s(E')}{\Sigma_t(E')}e^{-\int_E^{E'}\frac{\Sigma_a(E'')}{\Sigma_t(E'')}\frac{dE''}{E''}}dE'\right]. \tag{219}$$

Unfortunately, for $A > 1$, it is not possible to perform these operations and solve (215). Thus, for $A > 1$, it is desirable to *accurately approximate* (215) in a form similar to (217), i.e., as an explicitly solvable first-order ordinary differential equation. Accomplishing this is the task at hand.

Before proceeding, we note that for any constant C,

$$\mathcal{L}\left[\frac{C}{E\Sigma_s(E)}\right] = \int_E^{E/\alpha} \frac{C}{(1-\alpha)(E')^2}dE' - \frac{C}{E} = 0. \tag{220}$$

Thus, for $\Sigma_a(E) = 0$ and $Q(E) = 0$,

$$\phi_{eq}(E) = \frac{C}{E\Sigma_s(E)} \tag{221}$$

is an *equilibrium solution* of (215a). For intervals of energy in which $\Sigma_a(E) = 0$ and $Q(E) = 0$, $\phi(E)$ is very well approximated by (221), with a suitably defined C.

Also, for any $\phi(E)$, we have

$$\int_0^\infty \mathcal{L}\phi(E)dE = \int_0^\infty \int_E^{E/\alpha} \frac{\Sigma s(E')\phi(E')}{(1-\alpha)E'}dE'dE - \int_0^\infty \Sigma_s(E)\phi(E)dE$$

$$= \int_{E'=0}^\infty \left(\int_{E=\alpha E'}^{E'} dE\right) \frac{\Sigma s(E')\phi(E')}{(1-\alpha)E'}dE' - \int_0^\infty \Sigma_s(E)\phi(E)dE = 0. \tag{222}$$

This equation states that scattering is *conservative*: the rate at which neutrons enter scattering events equals the rate at which neutrons exit scattering events.

In the following, we require any acceptable approximation of $\mathcal{L}$ to satisfy (220) and (222). Thus, an approximate scattering operator should preserve the equilibrium solution $\phi_{eq}(E)$, and it should be conservative. (In fact, we will demand more, but we state these first two conditions here.)

7.2 The "Conservative" Form of the Neutron Transport Equation

The out-scattering (integral) operator in (215a) contains the differential scattering cross section:

$$\Sigma_s(E' \to E'') = \begin{cases} \dfrac{\Sigma_s(E')}{(1-\alpha)E'}, & E'' < E' < E''/\alpha \\ 0, & \text{otherwise.} \end{cases} \tag{223}$$

Using this, it is possible to determine the *slowing-down density* $F(E)$, defined by:

$$F(E) = \text{the rate per unit volume at which neutrons slow down from}$$
$$\text{energies } (E') \text{ greater than } E \text{ to energies } (E'') \text{ less than } E. \tag{224}$$

As depicted in ❯ *Fig. 27*, a neutron with energy E' in the interval $E < E' < E/\alpha$ can directly scatter into an energy $E'' < E$ only if E'' is in the interval $\alpha E' < E'' < E$.
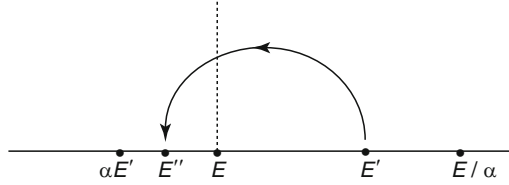
◾ **Figure 27**
Scattering from $E' > E$ to $E'' < E$

From (223), we have

$$\Sigma_s(E' \to E'')\phi(E')dE'dE'' = \text{the rate per unit volume at which neutrons scatter from}$$
$$\text{the interval } (E', E' + dE') \text{ to the interval } (E'', E'' + dE'').$$

Integrating this expression over $\alpha E' < E'' < E$ and then over $E < E' < E/\alpha$, and using the definition (224), we obtain:

$$F(E) = \int_{E'=E}^{E/\alpha} \int_{E''=\alpha E'}^{E} \frac{\Sigma_s(E')\phi(E')}{(1-\alpha)E'} dE'' dE' = \int_{E'=E}^{E/\alpha} \frac{E - \alpha E'}{(1-\alpha)E'} \Sigma_s(E')\phi(E')dE'. \quad (225)$$

Differentiating $F(E)$, we get:

$$\frac{dF}{dE}(E) = \int_{E}^{E/\alpha} \frac{\Sigma_s(E')\phi(E')}{(1-\alpha)E'} dE' - \Sigma_s(E)\phi(E)$$
$$= \mathcal{L}\phi(E). \quad (226)$$

Therefore, the infinite-medium spectrum equation (215b) can be written in the advantageous *conservative* form:

$$\Sigma_a(E)\phi(E) = \frac{dF}{dE}(E) + Q(E), \quad (227a)$$

where:

$$F(E) = \frac{1}{1-\alpha} \int_{E'=E}^{E/\alpha} \frac{E - \alpha E'}{E'} \Sigma_s(E')\phi(E')dE'. \quad (227b)$$

To illustrate the utility of (227), let us consider for any mass number $A \geq 1$ a purely scattering problem $[\Sigma_a(E) = 0]$ with $Q(E) > 0$ only for $E_1 < E < E_0$ (❯ *Fig. 28*). Then, operating on (227a) by $\int_{E}^{E_0}(\cdot)dE'$, we obtain for $E < E_1$:

$$F(E) = \int_{E_1}^{E_0} Q(E')dE' = \text{constant} \quad \text{(independent of } E). \quad (228a)$$

However, since $\Sigma_a(E) = 0$ and $Q(E) = 0$ for $E < E_1$, then for $E \ll E_1$, $\phi_A(E)$ is very well-represented by (221):

$$\phi_A(E) \approx \frac{C}{E\Sigma_s(E)}, \quad (228b)$$
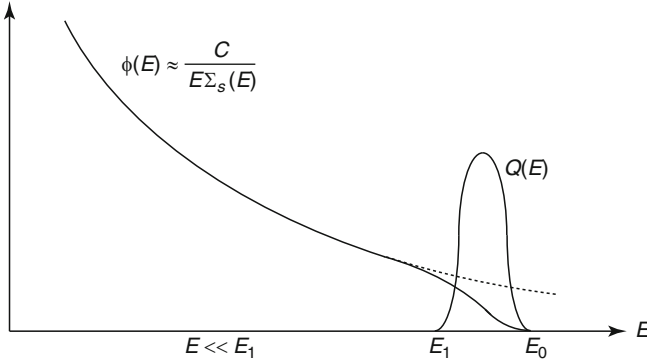
■ Figure 28
Purely scattering problem with $\Sigma_a(E) = 0$

where the constant C is undetermined. Assuming $E \ll E_1$, and introducing (228a) into the left side of (227b) and (228b) into the right side of (227b), we obtain

$$\int_{E_1}^{E_0} Q(E)dE \approx \frac{1}{1-\alpha} \int_{E'=E}^{E/\alpha} \frac{E - \alpha E'}{E'} \left(\frac{C}{E'}\right) dE'$$

$$= \frac{C}{1-\alpha} \int_{E'=E}^{E/\alpha} \frac{E - \alpha E'}{(E')^2} dE' = C\xi, \tag{228c}$$

where (see ❯ *Fig. 29*):

$$\xi = 1 + \frac{\alpha \ln \alpha}{1 - \alpha}$$

$$= \begin{cases} 1, & \alpha = 0 \quad (A = 1) \\ \dfrac{1-\alpha}{2} + O(1-\alpha)^2, & \alpha \approx 1 \quad (A \gg 1). \end{cases} \tag{229}$$

Solving (228c) for C and introducing this expression into (228b), we obtain:

$$\phi_A(E) \approx \frac{1}{E\Sigma_s(E)} \left[\frac{1}{\xi} \int_{E_1}^{E_0} Q(E')dE' \right]. \tag{230}$$

Equation (230) is essentially exact for all α and for all $E < E_1$. We note that since $\xi = 1$ for $A = 1$ (see [229]), then (230) agrees with (219) for $A = 1$ and $\Sigma_a(E) = 0$.

As the mass number A of the scattering nuclei increases, α increases, so ξ decreases, and so $\phi(E)$ in (230) increases. Physically, this happens because for larger A, neutrons on the average lose less energy per collision, i.e., the slowing-down process becomes less efficient. Thus, neutrons increasingly "pile up" as they slow down. The constant ξ in (229) and (230) exactly calibrates this "piling-up" effect for the purely scattering problems considered above:

$$\frac{\phi_A(E)}{\phi_1(E)} = \frac{1}{\xi}, \quad E < E_1, \tag{231}$$
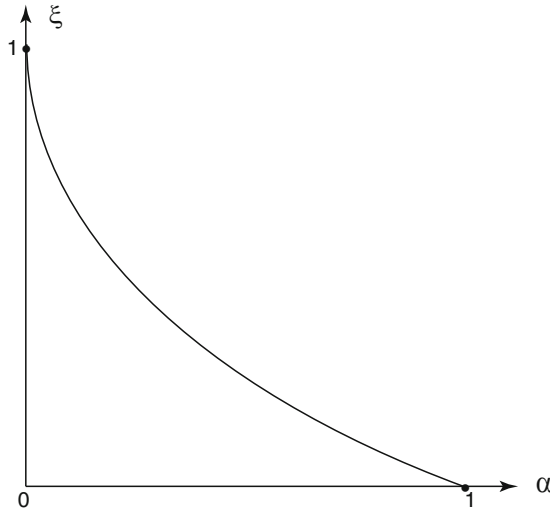
■ **Figure 29**
ξ versus α

7.3 The Age Approximation

In (227), let us consider $A \gg 1$. Then

$$\alpha = \left(\frac{A-1}{A+1}\right)^2 = 1 - \frac{4}{A} + O\left(\frac{1}{A^2}\right), \tag{232}$$

so the width of the interval of integration in (225) is $O(1/A)$. (This implies $F(E) = O(1/A)$.) We approximate (225) as:

$$\begin{aligned} F(E) &= \int_{E'=E}^{E/\alpha} \frac{E - \alpha E'}{(1-\alpha)(E')^2}[E'\Sigma_s(E')\phi(E')]dE' \\ &= \int_{E'=E}^{E/\alpha} \frac{E - \alpha E'}{(1-\alpha)(E')^2}[E\Sigma_s(E)\phi(E) + O(E' - E)]dE' \\ &= \xi E\Sigma_s(E)\phi(E) + O\left(\frac{1}{A^2}\right). \end{aligned} \tag{233}$$

(The remainder term is $O(1/A^2)$ because $E' - E = O(1/A)$ and the interval of integration is $O(1/A)$.)

Introducing (233) into (227a) and ignoring the $O(1/A^2)$ terms, we obtain the following *Age Approximation* to the infinite-medium neutron spectrum equation:

$$\Sigma_a(E)\phi(E) = \xi\frac{d}{dE}E\Sigma_s(E)\phi(E) + Q(E) . \tag{234}$$

(For electron transport problems, this result is called the *continuous slowing down* (CSD) approximation.) Equation (234) contains the basic approximation:

$$\mathcal{L}_A \phi(E) = \xi \frac{d}{dE} E \Sigma_s(E) \phi(E), \tag{235}$$

which satisfies (220) and (222), provided only that $E\Sigma_s(E)\phi(E)$ vanishes at $E = 0$ and ∞.

The Age equation has $O(1/A^2)$ error for $A \gg 1$, so at this point its validity for small mass numbers A is unclear. For all A, (234), applied to the purely scattering problem discussed above yields the solution defined by (230) for all $E < E_1$. This shows that the Age approximation is valid for *some* problems for all A.

Equation (234) can be solved in closed form, yielding:

$$\phi(E) = \frac{1}{\xi E \Sigma_s(E)} \int_E^{E_0} e^{-\frac{1}{\xi} \int_E^{E'} \frac{\Sigma_a(E'')}{E'' \Sigma_s(E'')} dE''} Q(E') dE'. \tag{236}$$

For $A = 1$ ($\xi = 1$), this result reduces to the exact $A = 1$ solution given in (219) only if $E < E_1$ and $\Sigma_a(E) = 0$. Thus, the Age approximation is generally not accurate unless $A \gg 1$, $E < E_1$, and $\Sigma_a(E) \ll \Sigma_s(E)$.

A more accurate approximation, derived by Wigner, has the desirable features of the Age approximation *and* the additional desirable properties that it is exact for $A = 1$ and is generally much more accurate than the Age approximation. We discuss this next.

7.4 The Wigner Approximation

For $A \gg 1$, (234) holds with $O(1/A^2)$ error. Adding $\Sigma_s(E)\phi(E)$ to both sides of this equation and using $\xi = O(1/A)$, we obtain:

$$\begin{aligned} \Sigma_t(E)\phi(E) &= \left[\Sigma_s(E)\phi(E) + \xi \frac{d}{dE} E \Sigma_s(E)\phi(E) \right] + Q(E) + O\left(\frac{1}{A^2}\right) \\ &= \frac{1}{E}\left(I + \xi E \frac{d}{dE} \right) E\Sigma_s(E)\phi(E) + Q(E) + O\left(\frac{1}{A^2}\right) \\ &= \frac{1}{E}\left(I - \xi E \frac{d}{dE} \right)^{-1} E\Sigma_s(E)\phi(E) + Q(E) + O\left(\frac{1}{A^2}\right). \end{aligned} \tag{237}$$

Ignoring the $O(1/A^2)$ terms, we obtain the basic form of the *Wigner approximation* to the infinite-medium neutron spectrum equation:

$$\Sigma_t(E)\phi(E) = \frac{1}{E}\left(I - \xi E \frac{d}{dE} \right)^{-1} E\Sigma_s(E)\phi(E) + Q(E). \tag{238a}$$

The first term on the right side:

$$H_W(E) = \frac{1}{E}\left(I - \xi E \frac{d}{dE} \right)^{-1} E\Sigma_s(E)\phi(E) \tag{238b}$$

satisfies the first-order ordinary differential equation:

$$\left(I - \xi E \frac{d}{dE} \right) E H_W(E) = E \Sigma_s(E) \phi(E),$$

or:

$$H_W(E) - \xi \frac{d}{dE} E H_W(E) = \Sigma_s(E) \phi(E).$$

The solution of this equation is:

$$H_W(E) = \frac{1}{\xi E} \int_E^\infty \left(\frac{E}{E'} \right)^{1/\xi} \Sigma_s(E') \phi(E') dE'. \tag{238c}$$

Introducing (238c) into (238a), we get:

$$\Sigma_t(E) \phi(E) = \frac{1}{\xi E} \int_E^\infty \left(\frac{E}{E'} \right)^{1/\xi} \Sigma_s(E') \phi(E') dE' + Q(E). \tag{238d}$$

Thus, unlike the Age approximation, the Wigner approximation approximates the scattering integral by an actual integral, $H_W(E)$. For $A \gg 1$, $H_W(E)$ is an $O(1/A^2)$ approximation to the exact scattering integral in (215b):

$$H(E) = \frac{1}{1 - \alpha} \int_E^{E/\alpha} \frac{\Sigma_s(E') \phi(E')}{E'} dE'. \tag{239}$$

However, for $A = 1$, $\alpha = 0$ and $\xi = 1$, so $H_W(E) = H(E)$, and Wigner's approximation is exact!

Also, the Wigner approximation to the scattering operator $\mathcal{L}$:

$$\mathcal{L}_W \phi(E) = \left[\frac{1}{E} \left(I - \xi E \frac{d}{dE} \right)^{-1} E - I \right] \Sigma_s(E) \phi(E)$$

$$= \frac{1}{E} \left[\left(I - \xi E \frac{d}{dE} \right)^{-1} - I \right] E \Sigma_s(E) \phi(E) \tag{240}$$

can be written in two equivalent forms:

$$\mathcal{L}_W \phi(E) = \frac{1}{E} \left(I - \xi E \frac{d}{dE} \right)^{-1} \left[I - \left(I - \xi E \frac{d}{dE} \right) \right] E \Sigma_s(E) \phi(E)$$

$$= \frac{\xi}{E} \left(I - \xi E \frac{d}{dE} \right)^{-1} E \frac{d}{dE} E \Sigma_s(E) \phi(E), \tag{241}$$

and:

$$\mathcal{L}_W \phi(E) = \frac{1}{E} \left[I - \left(I - \xi E \frac{d}{dE} \right) \right] \left(I - \xi E \frac{d}{dE} \right)^{-1} E \Sigma_s(E) \phi(E)$$

$$= \xi \frac{d}{dE} \left(I - \xi E \frac{d}{dE} \right)^{-1} E \Sigma_s(E) \phi(E). \tag{242}$$

Equation (241) shows that $\mathcal{L}_W$ preserves $\phi_{eq}(E)$, and (242) shows that $\mathcal{L}_W$ is conservative. Wigner's equation (238) can also be written:

$$\left(I - \xi E \frac{d}{dE}\right) E\left[\Sigma_t(E)\phi(E) - Q(E)\right] = E\Sigma_s(E\phi(E),$$

or:

$$\Sigma_t(E)\phi(E) - Q(E) - \xi \frac{d}{dE} E\left[\Sigma_t(E)\phi(E) - Q(E)\right] = \Sigma_s(E\phi(E)$$

or:

$$\Sigma_a(E)\phi(E) = \xi \frac{d}{dE} E\left[\Sigma_t(E)\phi(E) - Q(E)\right] + Q(E). \tag{243}$$

Solving this first-order ordinary differential equation with $\phi(E_0) = 0$, we obtain:

$$\phi_W(E) = \frac{1}{\Sigma_t(E)}\left[Q(E) + \frac{1}{\xi E}\int_E^{E_0} e^{-\frac{1}{\xi}\int_E^{E'}\frac{\Sigma_a(E'')}{E''\Sigma_t(E'')}dE''}\frac{\Sigma_s(E')}{\Sigma_t(E')}Q(E')dE'\right]. \tag{244}$$

This result is exact for $A = 1$ and has $O(1/A^2)$ error for $A \gg 1$.

If we consider a monoenergetic source:

$$Q(E) = Q_0\delta(E - E_0),$$

then for $E < E_0$, (244) can be written as the product of four factors:

$$\phi_W(E) = \left[\frac{Q_0}{\xi E\Sigma_s(E)}\right]\left[\frac{\Sigma_s(E_0)}{\Sigma_t(E_0)}\right]\left[e^{-\frac{1}{\xi}\int_E^{E_0}\frac{\Sigma_a(E')}{E'\Sigma_t(E')}dE'}\right]\left[\frac{\Sigma_s(E)}{\Sigma_t(E)}\right], \tag{245}$$

each of which has a straightforward physical interpretation.

The first factor is the equilibrium solution for a problem emitting Q_0 neutrons per cm^3 per s with $\Sigma_a(E) = 0$:

$$\phi_{eq}(E) = \frac{Q_0}{\xi E\Sigma_s(E)}. \tag{246a}$$

If $\Sigma_a(E) = 0$, the remaining three factors on the right side of (245) all equal unity, and then $\phi_W(E) = \phi_{eq}(E)$. The three terms suppress $\phi_W(E)$ in ways that account for absorption.

The second factor is the *scattering ratio at energy E_0*:

$$c(E_0) = \frac{\Sigma_s(E_0)}{\Sigma_t(E_0)} = \text{ the probability that a (source) neutron}$$

$$\text{with energy } E_0 \text{ will not be absorbed.} \tag{246b}$$

This factor is necessary because only the source neutrons (all of which are born at energy E_0) that scatter can contribute to $\phi(E)$. Effectively, the product

$$q_0 = Q_0\frac{\Sigma_s(E_0)}{\Sigma_t(E_0)}$$

is a *reduced source rate*, which accounts for source neutrons born at E_0 that are immediately absorbed and hence do not slow down.

The third factor on the right side of (245) is the *resonance escape probability*:

$$p(E_0 \to E) = e^{-\frac{1}{\xi} \int_E^{E_0} \frac{\Sigma_a(E')}{E' \Sigma_t(E')} dE'}$$

$$= \text{the probability that a neutron will not be absorbed}$$

$$\text{while slowing down from } E_0 \text{ to } E. \tag{246c}$$

The fourth factor is the scattering ratio $c(E)$, to account for the suppression of $\phi(E)$ due to absorption at energy E.

Equation (245) is therefore not only an accurate result, but it has an intuitive physical interpretation. (The expression for the resonance escape probability in (245) is especially accurate and useful.) We now turn to providing a general sketch of $\phi_W(E)$.

For heavy nuclei, $\Sigma_a(E)$ often consists of narrow, isolated absorption resonances, while $\Sigma_s(E)$ is relatively constant (see ❯ *Fig. 30*). In this situation, $c(E)$ has the form depicted in ❯ *Fig. 31*, and $p(E_0 \to E)$ has the form depicted in ❯ *Fig. 32*. Combining these, the product $\phi(E)$ expressed in (245) has the form depicted in ❯ *Fig. 33*.

Hence, as neutrons slow down through each absorption resonance, $\phi_W(E)$ experiences a narrow "dip" within the resonance and returns to a new equilibrium solution below the resonance (the amplitude is reduced because of neutrons that are absorbed within the resonance).
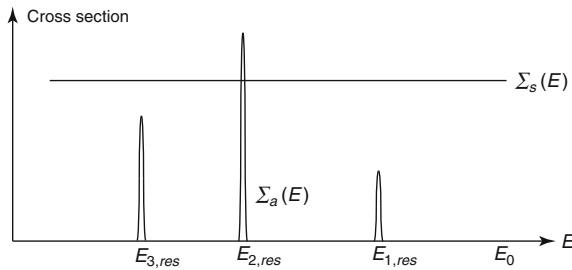
◼ **Figure 30**
$\Sigma_a(E)$ **and** $\Sigma_s(E)$
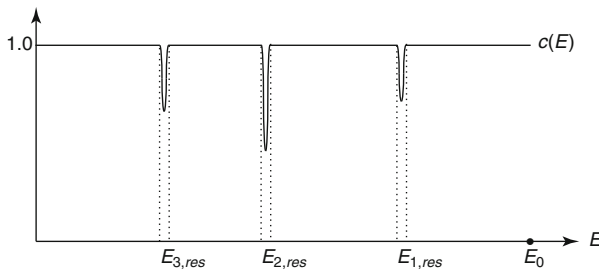
◼ **Figure 31**
c(E)
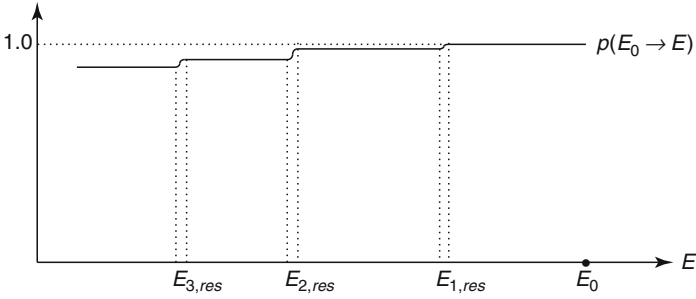
☐ **Figure 32**
$p(E_0 \rightarrow E)$
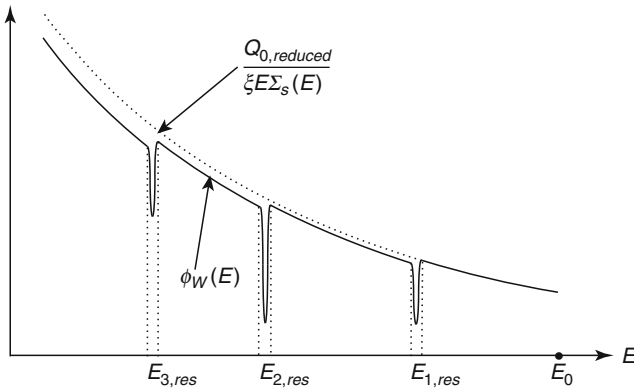
☐ **Figure 33**
$\phi_W(E)$

The above Wigner depiction of $\phi(E)$ is surprisingly accurate. The simpler Age depiction of $\phi(E)$ is usually less accurate, unless $\Sigma_a(E) \ll \Sigma_s(E)$.

7.5 Discussion

We have derived the *Age* (or CSD) approximation (234), and the *Wigner* approximation (243) of the infinite-medium neutron spectrum equation (215a). The Age and Wigner approximations both:

1. Are conservative.
2. Preserve the equilibrium solution $\phi_{eq}(E)$.
3. Are $O(1/A^2)$ asymptotic approximations to the spectrum equation for $A \gg 1$.
4. Yield for $E < E_1$ the solution (230) of the purely scattering problem.

However, the Wigner approximation is generally more accurate than the Age approximation, for the following reasons:

1. The Wigner approximation $H_W(E)$ of the out-scattering integral $H(E)$ is itself an integral [see (238c) and (239)], and $H_W(E) = H(E)$ for $A = 1$.
2. Because the Wigner approximation is exact for $A = 1$ and highly accurate for $A \gg 1$, it is also quite accurate for intermediate values of A.

Therefore, the Wigner approximation is quite accurate for all values of A, whereas the simpler Age approximation is generally only accurate for $A \gg 1$.

8   The Diffusion Approximation

Because of its relative simplicity and range of applicability, the diffusion approximation to the Boltzmann transport equation is widely used for reactor core simulations. However, the diffusion approximation has several subtleties, and even today there are issues in its use that are not fully understood.

　Here we derive the approximate diffusion equation for a 1-D planar-geometry problem, using a simplified version of asymptotic derivations that have been published during the past 35 years (Habetler and Matkowsky 1975; Larsen 1980; Larsen and Keller 1974; Larsen et al. 1996; Papanicolaou 1975). The choice of 1-D planar geometry enables us to perform the derivation with the Legendre polynomials, rather than the more complex spherical harmonic functions, which are necessary for 2-D, and 3-D problems. However, the basic underlying issues in 1-D, 2-D, and 3-D geometries are the same.

8.1   Derivation of the Diffusion Equation

We consider the energy-dependent, planar-geometry Boltzmann transport equation with anisotropic scattering:

$$\mu \frac{\partial \psi}{\partial x}(x, \mu, E) + \Sigma_t(x, E)\psi(x, \mu, E)$$
$$= \sum_{m=0}^{\infty} \frac{2m+1}{2} P_m(\mu) \int_0^{\infty} \int_{-1}^{1} P_m(\mu')\Sigma_{s,m}(x, E' \to E)\psi(x, \mu', E')d\mu' dE'$$
$$+ \frac{Q(x, E)}{2}, \tag{247a}$$

on the system $0 \le x \le X$, with boundary conditions:

$$\psi(0, \mu, E) = \psi(0, -\mu, E), \quad 0 < \mu \le 1, \tag{247b}$$

$$\psi(X, \mu, E) = \psi^b(\mu, E), \quad -1 \le \mu < 0. \tag{247c}$$

(Equation [247b] is a *reflection* or *symmetry* boundary condition; [247c] specifies the incident flux $\psi^b(\mu, E)$ on the right boundary of the system.)

To initiate the derivation of the diffusion approximation to (247), let us first consider (247a) for an *infinite homogeneous* medium having no spatial dependence:

$$\Sigma_t(E)\psi(\mu, E) = \sum_{m=0}^{\infty} \frac{2m+1}{2} P_m(\mu) \int_0^{\infty} \int_{-1}^{1} P_m(\mu') \Sigma_{s,m}(E' \to E)\psi(\mu', E')d\mu' dE' + \frac{Q(E)}{2}.$$
(248)

To represent the exact solution of (248), we operate on this equation by $\int_{-1}^{1} P_n(\mu)(\cdot)d\mu$. Defining the nth Legendre moment of the angular flux as:

$$\int_{-1}^{1} P_n(\mu)\psi(\mu, E)d\mu = \phi_n(E),$$

and using:

$$\int_{-1}^{1} P_n(\mu)P_m(\mu)d\mu = \delta_{m,n},$$

we obtain the system of equations:

$$\Sigma_t(E)\phi_n(E) = \int_0^{\infty} \Sigma_{s,n}(E' \to E)\phi_n(E')dE' + Q(E)\delta_{n,0}, \;\; 0 \le n.$$
(249)

Hence, for $n \ge 1$, $\phi_n(E) = 0$, and:

$$\psi(\mu, E) = \sum_{n=0}^{\infty} \frac{2n+1}{2} P_n(\mu)\phi_n(E) = \frac{1}{2}\phi_0(E),$$
(250)

where $\phi_0(E)$ satisfies (249) with $n = 0$. Equations (248–250) show that *for an infinite, spatially uniform problem with an isotropic source, the angular flux is independent of both space (x) and angle (μ).*

We now return to (247) and assume that the spatial derivative in ψ is *small* in comparison to the other terms. (Physically, the net leakage rate from a spatial increment dx is assumed to be small in comparison to the collision rate and scattering rates in dx.) To analytically describe this, we write (247a) as:

$$\varepsilon\mu\frac{\partial\psi}{\partial x}(x, \mu, E) + \Sigma_t(x, E)\psi(x, \mu, E)$$
$$= \sum_{m=0}^{\infty} \frac{2m+1}{2} P_m(\mu) \int_0^{\infty} \int_{-1}^{1} P_m(\mu')\Sigma_{s,m}(x, E' \to E)\psi(x, \mu', E')d\mu'dE'$$
$$+ \frac{Q(x, E)}{2},$$
(251)

where ε is a small dimensionless parameter, indicating that the leakage term is small. (At the conclusion of this analysis, we set $\varepsilon = 1$.)

Because ψ has a weak spatial dependence, we anticipate that ψ should also have a weak angular dependence. (As the spatial derivative of ψ limits to zero, ψ should become isotropic.) Consistent with this expectation, we show that the solution of (251) has the Legendre polynomial expansion:

$$\psi(x, \mu, E) = \sum_{m=0}^{\infty} \frac{2m+1}{2} \varepsilon^m P_m(\mu)\phi_m(x, E),$$
(252)

where $\phi_n(E) = O(1)$ for all n. (In (252), the mth Legendre moment of $\psi(x, \mu, E)$ is $\varepsilon^m \phi_m(x, E)$.)

Introducing (252) into (251), using the identity:

$$\mu P_m(\mu) = \frac{m+1}{2m+1} P_{m+1}(\mu) + \frac{m}{2m+1} P_{m-1}(\mu),$$

and operating by $\int_{-1}^{1} P_n(\mu)(\cdot)d\mu$, we obtain for all $n \geq 0$:

$$\frac{n}{2n+1} \frac{\partial \phi_{n-1}}{\partial x}(x, E) + \varepsilon^2 \frac{n+1}{2n+1} \frac{\partial \phi_{n+1}}{\partial x}(x, E) + \Sigma_t(x, E)\phi_n(x, E)$$

$$= \int_0^\infty \Sigma_{s,n}(x, E' \to E)\phi_n(x, E')dE' + \delta_{n,0}Q(x, E). \qquad (253)$$

These equations are consistent with the assumption in (252) that $\phi_n(x, E) = O(1)$, and thus that the nth Legendre moment of ψ is $O(\varepsilon^n)$.

Specifically, (253) with $n = 0$ and $n = 1$ yields:

$$\varepsilon^2 \frac{\partial \phi_1}{\partial x}(x, E) + \Sigma_t(x, E)\phi_0(x, E) = \int_0^\infty \Sigma_{s,0}(x, E' \to E)\phi_n(x, E')dE' + Q(x, E), \quad (254a)$$

$$\frac{1}{3}\frac{\partial \phi_0}{\partial x}(x, E) + \frac{2\varepsilon^2}{3}\frac{\partial \phi_2}{\partial x}(x, E) + \Sigma_t(x, E)\phi_1(x, E) = \int_0^\infty \Sigma_{s,1}(x, E' \to E)\phi_1(x, E')dE'.$$
$$(254b)$$

To derive the diffusion equation, we make the following two approximations to (254b):

1. We set:

$$\varepsilon^2 \frac{\partial \phi_2}{\partial x}(x, E) \approx 0. \qquad (255a)$$

(This introduces an error of $O(\varepsilon^2)$ in the equations for ϕ_0 and ϕ_1.)

2. We introduce the approximation:

$$\Sigma_{s,1}(E' \to E) \approx \Sigma_{s,1}(x, E')\delta(E' - E), \qquad (255b)$$

where:

$$\Sigma_{s,1}(x, E') = \int_0^\infty \Sigma_{s,1}(E' \to E)dE. \qquad (256)$$

(This creates an error of undetermined order with respect to ε. However, the following integral is preserved:

$$\int_0^\infty \left[\Sigma_{s1}(x, E' \to E)\right] dE = \int_0^\infty \left[\Sigma_{s1}(x, E')\delta(E' - E)\right] dE = \Sigma_{s,1}(x, E'),$$

and thus the integral of the right side of (254) over E is preserved.)

Making these two approximations, (254b) becomes:

$$\frac{1}{3}\frac{\partial \phi_0}{\partial x}(x, E) + \Sigma_t(x, E)\phi_1(x, E) = \Sigma_{s,1}(x, E)\phi_1(x, E). \qquad (257)$$

If we now define:

$$\Sigma_{tr}(x, E) = \Sigma_t(x, E) - \Sigma_{s,1}(x, E) = \textit{transport cross section,} \tag{258a}$$

then (257) yields *Fick's Law*:

$$\phi_1(x, E) = -\frac{1}{3\Sigma_{tr}(x, E)} \frac{\partial \phi_0}{\partial x}(x, E). \tag{258b}$$

Introducing (258a) into (254a), we obtain the following *energy-dependent diffusion equation*:

$$-\varepsilon^2 \frac{\partial}{\partial x} \frac{1}{3\Sigma_{tr}(x, E)} \frac{\partial \phi_0}{\partial x}(x, E) + \Sigma_t(x, E)\phi_0(x, E) = \int_0^\infty \Sigma_{s,0}(x, E' \to E)\phi_n(x, E')dE'$$
$$+ Q(x, E). \tag{259}$$

Also, from (252) and (258), we have the following representation of ψ:

$$\psi(x, \mu, E) = \frac{1}{2}\phi_0(x, E) - \frac{\varepsilon\mu}{2\Sigma_{tr}(x, E)} \frac{\partial \phi_0}{\partial x}(x, E) + O(\varepsilon^2). \tag{260}$$

Ignoring the $O(\varepsilon^2)$ component of ψ, we see that the transport reflection boundary condition (247b) at $x = 0$ is satisfied by (260) if:

$$\frac{\partial \phi_0}{\partial x}(0, E) = 0. \tag{261}$$

This is the diffusion *reflection* or *symmetry* boundary condition.

However, since ϕ_0 is independent of μ, the transport boundary condition at $x = X$:

$$\psi^b(X, \mu) = \psi(X, \mu)$$
$$= \frac{1}{2}\phi_0(X, E) - \frac{\varepsilon\mu}{2\Sigma_{tr}(X, E)} \frac{\partial \phi_0}{\partial x}(X, E), \quad -1 \le \mu < 0$$

cannot generally be satisfied. Operating on both sides of this equation by $\int_{-1}^0 w(|\mu|)(\cdot)d\mu$, where $w(\mu)$ is any positive function, which for convenience is normalized by $\int_0^1 w(\mu)d\mu = 1$, we obtain:

$$2\int_{-1}^0 w(|\mu|)\psi^b(\mu, E)d\mu = \phi_0(X, E) + \frac{\varepsilon}{\Sigma_{tr}(X, E)} \left(\int_0^1 \mu w(\mu)d\mu\right) \frac{\partial \phi_0}{\partial x}(X, E), \tag{262}$$

and this boundary condition *can* be used to determine ϕ_0. However, it is not clear how to choose $w(\mu)$.

A common, physically based choice of $w(\mu)$ is:

$$w(\mu) = 2\mu, \tag{263a}$$

which yields the *Marshak boundary condition*:

$$4J^-(X) = \phi_0(X, E) + \frac{2\varepsilon}{3\Sigma_{tr}(X, E)} \frac{\partial \phi_0}{\partial x}(X, E), \tag{263b}$$

where:

$$J^-(X) = \int_{-1}^{0} |\mu| \psi^b(\mu, E) d\mu$$

$$= \text{incident partial current at } x = X. \tag{263c}$$

This boundary condition preserves the rate at which neutrons enter the system on its incident-flux boundary.

A more accurate diffusion boundary condition can be obtained by appealing to transport theory, or to a variational analysis, which yields the following approximation to $w(\mu)$:

$$w(\mu) = \mu + \frac{3}{2}\mu^2. \tag{264a}$$

This yields:

$$2 \int_{-1}^{0} w(|\mu|) \psi^b(\mu, E) d\mu = \phi_0(X, E) + \frac{17\varepsilon}{24\Sigma_{tr}(X, E)} \frac{\partial \phi_0}{\partial x}(X, E). \tag{264b}$$

Setting $\varepsilon = 1$ in (259–263), we obtain the standard energy-dependent diffusion equation with Marshak boundary conditions. If the boundary condition (263) is replaced by (264), one obtains a more accurate result.

The diffusion solution is accurate for transport problems in which the angular flux ψ has a weak space-dependence (its spatial derivatives are small). In this case, ψ also has a weak angle-dependence (is nearly isotropic). In the diffusion equations (259), (261), and (262) the angular variable is entirely eliminated. The constraint that ψ must have weak spatial and angular dependences is often valid in reactor cores, but not in shields. For this reason, the diffusion approximation, or variants thereof, are generally used to simulate neutron transport in nuclear reactor cores, but not in shields.

8.2   Homogenized Diffusion Theory

The "variants" of diffusion theory mentioned in the previous paragraph refer to other approximations used in practical reactor core simulations. In many problems, an extra step is included that is difficult to justify theoretically: each reactor assembly in a core is *homogenized*, i.e., approximated by a fictitious homogeneous system in which the homogenized cross sections are defined to preserve certain features of the original heterogeneous system. Then, the diffusion approximation is applied to the homogenized system.

The homogenization process is not unique because different quantities can be preserved, and there has been considerable debate about the proper manner in which homogenization should be done (Benoist 1964; Dorning 2003; Gelbard 1974; Larsen and Hughes 1980). Different definitions work acceptably for different applications, but no one definition seems to work best for all (or even most) applications. As a consequence, the optimal definition of homogenized diffusion coefficients remains an unsolved problem.

8.3 Spherical Harmonic (P_N) and Simplified Spherical Harmonic (SP_N) Approximations

The diffusion approximation is the simplest useful approximation that has been derived from (251) and (252). Other higher-order in angle approximations can also be derived.

In particular, the 1-D P_N approximation (for N odd and ≥ 3) can be derived from (251) and (252) by calculating the first $N+1$ Legendre moments of (251) and using (252) with $\phi_n = 0$ for $n > N$ to truncate the series. The resulting equations are closely related to diffusion equations; for one-group problems, they can be written exactly as a coupled system of $(N+1)/2$ diffusion equations. Unfortunately, this relatively simple form of the P_N equations does not hold for 2-D and 3-D problems. The greater complexity of the P_N equations for 2-D and 3-D geometries has been a significant factor to their relative unpopularity.

A different class of approximations, which are less accurate but simpler than the P_N approximations, and more accurate than the diffusion approximation, has been developed; this is the so-called *simplified spherical harmonic* (SP_N) equations, originally proposed by Gelbard (1960, 1961, 1962). The 1-D SP_N equations are identical to the diffusion form of the 1-D P_N equations described in the previous paragraph. The multidimensional SP_N equations can be formally derived from the 1-D P_N or SP_N equations by replacing, in each equation, the 1-D diffusion operator by the multidimensional diffusion operator:

$$\frac{d}{dx} D(x) \frac{d\phi}{dx}(x) \rightarrow \nabla \cdot D(\boldsymbol{x}) \nabla \phi(\boldsymbol{x}).$$

(More mathematically rigorous derivations of the SP_N equations, using asymptotic and variational analyses, have been developed [Brantley and Larsen 2000; Larsen et al. 1996; Tomašević and Larsen 1996].) The multidimensional SP_N equations have the relatively simple form of coupled multidimensional diffusion equations, and they become equivalent to the P_N equations in 1-D.

Because of their diffusion form, the SP_N equations can be implemented in a multigroup diffusion code without significantly restructuring the code. In certain practical problems, the low-order SP_3 equations have been shown to capture "more than 80%" of the transport effects that are not present in the diffusion (P_1) solution (Gamino 1989, 1991). Generally, the SP_N equations are useful for problems in which the diffusion solution is a reasonable, but not sufficiently accurate, approximation to the transport solution. However, the SP_N equations are not always accurate for problems in which the diffusion solution is a poor approximation.

8.4 Discussion

The diffusion equation is used almost universally as an approximation to the Boltzmann transport equation for reactor core simulations, after the core has been suitably "homogenized." The principal advantage of the diffusion approximation is that the angular variable Ω is eliminated, thereby greatly reducing the amount of work and the expense necessary to solve the approximate problem. However, the diffusion solution has limited accuracy, and the proper definition of homogenized diffusion coefficients remains an open question.

9   The Point Kinetics Approximation

The point kinetics equations (PKEs) are a classic approximation of the time-dependent neutron transport and precursor density equations (Bell and Glasstone 1970; Henry 1975; Hetrick 1993; Lewis and Miller 1993; Ott 1985). For a *critical* system, the (i) neutron transport and precursor and (ii) PKEs both have steady-state solutions. For systems that are *nearly critical* and have solutions that *vary slowly* in t, the solutions of the PKEs can accurately approximate the corresponding solutions of the time-dependent transport and precursor density equations. Also, the PKEs are much simpler than the transport and precursor density equations and can be solved much more efficiently. For these reasons, the PKEs are widely used in time-dependent reactor simulations and stability studies. Previously, the PKEs have been derived by *variational approximations*; here they are derived from the full transport and neutron precursor equations, using an asymptotic analysis that is related to the analyses used in ❯ Sect. 8 to derive the diffusion approximation.

9.1   Preliminaries

We begin by restating the general time-dependent transport problem with neutron precursors for a system V with vacuum boundary conditions and no internal source. The problem consists of the time-dependent transport equation for the angular flux $\psi(\boldsymbol{x}, \boldsymbol{\Omega}, E, t)$:

$$
\begin{aligned}
\frac{1}{v} \frac{\partial \psi}{\partial t} &(\boldsymbol{x}, \boldsymbol{\Omega}, E, t) + \boldsymbol{\Omega} \cdot \nabla \psi(\boldsymbol{x}, \boldsymbol{\Omega}, E, t) + \Sigma_t(\boldsymbol{x}, E, t) \psi(\boldsymbol{x}, \boldsymbol{\Omega}, E, t) \\
&= \int_0^\infty \int_{4\pi} \Sigma_s(\boldsymbol{x}, \boldsymbol{\Omega}' \cdot \boldsymbol{\Omega}, E' \to E, t) \psi(\boldsymbol{x}, \boldsymbol{\Omega}', E', t) d\Omega' dE' \\
&\quad + \frac{\chi_p(\boldsymbol{x}, E, t)}{4\pi} \int_0^\infty \int_{4\pi} \left[1 - \beta(\boldsymbol{x}, E', t)\right] v \Sigma_f(\boldsymbol{x}, E', t) \psi(\boldsymbol{x}, \boldsymbol{\Omega}', E', t) d\Omega' dE' \\
&\quad + \frac{1}{4\pi} \sum_{j=1}^6 \chi_j(\boldsymbol{x}, E, t) \lambda_j C_j(\boldsymbol{x}, t), \quad \boldsymbol{x} \in V, \ \boldsymbol{\Omega} \in 4\pi, \ 0 < E < \infty, \ 0 < t, \quad (265)
\end{aligned}
$$

the time-dependent equations for the neutron precursor densities $C_j(\boldsymbol{x}, t)$:

$$
\begin{aligned}
\frac{\partial C_j}{\partial t} &(\boldsymbol{x}, t) + \lambda_j C_j(\boldsymbol{x}, t) \\
&= \int_0^\infty \int_{4\pi} \beta_j(\boldsymbol{x}, E', t) v \Sigma_f(\boldsymbol{x}, E', t) \psi(\boldsymbol{x}, \boldsymbol{\Omega}', E', t) d\Omega' dE', \quad \boldsymbol{x} \in V, \ 0 < t, \ 1 \le j \le 6,
\end{aligned}
$$
$$(266)$$

the specified initial conditions for ψ and C_j:

$$
\psi(\boldsymbol{x}, \boldsymbol{\Omega}, E, 0) = \psi^i(\boldsymbol{x}, \boldsymbol{\Omega}, E), \quad \boldsymbol{x} \in V, \ \boldsymbol{\Omega} \in 4\pi, \ 0 < E < \infty, \quad (267a)
$$
$$
C_j(\boldsymbol{x}, 0) = C_j^i(\boldsymbol{x}), \quad \boldsymbol{x} \in V, \ 1 \le j \le 6, \quad (267b)
$$

and the vacuum boundary condition for ψ:

$$\psi(\boldsymbol{x}, \boldsymbol{\Omega}, E, t) = 0, \quad \boldsymbol{x} \in \partial V, \quad \boldsymbol{\Omega} \cdot \boldsymbol{n} < 0, \quad 0 < E < \infty, \quad 0 < t. \tag{267c}$$

Also, β and β_j satisfy:

$$\beta(\boldsymbol{x}, E, t) = \sum_{n=1}^{6} \beta_j(\boldsymbol{x}, E, t). \tag{268}$$

Equations (265) and (266) explicitly allow space- and time-dependence of all cross sections to account for the time-dependent movement of control rods within the core. However, we do not (for simplicity) include a nonlinear temperature-dependence of the cross sections, and we assume that the cross sections are specified for $t \geq 0$.

Because the cross sections are known for $t > 0$, it is in principle possible to calculate the *reactivity* $\rho(t)$ and the corresponding *forward eigenfunction* $\Psi(\boldsymbol{x}, \boldsymbol{\Omega}, E, t)$ for $t > 0$. These are defined by the familiar eigenvalue problem:

$$\boldsymbol{\Omega} \cdot \nabla \Psi(\boldsymbol{x}, \boldsymbol{\Omega}, E, t) + \Sigma_t(\boldsymbol{x}, E, t) \Psi(\boldsymbol{x}, \boldsymbol{\Omega}, E, t)$$

$$= \int_0^\infty \int_{4\pi} \Sigma_s(\boldsymbol{x}, \boldsymbol{\Omega}' \cdot \boldsymbol{\Omega}, E' \to E, t) \Psi(\boldsymbol{x}, \boldsymbol{\Omega}', E', t) d\Omega' dE'$$

$$+ \left[1 - \rho(t)\right] \frac{\chi_p(\boldsymbol{x}, E, t)}{4\pi} \int_0^\infty \int_{4\pi} \nu \Sigma_f(\boldsymbol{x}, E', t) \Psi(\boldsymbol{x}, \boldsymbol{\Omega}', E', t) d\Omega' dE',$$

$$\boldsymbol{x} \in V, \quad \boldsymbol{\Omega} \in 4\pi, \quad 0 < E < \infty, \tag{269a}$$

$$\Psi(\boldsymbol{x}, \boldsymbol{\Omega}, E, t) = 0, \quad \boldsymbol{x} \in \partial V, \quad \boldsymbol{\Omega} \cdot \boldsymbol{n} < 0, \quad 0 < E < \infty. \tag{269b}$$

In these equations, t appears only as a parameter, and we normalize the eigenfunction Ψ by:

$$\int \int_0^\infty \int_{4\pi} \frac{1}{v} \Psi(\boldsymbol{x}, \boldsymbol{\Omega}, E, t) d\Omega dE dV = 1. \tag{269c}$$

Equations (269a) and (269b) have no external sources, and the eigenvalue $\rho(t)$ must be determined so that a positive solution Ψ exists. If $\rho(t) < 0$, the fission term in (269a) is increased by the factor $[1 - \rho(t)]$ to produce a steady-state solution, so the system is *subcritical*. If $\rho(t) > 0$, the fission term is reduced by the factor $[1 - \rho(t)]$ to produce a steady-state solution, so the system is *supercritical*. If $\rho(t) = 0$, then no adjustment to the fission term is made, and the system is *critical*.

The time-dependent cross sections, the reactivity $\rho(t)$, the forward eigenfunction $\Psi(\boldsymbol{x}, \boldsymbol{\Omega}, E, t)$, and the adjoint eigenfunction $\Psi^\dagger(\boldsymbol{x}, \boldsymbol{\Omega}, E, t)$ (of the problem which is adjoint to [269]) all explicitly occur in the asymptotic analysis. In the following, we assume that all of these quantities are known. (Then the forward and adjoint scalar fluxes $\Phi(\boldsymbol{x}, E, t) = \int_{4\pi} \Psi(\boldsymbol{x}, \boldsymbol{\Omega}, E, t) d\Omega$ and $\Phi^\dagger(\boldsymbol{x}, E, t) = \int_{4\pi} \Psi^\dagger(\boldsymbol{x}, \boldsymbol{\Omega}, E, t) d\Omega$ are also known.) The asymptotic analysis determines time-dependent equations for ψ and C_j having coefficients that

are expressed in terms of the time-dependent cross sections $\Sigma(x, E, t)$, reactivity $\rho(t)$, and eigenfunctions $\Psi(x, \Omega, E, t)$ and $\Psi^\dagger(x, \Omega, E, t)$.

9.2 The Scaled Transport and Neutron Precursor Equations

Next, we make physical assumptions that are consistent with the basic overall requirement that the system V be *nearly critical* and *slowly varying in time*.

- The reactivity $\rho(t)$ is small. (The system is *nearly critical* for all $t > 0$.)
- β_j and β are small. In practice, this assumption is valid; β is dimensionless and ≈ 0.01.
- If t is measured on the timescale for precursor decay (e.g., in seconds), then the mean neutron speed is large. In practice, this assumption is valid.
- Since the mean neutron speed is large and $\psi = vN$, then ψ is large.
- All specified time-dependent quantities in (265–266) vary on the same slow timescale (seconds) on which the neutron precursors decay.

To express these conditions mathematically, we introduce a small positive dimensionless parameter ε and define:

$$\rho(t) = \varepsilon\hat{\rho}(t), \tag{270a}$$

$$\beta_j(x, E, t) = \varepsilon\hat{\beta}_j(x, E, t) \quad \text{and} \quad \beta(x, E, t) = \varepsilon\hat{\beta}(x, E, t), \tag{270b}$$

$$v = \frac{\hat{v}}{\varepsilon}, \tag{270c}$$

$$\psi(x, \Omega, E, t) = \frac{\hat{\psi}(x, \Omega, E, t)}{\varepsilon}, \tag{270d}$$

$$\psi^i(x, \Omega, E, t) = \frac{\hat{\psi}^i(x, \Omega, E, t)}{\varepsilon}. \tag{270e}$$

In these equations, all the hatted quantities are assumed to be $O(1)$.

Introducing (270) into (265–268), we obtain:

$$\frac{1}{\hat{v}}\frac{\partial\hat{\psi}}{\partial t}(x, \Omega, E, t) + \frac{1}{\varepsilon}\Omega \cdot \nabla\hat{\psi}(x, \Omega, E, t) + \frac{1}{\varepsilon}\Sigma_t(x, E, t)\hat{\psi}(x, \Omega, E, t)$$

$$= \frac{1}{\varepsilon}\int_0^\infty \int_{4\pi} \Sigma_s(x, \Omega' \cdot \Omega, E' \to E, t)\hat{\psi}(x, \Omega', E', t)d\Omega'dE'$$

$$+ \frac{\chi_p(x, E, t)}{4\pi\varepsilon}\int_0^\infty \int_{4\pi}\left[1 - \rho(t) + \varepsilon\hat{\rho}(t) - \varepsilon\hat{\beta}(x, E', t)\right]$$

$$\times v\Sigma_f(x, E', t)\hat{\psi}(x, \Omega', E', t)d\Omega'dE'$$

$$+ \frac{1}{4\pi}\sum_{j=1}^{6}\chi_j(x, E, t)\lambda_j C_j(x, t) + \frac{Q(x, E, t)}{4\pi}, \tag{271a}$$

$$\frac{\partial C_j}{\partial t}(x, t) + \lambda_j C_j(x, t) = \int_0^\infty \int_{4\pi}\hat{\beta}_j(x, E', t)v\Sigma_f(x, E', t)\hat{\psi}(x, \Omega', E', t)d\Omega'dE', \tag{271b}$$

where the expression $-\rho(t) + \varepsilon\hat{\rho}(t) = 0$ has been included in the integrand of the prompt fission term in (271a) so that the small reactivity $\rho(t) = \varepsilon\hat{\rho}(t)$ occurs in the scaled equations to leading order. We also have the boundary and initial conditions:

$$\hat{\psi}(x, \Omega, E, t) = 0, \quad x \in \partial V, \ \Omega \cdot n < 0, \ 0 < E < \infty, \ 0 < t, \tag{272}$$

$$\hat{\psi}(x, \Omega, E, 0) = \hat{\psi}^i(x, \Omega, E), \quad x \in V, \ \Omega \in 4\pi, \ 0 < E < \infty, \tag{273a}$$

$$C_j(x, 0) = C_j^i(x), \quad x \in V, \tag{273b}$$

and:

$$\hat{\beta}(x, E, t) = \sum_{j=1}^{6} \hat{\beta}_j(x, E, t). \tag{274}$$

The scaled equations (271–274) for $\hat{\psi}$ and C_j are equivalent to the original equations (265–268) for ψ and C_j; no approximations have yet been made.

9.3   Asymptotic Derivation of the Point Kinetics Equations

To proceed, we introduce the *ansatz*:

$$\hat{\psi}(x, \Omega, E, t) = \sum_{n=0}^{\infty} \varepsilon^n \hat{\psi}_n(x, \Omega, E, t), \tag{275a}$$

$$C_j(x, t) = \sum_{n=0}^{\infty} \varepsilon^n C_{j,n}(x, t), \tag{275b}$$

into (271–273) and equate the coefficients of different powers of ε. The sole $O(\varepsilon^{-1})$ equation is:

$$\Omega \cdot \nabla \hat{\psi}_0(x, \Omega, E, t) + \Sigma_t(x, E, t)\hat{\psi}_0(x, \Omega, E, t)$$
$$- \int_0^{\infty} \int_{4\pi} \Sigma_s(x, \Omega' \cdot \Omega, E' \to E, t)\hat{\psi}_0(x, \Omega', E', t)d\Omega'dE'$$
$$- [1 - \rho(t)]\frac{\chi_p(x, E, t)}{4\pi}\int_0^{\infty}\int_{4\pi}\nu\Sigma_f(x, E', t)\hat{\psi}_0(x, \Omega', E', t)d\Omega'dE' = 0, \tag{276}$$

with the vacuum boundary condition for $\hat{\psi}_0$. By (269), the general solution of these equations is:

$$\hat{\psi}_0(x, \Omega, E, t) = \Psi(x, \Omega, E, t)\, N_0(t), \tag{277}$$

where $N_0(t)$ is, at this point, undetermined. We note that by (269c),

$$\int_V \int_0^{\infty}\int_{4\pi}\frac{1}{\nu}\hat{\psi}_0(x, \Omega, E, t)d\Omega dEdV = N_0(t), \tag{278a}$$

so:

$$N_0(t) = \text{ the number of neutrons in } V \text{ at time } t. \tag{278b}$$

Next, we introduce (277) for $\hat{\psi}_0$ into the $O(1)$ components of (271) and obtain the following equations for $\hat{\psi}_1$ and $C_{j,0}$:

$$\boldsymbol{\Omega} \cdot \nabla \hat{\psi}_1(\boldsymbol{x}, \boldsymbol{\Omega}, E, t) + \Sigma_t(\boldsymbol{x}, E, t)\hat{\psi}_1(\boldsymbol{x}, \boldsymbol{\Omega}, E, t)$$

$$- \int_0^\infty \int_{4\pi} \Sigma_s(\boldsymbol{x}, \boldsymbol{\Omega}' \cdot \boldsymbol{\Omega}, E' \to E, t)\hat{\psi}_1(\boldsymbol{x}, \boldsymbol{\Omega}', E', t)d\Omega'dE'$$

$$- [1 - \rho(t)]\frac{\chi_p(\boldsymbol{x}, E, t)}{4\pi}\int_0^\infty \int_{4\pi} v\Sigma_f(\boldsymbol{x}, E', t)\hat{\psi}_1(\boldsymbol{x}, \boldsymbol{\Omega}', E', t)d\Omega'dE'$$

$$= -\frac{1}{v}\frac{\partial}{\partial t}\Psi(\boldsymbol{x}, \boldsymbol{\Omega}, E, t)N_0(t)$$

$$+ \frac{\chi_p(\boldsymbol{x}, E, t)}{4\pi}\int_0^\infty [\hat{\rho}(t) - \hat{\beta}(\boldsymbol{x}, E', t)]v\Sigma_f(\boldsymbol{x}, E', t)\Phi(\boldsymbol{x}, E', t)dE'\, N_0(t)$$

$$+ \frac{1}{4\pi}\sum_{j=1}^6 \chi_j(\boldsymbol{x}, E, t)\lambda_j C_{j,0}(\boldsymbol{x}, t) + \frac{Q(\boldsymbol{x}, E, t)}{4\pi}, \tag{279}$$

$$\frac{\partial C_{j,0}}{\partial t}(\boldsymbol{x}, t) + \lambda_j C_{j,0}(\boldsymbol{x}, t) = \left(\int_0^\infty \hat{\beta}_j(\boldsymbol{x}, E', t)v\Sigma_f(\boldsymbol{x}, E', t)\Phi(\boldsymbol{x}, E', t)dE'\right)N_0(t). \tag{280}$$

The operator on the left side of (279) is the same as the operator on the left side of (276). Operating on both sides of (279) by:

$$\int \int_0^\infty \int_{4\pi} \Psi^\dagger(\boldsymbol{x}, \boldsymbol{\Omega}, E, t)\, (\cdot)\, d\Omega dE dV,$$

the left side vanishes, and we obtain the *solvability condition*:

$$0 = -\int \int_0^\infty \int_{4\pi} \Psi^\dagger \frac{1}{v}\frac{\partial}{\partial t}\Psi\, N_0(t)\, d\Omega dE dV$$

$$+ \frac{\hat{\rho}(t)}{4\pi}\int \left(\int_0^\infty \Phi^\dagger \chi_p\, dE\right)\left(\int_0^\infty v\Sigma_f\Phi dE\right)dV\, N_0(t)$$

$$- \frac{1}{4\pi}\int \left(\int_0^\infty \Phi^\dagger \chi_p\, dE\right)\left(\int_0^\infty \hat{\beta}v\Sigma_f\Phi dE\right)dV\, N_0(t)$$

$$+ \sum_j \frac{\lambda_j}{4\pi}\int \int_0^\infty \Phi^\dagger C_{j,0}\chi_j\, dE dV + \frac{1}{4\pi}\int \int_0^\infty \Phi^\dagger Q\, dE dV. \tag{281}$$

To simplify this result, we define the functions:

$$\theta(t) = \frac{\int \int_0^\infty \int_{4\pi} \Psi^\dagger \frac{1}{v}\frac{d\Psi}{dt}d\Omega dE dV}{\int \int_0^\infty \int_{4\pi} \Psi^\dagger \frac{1}{v}\Psi d\Omega dE dV}, \tag{282a}$$

$$\frac{1}{\Lambda(t)} = \frac{\int \left(\int_0^\infty \Phi^\dagger \chi_p\, dE\right)\left(\int_0^\infty v\Sigma_f\Phi dE'\right)dV}{4\pi \int \int_0^\infty \int_{4\pi} \Psi^\dagger \frac{1}{v}\Psi d\Omega dE dV}, \tag{282b}$$

$$\hat{\beta}(t) = \frac{\int \left(\int_0^\infty \Phi^\dagger \chi_p\, dE\right)\left(\int_0^\infty \hat{\beta}v\Sigma_f\Phi dE'\right)dV}{\int \left(\int_0^\infty \Phi^\dagger \chi_p\, dE\right)\left(\int_0^\infty v\Sigma_f\Phi dE'\right)dV}, \tag{282c}$$

$$c_j(t) = \frac{\int \int_0^\infty \Phi^\dagger C_{j,0}\chi_j\, dE dV}{4\pi \int \int_0^\infty \int_{4\pi} \Psi^\dagger \frac{1}{v}\Psi d\Omega dE dV}, \tag{282d}$$

$$q(t) = \frac{\int \int_0^\infty \Phi^\dagger Q \, dE \, dV}{4\pi \int \int_0^\infty \int_{4\pi} \Psi^\dagger \frac{1}{v} \Psi \, d\Omega \, dE \, dV};\tag{282e}$$

then (281) becomes:

$$\frac{dN_0}{dt}(t) + \theta(t)N_0(t) = \frac{\hat{\rho}(t) - \hat{\beta}(t)}{\Lambda(t)} N_0(t) + \sum_j \lambda_j c_j(t) + q(t).\tag{283}$$

To obtain equations for $c_j(t)$, we analytically solve (280) for $C_{j,0}(\boldsymbol{x}, t)$, obtaining:

$$C_{j,0}(\boldsymbol{x}, t) = C_j^i(\boldsymbol{x})e^{-\lambda_j t} + \int_0^t e^{-\lambda_j(t-t')} \left(\int_0^\infty \hat{\beta}_j v \Sigma_f \Phi \, dE' \right) N_0(t') \, dt'.$$

Then we operate on this result by:

$$\frac{1}{4\pi \int \int_0^\infty \int_{4\pi} \Psi^\dagger \frac{1}{v} \Psi \, d\Omega \, dE \, dV} \int \int_0^\infty \Phi^\dagger \chi_j [\,\cdot\,] dE \, dV$$

and use the definition (282d) to obtain:

$$c_j(t) = c_j^i e^{-\lambda_j t} + \frac{\int \left(\int_0^\infty \Phi^\dagger \chi_j \, dE \right) \left[\int_0^t e^{-\lambda_j(t-t')} \left(\int_0^\infty \hat{\beta}_j v \Sigma_f \Phi \, dE' \right) N_0(t') \, dt' \right] dV}{4\pi \int \int_0^\infty \int_{4\pi} \Psi^\dagger \frac{1}{v} \Psi \, d\Omega \, dE \, dV}.\tag{284}$$

Equations (283) and (284) define $N_0(t)$ and $c_j(t)$ for $t > 0$.

Next, we convert these results back to the original unscaled (unhatted) variables. This is done by using (270) to systematically replace all scaled (hatted) quantities in (277) and (282–284) by unscaled (unhatted) quantities. Defining $N(t) = N_0(t)/\varepsilon$ and omitting the straightforward details, we obtain for $t > 0$:

$$\psi(\boldsymbol{x}, \boldsymbol{\Omega}, E, t) \approx \Psi(\boldsymbol{x}, \boldsymbol{\Omega}, E, t) \, N(t),\tag{285}$$

where $N(t)$ satisfies the equations:

$$\frac{dN}{dt}(t) + \theta(t)N(t) = \frac{\rho(t) - \beta(t)}{\Lambda(t)} N(t) + \sum_{j=1}^6 \lambda_j c_j(t) + q(t),\tag{286}$$

and:

$$c_j(t) = c_j^i e^{-\lambda_j t} + \frac{\int \left(\int_0^\infty \Phi^\dagger \chi_j \, dE \right) \left[\int_0^t e^{-\lambda_j(t-t')} \left(\int_0^\infty \beta_j v \Sigma_f \Phi \, dE' \right) N(t') \, dt' \right] dV}{4\pi \int \int_0^\infty \int_{4\pi} \Psi^\dagger \frac{1}{v} \Psi \, d\Omega \, dE \, dV},\tag{287}$$

where:

$$\beta(t) = \frac{\int \left(\int_0^\infty \Phi^\dagger \chi_p \, dE \right) \left(\int_0^\infty \beta v \Sigma_f \Phi \, dE \right) dV}{\int \left(\int_0^\infty \Phi^\dagger \chi_p \, dE \right) \left(\int_0^\infty v \Sigma_f \Phi \, dE \right) dV}.\tag{288}$$

Also, (267), (285), and (282d) yield the following initial conditions for $N(t)$ and $c_j(t)$:

$$N(0) = \int \int_0^\infty \int_{4\pi} \frac{1}{v} \psi^i(\boldsymbol{x}, \boldsymbol{\Omega}, E) d\Omega dE dV, \tag{289}$$

$$c_j(0) = c_j^i = \frac{\int \int_0^\infty \Phi^\dagger(\boldsymbol{x}, E, 0) C_j^i(\boldsymbol{x}) \chi(\boldsymbol{x}, E, 0) dE dV}{4\pi \int \int_0^\infty \int_{4\pi} \Psi^\dagger(\boldsymbol{x}, \boldsymbol{\Omega}, E, 0) \frac{1}{v} \Psi(\boldsymbol{x}, \boldsymbol{\Omega}, E, 0) d\Omega dE dV}. \tag{290}$$

To obtain the standard PKEs, it is necessary to make two further assumptions. The first assumption is:

$$\frac{\partial}{\partial t} \left(\frac{\int_0^\infty \Phi^\dagger \chi_j dE}{\int \int_0^\infty \int_{4\pi} \Psi^\dagger \frac{1}{v} \Psi d\Omega dE dV} \right) \approx 0. \tag{291}$$

Then (287) can be written:

$$c_j(t) = c_j^i e^{-\lambda_j t} + \int_0^t e^{-\lambda_j(t-t')} \frac{\beta_j(t')}{\Lambda(t')} N(t') dt', \tag{292}$$

where:

$$\beta_j(t) = \frac{\int \left(\int_0^\infty \Phi^\dagger \chi_p \, dE \right) \left(\int_0^\infty \beta_j v \Sigma_f \Phi dE \right) dV}{\int \left(\int_0^\infty \Phi^\dagger \chi_p \, dE \right) \left(\int_0^\infty v \Sigma_f \Phi dE \right) dV}. \tag{293}$$

The second assumption is:

$$\theta(t) = \frac{\int \int_0^\infty \int_{4\pi} \Psi^\dagger \frac{1}{v} \frac{d\Psi}{dt} d\Omega dE dV}{\int \int_0^\infty \int_{4\pi} \Psi^\dagger \frac{1}{v} \Psi d\Omega dE dV} \approx 0. \tag{294}$$

If (291) and (294) both hold, then (286) and (292) reduce to the standard PKEs:

$$\frac{dN}{dt}(t) = \frac{\rho(t) - \beta(t)}{\Lambda(t)} N(t) + \sum_{j=1}^6 \lambda_j c_j(t) + q(t), \tag{295a}$$

$$\frac{dc_j}{dt}(t) + \lambda_j c_j(t) = \frac{\beta_j(t)}{\Lambda(t)} N(t), \quad 1 \le j \le 6. \tag{295b}$$

Also, from (274), (288), and (293), we have:

$$\beta(t) = \sum_{n=1}^6 \beta_j(t). \tag{296}$$

Thus, the neutron angular flux $\psi(\boldsymbol{x}, \boldsymbol{\Omega}, E, t)$ is asymptotically given by (285), where $N(t)$ is obtained by solving the PKEs (295) and (296), with initial conditions given by (289) and (290). Because of the very specific angular and energy dependence of the asymptotic solution (285), this solution cannot generally satisfy the arbitrary initial conditions specified in (267). This deficiency can be overcome by including an *initial-layer* solution, which describes the rapid transition from the general initial conditions for ψ and C_j to the near-equilibrium solution that forms the basis of the PKEs. The asymptotic initial-layer analysis is not presented here because this analysis has no effect on the PKEs.

9.4   Discussion

For a fissile system that is nearly critical and slowly varying, in the sense described by the scalings in (270), we have shown that the time-dependent angular flux is described asymptotically by (285–290). Furthermore, if (291) and (294) hold, then the approximating equations simplify to the standard PKEs (295), (296).

The PKEs have been obtained previously using derivations that are tantamount to variational approximations. In these earlier derivations, $\Psi(\boldsymbol{x}, \boldsymbol{\Omega}, E, t)$ is called the *shape function* and is not necessarily an eigenfunction; it is chosen. Also, $\Psi^\dagger(\boldsymbol{x}, \boldsymbol{\Omega}, E, t)$ is called the *weight function*; it too is not necessarily an (adjoint) eigenfunction and is chosen. The subsequent derivations lead to equations of the form of (285) and (295), but with the coefficients in these equations usually defined differently than in (282) and (288). In particular, in the asymptotic analysis presented here, $\rho(t)$ is the true reactivity of the system at time t, as defined by the eigenvalue problem (269). In other formulations, $\rho(t)$ is not always the true reactivity. The analysis presented here suggests that these earlier formulations of the PKEs may not represent asymptotic approximations of the time-dependent transport equations. However, the asymptotic result derived here is potentially more expensive to implement because $\rho(t)$, $\Psi(\boldsymbol{x}, \boldsymbol{\Omega}, E, t)$, and $\Psi^\dagger(\boldsymbol{x}, \boldsymbol{\Omega}, E, t)$ must be calculated by solving eigenvalue problems for each time t. (This point is discussed further below.) It is possible that by using a less sophisticated approximation to Ψ and ρ, one can reduce the cost of the calculation and still obtain acceptably accurate results.

In previous derivations of the PKEs, the shape and weight functions are often assumed to be independent of time (at least, for specified time intervals). If this were true in the asymptotic analysis, and if the time-dependent variations of the system occur only in non-fissile regions, then (291) and (294) would be valid. This situation can effectively occur if, for a critical reactor, control rods are *very slowly and slightly* moved in or out, thereby making the reactor slightly subcritical or supercritical. Then the temporal changes in $\Psi(\boldsymbol{x}, \boldsymbol{\Omega}, E, t)$ and $\Psi^\dagger(\boldsymbol{x}, \boldsymbol{\Omega}, E, t)$ would be very small and, effectively, $\theta(t) = 0$, $\Lambda(t) = \Lambda = $ constant, and $\beta_j(t) = \beta_j = $ constant.

Also, we note that by suitably altering the normalization (269c) on Ψ, then by (277) and (278), $N(t) = $ the power output of the reactor at time t.

The asymptotic analysis shows that the neutron flux can be predicted by means of PKEs that depend on time-dependent knowledge of the cross sections, the reactivity, and the forward and adjoint eigenfunctions. Although it is not practical to calculate ρ, Ψ, and $\Psi^\dagger$ *continuously* for all $t > 0$, it is possible to calculate these quantities at discrete times, e.g., $t_n = n\Delta t$, and to evaluate $\rho(t)$ and the time-dependent parameters in (288) by linearly interpolating between t_n and t_{n+1}. By doing this, the asymptotic result obtained here could be the basis of a realistic point kinetics model.

Other asymptotic expansions that lead to results of the form of the PKEs are possible. For example, in the analysis presented here, the reactivity ρ of the system is calculated by neglecting the delayed neutrons (see [269]). By including a steady-state term in (269) to account for the different energy spectrum of the delayed neutrons, a different and possibly more accurate expression for ρ might be obtained. Also, a more sophisticated asymptotic analysis could include temperature-dependent cross sections, with an extra equation relating the temperature $T(\boldsymbol{x}, t)$ within the reactor as a function of the neutron flux. In addition, an asymptotic derivation of the PKEs can be based on the α-eigenvalues and eigenfunctions of the transport

equation (Lewis and Miller 1984), rather than the k-eigenvalues and eigenfunctions. (Such a derivation would actually be more natural, because the α-eigenvalues are associated with the time-behavior of the system.) However, none of these generalizations can be discussed further here.

10   Computational Neutron Transport

Analytic solutions of the Boltzmann transport equation can be obtained only for the simplest problems. For realistic, multidimensional, energy-dependent problems, it is necessary to calculate numerical solutions as accurately and efficiently as possible. This can be an extremely daunting task. Research on computational methods for the Boltzmann transport equation has been actively pursued from the 1950s up to the present (Adams and Larsen 2002; Carlson and Lathrop 1968; Carter and Cashwell 1975; Haghighat and Wagner 2003; Kalos and Whitlock 1986; Larsen 1992; Larsen and Morel 2009; Lewis and Miller 1993; Lux and Koblinger 1991; Marchuk and Lebedev 1981; Sanchez and McCormick 1982; Spanier and Gelbard 2008; X-5 Monte Carlo Team 2003). During this time, the speed and memory of computers has increased by many orders of magnitude. Nonetheless, it has been argued that the gains in efficiency of simulations of particle transport problems, due to improvements in computational algorithms, exceeds the gains due to improvements in computer hardware. Here, we give a brief overview of the major advances in computational neutron transport algorithms. For details, we refer the reader to previous publications.

The history of computational transport methods is basically the history of two fundamentally different approaches, commonly called *stochastic* and *deterministic*. Stochastic (or *Monte Carlo*) methods are based on a probabilistic interpretation of the transport process. In this approach, the random *histories* of individual particles are calculated using pseudorandom number sequences and the results are averaged over a large number of histories. Stochastic methods have no need of a Boltzmann transport equation; they rely only on the detailed physics of interactions between individual neutrons and nuclei. Deterministic methods instead are based on (i) discretizing the Boltzmann transport equation in each of its independent variables, resulting in a (typically very large) algebraic system of equations, and then (ii) solving this algebraic system.

For the past 50 years, Monte Carlo and deterministic algorithms have been developed independently. The two approaches were viewed as being incompatible, and two basically disjoint technical communities evolved to develop codes for them. Major technical advances for one type of method (e.g., acceleration techniques for deterministic methods, variance reduction techniques for Monte Carlo methods) had no impact on the other method. Except for specialized applications, the two methods were not implemented in the same (production) computer code. Monte Carlo and deterministic methods became viewed as complementary: one approach was advantageous for certain problems, the other advantageous for different problems. Because of their complementarity, both methods have survived and matured.

However, during the past 10 years, it has become fairly widely understood that *hybrid* methods – which combine aspects of both Monte Carlo and deterministic methods – can be used to enhance the strengths and overcome the weaknesses of the individual approaches. Although hybrid methods are in the early stages of their development and implementation, they have already demonstrated that they can yield major improvements in efficiency and accuracy for difficult problems. It now appears that hybrid methods represent a promising third

approach, offering a way to significantly improve the efficiency and ease of simulations for difficult practical particle transport problems.

In the following, we discuss the general issues associated with deterministic, stochastic, and hybrid particle transport methodologies.

10.1   Monte Carlo Methods

In the physical process of *particle transport*, typically a *very* large number of particles undergo random and independent histories. Each element of an individual particle's history (distance to collision, probability of scattering, post-scattering energy, and direction of flight) has a specific probability distribution function. Because of this, the collective behavior of the particle population is predictable, with a small statistical noise that decreases as the number of particles $N \to \infty$.

Stochastic or *Monte Carlo* methods model this process by applying the known distribution functions to simulate the random histories of N_{MC} fictitious *Monte Carlo particles*, and averaging the results over the histories (Carter and Cashwell 1975; Kalos and Whitlock 1986; Lux and Koblinger 1991; Spanier and Gelbard 2008; X-5 Monte Carlo Team 2003). However, because the number of simulated particles $[N_{MC} \approx O(10^7)]$ is usually much smaller than the number of physical particles $[N \approx O(10^{15})]$, Monte Carlo simulations usually have orders of magnitude more statistical noise than the actual physical process. This is a significant issue when Monte Carlo methods are used to estimate *rare events*, such as the response rate in a detector located far from a source.

Nonetheless, Monte Carlo methods have certain basic advantages. If the geometry of the system and its cross sections are known, then the results of the Monte Carlo simulation contain only statistical errors. By processing a sufficient number of Monte Carlo particles, it is possible to reduce the probable statistical error below any specified level.

According the *central limit theorem*, for any Monte Carlo simulation, the statistical error in the estimation of a given quantity is, with probability 0.68, bounded by:

$$\text{Statistical error} \leq \frac{\sigma}{\sqrt{N_{MC}}}, \tag{297}$$

where σ (the *standard deviation*) is specific to the given problem and the quantity estimated, and (297) holds only for N_{MC} sufficiently large. The positive feature of (297) is that as N_{MC} increases, the statistical error will, with high probability, also decrease. The negative feature is that the rate of decrease of the statistical error is slow. For instance, (297) shows that to decrease the statistical error by a factor of 10, it is necessary to increase N_{MC} (and hence the computational expense) by a factor of 100.

Monte Carlo methods are widely used because of their relative ease of implementation, their ability to treat complex geometries with great fidelity, and their ability to solve problems accurately with cross-sectional data that can have extremely complex energy-dependence. However, Monte Carlo simulations can be costly, both to set up and to run.

In particular, when attempting to calculate a rare event, such as a detector response far from a source, such a small fraction of the physical particles participate in this event that the number of Monte Carlo particles that create a "score" is *very* small – and the resulting statistical error is unacceptably large. In this situation, the "rules" of the Monte Carlo "game" can be

altered so that Monte Carlo particles are "encouraged" to travel from the source to the detector region. The result is that the desired response is estimated with smaller statistical error and computational effort. In effect, the Monte Carlo process is changed so that the estimate of the response is preserved, but the standard deviation in this estimate (the constant σ in [297]) is reduced.

To accomplish this alteration of the Monte Carlo process, the code user must input a (generally) large number of *biasing parameters* that successfully "encourage" Monte Carlo particles to migrate from the source to the specified detector region. These parameters are strongly problem-dependent, and generating them can be a slow and laborious task. For difficult problems, a lengthy process of trial and error may be necessary, and there is no guarantee that at the end of this process, the code user will have been successful.

Another difficulty with Monte Carlo simulations is that they operate most efficiently when calculating limited information, such as a single detector response. If several detector responses are desired, and the detectors are located far from the source and far from each other, then often the best solution is to run several different Monte Carlo simulations, each with its own specially defined set of biasing parameters.

Thus, while Monte Carlo codes are widely used, running these codes efficiently is problematic for complex problems. In these situations, Monte Carlo codes are not a "black box" into which a user can simply specify the problem, press the "start" button, and expect reliable answer in a short time. *In addition to specifying the physical problem, the user must also specify the problem-dependent biasing parameters*, and this can be a formidable task.

Historically, research on Monte Carlo methods has focused on new approaches that show hope of alleviating the major difficulties associated with the method. For example, different biasing methods to encourage Monte Carlo particles to travel toward specified detector regions have been developed and tested. Also, methods have been developed to obtain, via the Monte Carlo process itself, the biasing parameters for difficult problems. In addition, sophisticated statistical methods have been developed to analyze Monte Carlo simulations and better determine the magnitude of the statistical errors. (For example, obtaining accurate estimates of the standard deviation σ, and hence of the true statistical error, can be problematic, particularly for eigenvalue problems.)

During the past 50 years, many significant advances in Monte Carlo techniques have been developed and implemented in large-scale codes. However, the difficulties described above remain significant obstacles to running these codes optimally.

10.2   Deterministic Methods

Because the particle transport process is governed by specified probability distribution functions, the Boltzmann transport equation exists for predicting the *mean* or *average* flux of particles at each location in phase space. *Deterministic*, or *discrete-ordinates*, or S_N methods are based on discretizing the Boltzmann equation in each of its independent variables, and solving the resulting (typically very large) system of algebraic equations (Adams and Larsen 2002; Carlson and Lathrop 1968; Larsen 1992; Larsen and Morel 2009; Lewis and Miller 1993; Marchuk and Lebedev 1986; Sanchez and McCormick 1982).

Because the Boltzmann equation depends on its independent variables in significantly different ways, different methods have been developed for their discretization.

For time-dependent problems, the most common method for discretizing the time variable t is the *implicit*, or *backward Euler* method. Other methods are possible and have been tested, but the implicit method is the most widely used because of its simplicity and robustness.

Of all the independent variables in the transport equation, the energy variable E is the most problematic. The reason for this is that typically, the material cross sections, and hence the particle flux itself, have an extraordinarily complex energy-dependence. If the simple rule of thumb is followed that an energy grid should be chosen for which the solution varies in energy from one grid point to the next by no more than about 15%, then for typical problems, *millions* of grid points in E would be required. This constraint would render the solution of typical problems to be outside the range of possibility.

However, the *multigroup* method (discussed previously in ❯ Sect. 6) has been developed to deal with this difficulty, and because of its success, it is almost universally used. This method requires the user to carefully specify a set of *multigroup* cross sections, whose values are determined by calculating integrals over E of the flux and the flux times the cross section. The optimal specification of a multigroup cross section depends on the given problem. From the user standpoint, determining accurate problem-dependent multigroup cross sections is the most challenging and time-consuming aspect of deterministic calculations.

The angular, or direction-of-flight variable Ω is generally discretized in one of two ways: *discrete-ordinates*, or *collocation* (or S_N) methods, and *spherical harmonic* (or P_N) methods. S_N methods are more commonly used because the structure of the resulting discrete equations is more closely linked to the innate physical interpretation of particle transport. (In Cartesian geometries, S_N methods can be interpreted as ones in which particles travel only in a finite, specified set of directions Ω_m.) However, S_N and P_N methods have characteristic errors. In particular, S_N methods have *ray effects*, which are most apparent in problems with strong absorption and localized sources. For problems whose solutions have a strong direction-dependence, such as neutron streaming through a voided channel, it is necessary to use a very high-order angular quadrature set. P_N methods also have angular truncation errors, but of a different nature. Like S_N methods, P_N methods cannot easily describe an angular flux with a complicated direction-dependence. Also, the P_N equations have a form and structure that are more difficult (than the S_N equations) to interpret in terms of the physics of particle transport.

The spatial variable x has probably been subjected to a greater variety of discretization methods than any other independent variable in the Boltzmann transport equation. In the early years, relatively simple *finite difference* (diamond difference and weighted diamond difference) methods were favored. Later, more sophisticated *finite element*, *nodal*, *characteristic*, and *corner balance* methods were introduced (Larsen and Morel 2009). Each of these types of methods tends to have its own advantages and disadvantages (Azmy 1992; Duo and Azmy 2007). For example, finite difference and (to a certain extent) nodal methods are relatively easy to implement on Cartesian (orthogonal, or box-like) spatial grids, while finite element, characteristic, and corner balance methods are better adapted to non-Cartesian (*triangular*, *tetrahedral*, or *unstructured*) spatial grids.

Cartesian grids were favored in early computer codes; but more recently, non-Cartesian grids have been employed, to better enable the spatial grid to fit the curved or non-right-angular surfaces occurring on material boundaries in many realistic applications.

A major issue in discretizing the spatial variable is the number of unknowns that must be calculated (and stored) per spatial cell. Methods that require a minimum amount of storage are generally less accurate on a specified grid, but the storage demand of particle transport problems is so high that in many problems, the simpler methods are preferred.

Another issue in spatial discretizations concerns accuracy in optically thick, scattering-dominated (*diffusive*) regions. For example, in electron and thermal radiation transport problems, the cross sections (or *opacities*) can be so high that it is not possible, due to computer storage limitations, to solve problems using a spatial grid in which the spatial cell widths are on the order of a mean free path or less. (In many neutron transport problems, spatial cell widths are chosen to be fractions of mean free paths.) Some discretization methods are significantly more accurate than others for problems in which the spatial grid is not optically thin; these methods tend to have a greater number of unknowns per cell (Adams et al. 1998; Adams 2001; Larsen 1992; Larsen and Morel 2009).

In practical neutron/photon transport problems, the total number of unknowns can be extraordinarily large. To estimate this number, let us consider a steady-state, 3-D, multigroup S_N problem.

The number G of energy groups can range from $G = 2$ for special light water reactor core problems to $G = 200$ for difficult shielding problems.

The number M of directions of flight in a typical 3-D S_N calculation varies, depending on the nature and order of the quadrature set. The 3-D S_N level-symmetric quadrature sets have $M = N(N+2)$ directions. Thus, the commonly used S_4 and S_8 level-symmetric quadrature sets have 24 and 80 directions of flight, respectively.

The number of spatial cells can also vary. It is not atypical for a Cartesian spatial grid to have each independent variable (x, y, and z) defined on a grid of 100 points. Thus, the number I of discrete values of x is 100, and the same is true for J = the number of discrete values of y and K = the number of discrete values of z.

Thus, if we consider "typical" values $G = 20$, $M = 50$, and $I = J = K = 100$, then the total number N_{tot} of unknowns is

$$N_{tot} = G \times M \times I \times J \times K = 10^9.$$

This extremely large number (and in many problems the number is much higher) is a direct consequence of the fact that steady-state 3-D transport problems require a 6-D phase space.

To minimize the number of unknowns, computer codes have been written for 3-D problems with 1-D or 2-D spatial symmetry. This reduces the number of independent spatial variables from 3 to 2 or 1, and it possibly reduces the number of angular variables from 2 to 1. The problems that can be accurately treated by 1-D or 2-D codes are geometrically constrained but, fortunately, many important applications can be adequately represented by a 1-D or 2-D geometric model.

In addition to the issue of storing and processing the unknowns in the discretized Boltzmann equation, there is the fact that a linear algebraic system of equations with $N \approx 10^9$ equations and unknowns cannot be solved by direct matrix inversion. For most practical problems, it is necessary to use *iterative methods* to calculate solutions.

The simplest iteration strategy is based on *sweeping*, which itself is based on the observation that with standard discretization schemes, problems with no scattering or fission can be solved directly and noniteratively by *marching* through the spatial grid in the direction of particle flow. (Different directions of flow can require a different direction of marching, or sweeping.) The angular flux solution of such a problem is termed the *uncollided flux*; it consists of all particles that have not experienced a collision. (When a particle does experience a collision, it is absorbed. See ❯ Subsect. 2.10.12.)

For problems with scattering, the *source iteration* strategy consists of performing sweeps and iterating on the scattering source. If the first sweep is performed with the scattering source

estimated to be zero, then at the end of the first sweep, the estimated angular flux is the uncollided flux. If this (uncollided) flux is used to estimate the scattering source and a second sweep is performed, then at the end of the second sweep, the estimated angular flux is the sum of the uncollided and the *once-collided* fluxes. At the end of N sweeps, the estimated angular flux $\psi^{(N)}$ is:

$$\psi^{(N)} = \sum_{n=0}^{N} \psi_n, \tag{298}$$

where ψ_n is the angular flux of particles that have scattered exactly n times. (See ❯ Subsect. 2.10.12.)

If a physical system is small and "leaky," or has significant absorption, then particles will generally have short histories, and the series (298) will converge rapidly. However, if a problem has a subregion which is many mean free paths thick and dominated by scattering (rather than capture), then particles in that subregion will have long histories, and the series (298) will converge slowly. In the former case, the source iteration strategy converges rapidly, but in the latter case, source iteration converges slowly (Carlson and Lathrop 1968; Larsen and Morel 2009).

To speed up the convergence of source iterations for problems with optically thick, scattering-dominated subregions, *iterative acceleration* strategies have been devised. The earliest of these was the *Chebyschev acceleration*, a technique based on concepts from matrix algebra. This method worked to a limited extent, but it was not sufficiently efficient for many problems.

Later, the *rebalance* method was developed and used widely for a number of years. This method operates by calculating and applying, at the end of each sweep, *rebalance factors* on a fine or coarse space-energy grid. The rebalance method tends to become unstable when used on a fine space-energy grid, and to become stable but inefficient when used on a very coarse grid. The optimal (intermediate) grid is problem-dependent and must found by trial and error. Even when the optimal grid is found, the resulting method is often not as efficient as desired (Adams and Larsen 2002).

Later still, *diffusion synthetic acceleration* (DSA) was developed to speed up the convergence of source iterations. DSA is based on the following concept. At the end of a transport sweep, an exact transport equation is derived for the iteration error (the difference between the latest iterate and the converged solution). This equation is just as difficult to solve as the original transport equation for the angular flux. In DSA, this *exact transport equation for the iteration error* is replaced by an *approximate diffusion equation for the iterative error*; the diffusion equation is solved; and the diffusion estimate of the iterative error is combined with the most recent estimate of the flux to obtain an updated and much more accurate estimate of the angular flux (Adams and Larsen 2002; Alcouffe 1977).

In practice, DSA is highly efficient for optically thin spatial grids. Unfortunately, unless great care is taken in the discretization of the diffusion part of the algorithm, it can become inefficient or unstable for optically thick spatial grids (Adams and Larsen 2002; Azmy 1998).

More recently, *Krylov methods* have been used, often in conjunction with DSA. Although Krylov methods require significant extra storage, they can be remarkably effective at stabilizing and speeding up the iterative convergence of methods based on source iterations, or on DSA (Adams and Larsen 2002; Faber and Mantueffel 1989).

All the work cited above describes advances in the basic mathematical algorithms for solving transport problems. Other equally important work has taken advantage of changes in computer architecture, i.e., on the details of how computers process arithmetic for large-scale problems

(Baker and Koch 1998). This type of research is becoming increasingly important as computers are becoming increasingly parallel in nature.

Historically, the research on S_N methods has tended to focus on (i) advanced discretization methods in space, angle, energy, and time, and (ii) advanced iterative methods that converge the iterative solution more rapidly and efficiently. In the past 50 years, major advances in all these areas have been made. The discretization and iteration schemes used in many advanced simulation codes today have little resemblance to the methods used 50 years ago.

However, a fundamental difficulty remains at the heart of deterministic calculations: the costly and time-consuming task of obtaining adequate multigroup cross sections for a specified difficult problem. This aspect of deterministic simulations remains the most significant obstacle to obtaining useful, accurate deterministic solutions of practical transport problems in a reliable, efficient, and user-friendly manner.

10.3   Hybrid Monte Carlo/Deterministic Methods

In the last 10–15 years, it has become understood that the most challenging aspect of difficult Monte Carlo simulations – the determination of problem-dependent biasing parameters – can be done efficiently by a deterministic simulation.

Specifically, for source-detector problems, the biasing parameters can be obtained by (i) solving an adjoint problem in which the detector response function is the source, as discussed in ❯ Sect. 5, and (ii) processing the resulting adjoint scalar or angular fluxes. The original "hybrid" concept is to use a deterministic code to perform this task (Chucas and Grimstone 1994; Haghighat and Wagner 2003; Smith and Wagner 2005; Van Riper et al. 1997).

The advantages to this procedure are that (i) it removes from the code user the burdensome task of calculating the biasing parameters, and (ii) the resulting computer-generated biasing parameters are usually much more efficient at reducing the Monte Carlo variance than the biasing parameters obtained by human trial and error (Smith and Wagner 2005).

The principal disadvantage is that two separate codes (Monte Carlo and deterministic) must be set up to run the same geometric problem, and the results of the deterministic code must be processed, formatted properly, and then input to the Monte Carlo code. This process can be unwieldy unless a suitable investment has been made in the computing infrastructure, enabling the process to occur automatically.

Most public particle transport codes are either Monte Carlo or deterministic, but a small number of user-friendly hybrid codes are now available. For example, the hybrid code MCBEND (Chucas and Grimstone 1994) uses a multigroup diffusion solver to determine weight windows for Monte Carlo simulation. Also, the recent SCALE 6.0 package from Oak Ridge National Laboratory contains software that enables, with one geometric input deck, deterministically generated multigroup S_N solutions to be calculated, turned into weight windows, and then used in Monte Carlo simulations (Haghighat and Wagner 2003; Smith and Wagner 2005).

The type of problem for which deterministic methods have been most widely used to derive biasing parameters for Monte Carlo simulations is the classic source-detector problem – in which particles are born in a source, and a single detector response, in a possibly distant detector, is desired. The biasing parameters for this problem "encourage" Monte Carlo particles to migrate from the source to the specified detector region in such a way that estimates of the desired response have a significantly reduced variance. The biasing parameters can be obtained by solving an adjoint transport problem. In the resulting *nonanalog* Monte Carlo simulations

of source-detector problems, Monte Carlo particles are discouraged from migrating to regions far from the detector. Consequently, estimates of reaction rates at these locations generally have larger variances than before.

One of the features of deterministic calculations is that at the end of a simulation, estimates of the flux are inherently available at *all* points in the 6-D phase space. For the reasons discussed in the previous paragraph, this *global* information is generally not considered to be available in a useful sense from Monte Carlo simulations.

However, recent work has shown that if weight windows are properly defined using information from both adjoint *and* forward calculations, then Monte Carlo particles are "encouraged" to become distributed throughout the system in a manner that is much more uniform than the distribution of physical particles. In this case, accurate (low-variance) estimates of reaction rates throughout a physical system can be obtained from a *single* Monte Carlo calculation (Becker and Larsen 2009; Cooper and Larsen 2001; Wagner et al. 2007, 2009).

To date, the term "hybrid" has implied a method in which a deterministic simulation is used to assist – through the calculation of biasing parameters – a Monte Carlo simulation. However, deterministic and Monte Carlo techniques can be merged in different advantageous ways. For example, it has been demonstrated that for source-detector problems, an adjoint calculation can be used to *actively* modify the physical scattering process, so that Monte Carlo particles are encouraged to scatter into directions and energies that will bring them from regions of low importance to regions of greater importance (Turner and Larsen 1997). This *local importance function transform* method requires a greater amount of computation per particle history. However, for optically thick, deep-penetration source-detector problems, the method can be significantly more efficient than a standard weight window. It has also been shown that for problems with high scattering ratios, hybrid methods based on variational principles can yield estimates of reaction rates and eigenvalues that are significantly more efficient than standard estimates (Densmore and Larsen 2004). In addition, recent work on the *functional Monte Carlo* method has shown that even more accurate estimates of eigenvalues and eigenfunctions can be obtained by a hybrid method in which the Monte Carlo simulation is *not* used to obtain estimates of the flux, but rather to obtain estimates of certain *nonlinear functionals*, which are then used to obtain estimates of the flux (Larsen and Yang 2008).

Is there a class of hybrid methods for which Monte Carlo can be used to directly assist the accurate calculation of deterministic solutions? Possibly, the answer to this question is *yes*. As discussed previously, the principal difficulty with deterministic methods is the laborious calculation of multigroup cross sections. If continuous-energy Monte Carlo simulations could be efficiently run, to automatically determine (problem-dependent) multigroup cross sections, then this would be a way in which Monte Carlo simulations could significantly influence deterministic solutions. Promising work in this area has recently been reported (Wolters et al. 2009; Yang and Larsen 2009).

If such methods can be developed, then it is possible to imagine a future particle transport code, containing both Monte Carlo and deterministic modules, in which the Monte Carlo module "supplies" multigroup cross sections to the deterministic module, and the deterministic module "supplies" biasing parameters to the Monte Carlo module. (It might be necessary to perform these tasks iteratively.) One would then have a particle transport code that is much closer to a "black box" than present-day transport codes; it would require the user to input neither the biasing parameters for Monte Carlo simulations, nor the multigroup cross sections for deterministic simulations; it would determine these quantities automatically, and more accurately.

In principle, a code containing these features could make effective use of future advances in Monte Carlo, deterministic, and hybrid methods. Such a hybrid code does not exist today, but it is a distinctly logical possibility, given the thrust of past and current research in computational particle transport methods and the practical difficulties experienced by current-day code users.

10.4 Discussion

During the past 50 years, computational methods for performing neutron and coupled neutron/photon simulations have been an active and vibrant area of research in the nuclear engineering community. Major advances in algorithms for Monte Carlo and deterministic simulations have been made. There is little doubt that, due to the increasing demands on increased realism in simulations, research will continue on different fronts to improve the accuracy and efficiency of these simulations. Also, hybrid methods may become a distinct third approach, which would have its own class of difficult problems for which it is best suited.

11 Concluding Remarks

This concludes the chapter on *general principles of neutron transport*. The theory and methods discussed here apply to photon as well as neutron transport, although photon transport is of practical interest mainly in radiation shields. Important topics could not be presented, including (for example) (i) a discussion on variational methods, which are heavily dependent on the adjoint transport equation discussed in ❯ Sect. 5; (ii) a more complete discussion on homogenized diffusion theory, which is used in most practical reactor core simulations; and (iii) a detailed exposition of computational methods for neutron and photon transport. Nonetheless, the authors hope that the material presented in this chapter, and the references provided below, will give the reader a useful foundation for more applied techniques described in other chapters of this handbook, and elsewhere.

References

Adams ML (2001) Discontinuous finite element transport solutions in thick diffusive problems. Nucl Sci Eng 137:298

Adams ML Larsen EW (2002) Fast iterative methods for discrete-ordinates particle transport calculations. Prog Nucl Energy 40:3 [Review article]

Adams ML, Wareing TA, Walters WF (1998) Characteristic methods in thick diffusive problems. Nucl Sci Eng 130:18

Alcouffe RE (1977) Diffusion synthetic acceleration methods for the diamond-differenced discrete-ordinates equations. Nucl Sci Eng 64:344

Azmy YY (1992) Arbitrarily high order characteristic methods for solving the neutron transport equation. Ann Nucl Energy 19:593

Azmy YY (1998) Impossibility of unconditional stability and robustness of diffusive acceleration schemes. In: Proceedings of the ANS topical meeting on radiation protection and shielding, Nashville, 19–23 April 1998, vol 1, p 480

Baker RS, Koch KR (1998) An SN algorithm for the massively parallel CM-200 computer. Nucl Sci Eng 128:312

Becker TL, Larsen EW (2009) The application of weight windows to "global" Monte Carlo problems. In: Proceedings of the 2009 international conference on advances in mathematics, computational methods, and reactor physics, Saratoga Springs, New York 3–7 May 2009

Bell GI (1965) On the stochastic theory of neutron transport. Nucl Sci Eng 21:390

Bell GI, Glasstone S (1970) Nuclear reactor theory. Van Nostrand Reinhold, New York

Benoist P (1964) Théorie du coefficient de diffusion des neutrons dans un reseau comportant des cavités. CEA-R2278, Centre d'Etudes Nucléaires – Saclay

Brantley PS Larsen EW (2000) The simplified P3 approximation. Nucl Sci Eng 134:1

Cacuci DG (2003) Sensitivity and uncertainty analysis: theory. Chapman & Hall/CRC Press, Boca Raton

Carlson BG, Lathrop KD (1968) Transport theory – the method of discrete ordinates. In: Greenspan H, Kelber CN, Okrent D (eds) Computing methods in reactor physics. Gordon & Breach, New York

Carter LL, Cashwell ED (1975) Particle transport simulation with the Monte Carlo method. TID-26607, National Technical Information Service, U.S. Department of Commerce

Case KM, Zweifel PF (1967) Linear transport theory. Addison-Wesley, Reading

Chucas SJ, Grimstone MJ (1994) The accelerated techniques used in the Monte Carlo code MCBEND. In: Proceedings of the eighth international conference on radiation shielding, Arlington, 24–28 April 1994, vol 2, p 1126

Cooper MA, Larsen EW (2001) Automated weight windows for global Monte Carlo deep penetration neutron transport calculations. Nucl Sci Eng 137:1

Densmore JD, Larsen EW (2004) Variational variance reduction for Monte Carlo eigenvalue and eigenfunction problems. Nucl Sci Eng 146:121

Dorning JJ (2003) Homogenized multigroup and energy-dependent diffusion equations as asymptotic approximations to the Boltzmann equation. Trans Am Nucl Soc 89:313

Duderstadt J, Hamilton L (1976) Nuclear reactor analysis. Wiley, New York

Duo JI, Azmy YY (2007) Error comparison of diamond difference, nodal, and characteristic methods for solving multidimensional transport problems with the discrete ordinates approximation. Nucl Sci Eng 156:139

Faber V, Mantueffel TA (1989) A look at transport theory from the viewpoint of linear algebra. In: Nelson P et al (eds) Transport theory, invariant imbedding, and integral equations (Lecture notes in pure and applied mathematics), vol 115. Marcel Dekker, New York, p 37

Gamino RG (1989) Simplified PL nodal transport applied to two-dimensional deep penetration problems. Trans Am Nucl Soc 59:149

Gamino RG (1991) 3-dimensional nodal transport using the simplified PL method. In: Proceedings of the ANS M&C conference on advances in mathematics, computations, and reactor physics, Pittsburgh, 29 April–2 May 1991, vol 2, section 7.1

Gelbard EM (1960) Application of spherical harmonics methods to reactor problems. WAPDBT-20, Bettis Atomic Power Laboratory

Gelbard EM (1961) Simplified spherical harmonics equations and their use in shielding problems. WAPD-T-1182, Bettis Atomic Power Laboratory

Gelbard EM (1962) Applications of the simplified spherical harmonics equations in spherical geometry. WAPD-TM-294, Bettis Atomic Power Laboratory

Gelbard EM (1974) Anisotropic neutron diffusion in lattices of the zero-power plutonium reactor experiments. Nucl Sci Eng 54:327

Habetler GJ, Matkowsky BJ (1975) Uniform asymptotic expansions in transport theory with small mean free paths, and the diffusion approximation. J Math Phys 16:846

Haghighat A, Wagner J (2003) Monte Carlo variance reduction with deterministic importance functions. Prog Nucl Energy 42:25 [Review article]

Henry AF (1975) Nuclear-reactor analysis. MIT Press, Cambridge

Hetrick DO (1993) Dynamics of nuclear reactors. American Nuclear Society, La Grange Park

Kalos MH, Whitlock PA (1986) Monte Carlo methods. Wiley, New York

Kellog RB (1974) First derivatives of solutions of the plane neutron transport equation. Technical Note BN-783, Institute for Fluid Dynamics and Applied Mathematics, University of Maryland

Larsen EW (1980) Diffusion theory as an asymptotic limit of transport theory for nearly critical systems with small mean free paths. Ann Nucl Energy 7:249 [Review article]

Larsen EW (1982) Spatial convergence properties of the diamond-difference method in X,Y geometry. Nucl Sci Eng 80:710

Larsen EW (1992) The asymptotic diffusion limit of discretized transport problems. Nucl Sci Eng 112:336 [Review article]

Larsen EW (2007) The description of particle transport problems with helical symmetry. Nucl Sci Eng 156:68

Larsen EW, Ahrens C (2001) The Greuling-Goertzel and Wigner approximations in the theory of neutron slowing down. Ann Nucl Energy 28:1809

Larsen EW, Hughes RP (1980) Homogenized diffusion approximations to the neutron transport equation. Nucl Sci Eng 73:274

Larsen EW, Keller JB (1974) Asymptotic solution of neutron transport problems for small mean free paths. J Math Phys 15:75

Larsen EW, Morel JE (2009) Advances in discrete-ordinates methodology. In: Azmy YY, Sartori E (eds) Nuclear computational science: a century in review. Springer, Berlin [Review article]

Larsen EW, Yang J (2008) A "functional Monte Carlo" method for k-eigenvalue problems. Nucl Sci Eng 159:107

Larsen EW, Morel JE, McGhee JM (1996) Asymptotic derivation of the multigroup P1 and simplified PN equations with anisotropic scattering. Nucl Sci Eng 123:328

Lewins J (1965) Importance: the adjoint function. Pergamon, Oxford

Lewins J (1968) Developments in perturbation theory. Adv Nucl Sci Technol 4:309

Lewis EE, Miller WF (1993) Computational methods of neutron transport. American Nuclear Society, Lagrange Park. Originally published by Wiley-Interscience, New York (1984)

Lux I, Koblinger L (1991) Monte Carlo particle transport methods: neutron and photon calculations. CRC Press, Boca Raton

Marchuk GI, Lebedev VI (1986) Numerical methods in the theory of neutron transport. Harwood, London. Originally published in Russian by Isdatel'stvo Atomizdat, Moscow (1981)

Ott KO (1985) Nuclear reactor dynamics. American Nuclear Society, La Grange Park

Papanicolaou GC (1975) Asymptotic analysis of transport processes. Bull Am Math Soc 81:330

Pomraning GC (1967a) A derivation of variational principles for inhomogeneous equations. Nucl Sci Eng 29:220

Pomraning GC (1967b) Variational principle for eigenvalue equations. J Math Phys 8:149

Prinja AK (1989) Forward-backward transport theories of ion-solid interactions: variational approach. Phys Rev B 39:8858

Sanchez R, McCormick NJ (1982) A review of neutron transport approximations. Nucl Sci Eng 80:481 [Review article]

Sigmund P (1969) Theory of sputtering. I. Sputtering yield of amorphous and polycrystalline targets. Phys Rev 184:383

Smith HP, Wagner JC (2005) A case study in manual and automated Monte Carlo variance reduction with a deep penetration reactor shielding problem. Nucl Sci Eng 149:23

Spanier J, Gelbard E (2008) Monte Carlo principles and neutron transport problems. Dover, New York. Originally published by Addison-Wesley, Reading (1969)

Stacey WM (1974) Variational methods in nuclear reactor physics. Academic, New York

Tomašević DI, Larsen EW (1996) The simplified P2 approximation. Nucl Sci Eng 122:309

Turner SA, Larsen EW (1997) Automatic variance reduction for 3-D Monte Carlo simulations by the local importance function transform – Part I: Analysis. Nucl Sci Eng 127:22; Part II: Numerical results. Nucl Sci Eng 127:36

Van Riper KA, Urbatsch TJ, Soran PD, Parsons DK, Morel JE, McKinney GW, Lee SR, Crotzer LA, Brinkley FW, Anderson JW, Alcouffe RE (1997) AVATAR – automatic variance reduction in Monte Carlo calculations. In: Proceedings of the ANS M&C international conference on mathematical methods and supercomputing in nuclear applications, Saratoga Springs, New York, 6–10 October 1997, American Nuclear Society, vol 1, p 661

Wagner JC, Blakeman ED, Peplow DE (2007) Forward-weighted CADIS method for global variance reduction. Trans Am Nucl Soc 97:630

Wagner JC, Blakeman ED, Peplow DE (2009) Forward-weighted CADIS method for variance reduction of Monte Carlo calculations of distributions and multiple localized quantities. In: Proceedings of the 2009 international conference on advances in mathematics, computational methods, and reactor physics, Saratoga Springs, New York, 3–7 May 2009

Weinberg AM, Wigner EP (1958) The physical theory of neutron chain reactors. University of Chicago Press, Chicago, pp 314–316

Williams MMR (1971) Mathematical methods in particle transport theory. Butterworth, London

Williams MMR (1979) The role of the Boltzmann equations in radiation damage calculations. Prog Nucl Energy 3:1

Wolters ER, Larsen EW, Martin WR (2009) A hybrid Monte Carlo-S2 method for preserving neutron transport effects. In: Proceedings of the 2009 international conference on advances in mathematics, computational methods, and reactor physics, Saratoga Springs, New York, 3–7 May 2009

X-5 Monte Carlo Team (2003) MCNP – a general Monte Carlo N-particle transport code, Version 5. Los Alamos National Laboratory, LA-UR-03-1987 (Revised October 2005)

Yang J, Larsen EW (2009) Application of the "functional Monte Carlo" method to estimate continuous energy k-eigenvalues and eigenfunctions. In: Proceedings of the 2009 international conference on advances in mathematics, computational methods, and reactor physics, Saratoga Springs, New York, 3–7 May 2009